ROLE OF GUKHOLDER IN ADHESION IN THE *DROSOPHILA* WING DISC

by

Rosalie Ho

B.Sc. Biology, The University of British Columbia, 2018

A THESIS SUBMITTED IN PARTIAL FULFILLMENT OF THE

REQUIREMENTS FOR THE DEGREE OF

MASTER OF SCIENCE

in

THE FACULTY OF GRADUATE AND POSTDOCTORAL STUDIES

(ZOOLOGY)

The University of British Columbia

(Vancouver)

December 2020

The following individuals certify that they have read, and recommend to the Faculty of Graduate and Postdoctoral Studies for acceptance, the thesis entitled:

Role of Gukholder in adhesion in the *Drosophila* wing disc

submitted by Rosalie Ho in partial fulfillment of the requirements for

the degree of Master of Science

in Zoology

Examining Committee:

Dr. Vanessa Auld, Zoology
Supervisor

Dr. Katie Marshall, Zoology
Supervisory Committee Member

Dr. Nelly Panté, Zoology
Additional Examiner

Additional Supervisory Committee Members:

Dr. Cal Roskelley, Cellular and Physiological Sciences
Supervisory Committee Member

Abstract

Cell adhesion plays an important role in maintaining tissue homeostasis and morphogenesis. In *Drosophila*, adhesion between neighbouring cells is mediated by adhesion junctions (AJ) and septate junctions (SJ) whereas the focal adhesion complex (FAC) adheres cells to the extracellular matrix. At the convergence of three neighbouring cells, a specialized junction is formed—the tricellular junction (TCJ). Both SJs and TCJs contribute to the formation of permeability barriers. Discs large (Dlg) and Scribble (Scrib) are scaffolding proteins responsible for recruiting the TCJ proteins Gliotactin and Anakonda. However, the mechanism that recruits Dlg and Scrib to the TCJ is not known. In the neuromuscular junction, Gukholder (Gukh) binds to the guanylate kinase (GUK) domain in Dlg, via the Dlg-binding domain, to facilitate the recruitment of Scrib. Thus, Gukh may mediate the recruitment of Dlg and Scrib to the TCJ. We found that within the wing imaginal disc epithelia Gukh is expressed at multiple locations including the SJ and TCJ, basolateral to the TCJ, and adjacent to the FAC on the basal side of the epithelium. We found that the knockdown of Gukh triggers severe cellular phenotypes including JNK-mediated apoptosis, cell migration, and cell delamination. However, Gukh is not necessary for the formation of the TCJ, SJ, or the FAC as RNAi-mediate knockdown of Gukh did not affect these junctional domains. Rather, TCJ proteins recruit Gukh to the TCJ, and β-integrin recruits Gukh to the basal domain. The exception was the lateral or intermediate zone where Gukh not only associated with the FAC but where loss of Gukh disrupted the recruitment of the FAC proteins as did overexpression of the Gukh C-terminal domain. This suggests a model where Gukh mediates the localization of focal adhesion-like structures in the lateral domain. Overall, we propose that Gukh is recruited to the TCJ and basal focal adhesion complex by two independent processes, and functions to mediate adhesion in the lateral domain.

Lay Summary

Cell adhesion, the ability for cells stick together in a continuous sheet, is important for biological processes. Junctions are specialized structures found between cells and their external environment to restrict the flow of undesired molecules or pathogens. Defects in junctions and barriers are implicated in many diseases and severe birth defects such as cancer and spina bifida. To better understand the role of how these junctions are formed and operate, we use the fruit fly as our model system to investigate the role of a protein named Gukholder (Gukh) in forming junctions. We found that Gukh is not important to the formation of junctions in the cell but reducing Gukh results in cell death and triggers cells to migrate. We also observed that Gukh stabilizes a specific cell junction that mediates adhesion to the external environment. We concluded the presence of Gukh in tissues is important to mediate cell adhesion.

Preface

Data presented in chapter 2 of this work was conducted at the Life Science Institute by Rosalie Ho and Dr. Vanessa Auld. I was responsible for performing all the experiments including animal crosses, fine dissections, immunostaining and western blot analysis. Dr. Auld contributed to the experimental design and data analysis, and supervised this project. I also analyzed and processed data I collected using Microsoft Excel, Image J, Adobe Photoshop, GraphPad Prism6. I created original illustrations with Adobe Illustrator.

Table Of Contents

List of Figures

List of Abbreviations

Abi	Abl interactor
AJ	Adheren Junction
Aka	Anakonda
Ap	Apterous
Arm	Armadillo
ATPα	Na+/K+ ATPase α subunit
α2M	α-2-macroglobulin
Bark	Barkbeetle
Bsk	Basket
BBB	Blood-brain-barrier
βPS	beta-integrin
Cora	Coracle
Cno	Canoe
DE-Cad/E-cad	DE-cadherin/E-cadherin
Dlg	Discs large
ECM	Extracellular matrix
FAC	Focal adhesion complex
FAK	focal adhesion kinase
Gli	Gliotactin
GUK	Guanylate kinase
GUKH	Gukholder

ILK	Integrin-linked kinase
JAMs	Junctional adhesion molecules
JNK	c-Jun N-terminal kinases
LSR	lipolysis-stimulated lipoprotein receptor
l(2)gl	Lethal (2) giant larvae
MAGUK	Membrane associated guanylate kinase
MARVEL	MAL and related proteins for vesicle trafficking and membrane link
Mcr	Macroglobulin complement-related
MDCK C7	Madin-Darby canine kidney cells clone 7
mys	myospheriod
NHS	Nance Horan Syndrome
NMJ	neuromuscular junctions
Nrg	Neuroglian
Nrv2	Nervana 2
NrxIV	Neurexin IV
PDZ	PSD95/Dlg/ZO-1 domain
pH3	phosphoHistone3
PJs	paranodal junctions
PSD95	Postsynaptic density 95
Scrib	Scribbled
Shot	Short stop
SH3	SRC homolog 3
SJ	Septate junction

TAJ	Tricellular adherens junctions
TCJ	Tricellular junction
TEP	thioester protein
tTJ	Tricellular tight junctions
UAS	upstream activating sequence
Vari	Varicose
Vinc	Vinculin
WASP	Wiskott–Aldrich syndrome protein
WHD	WAVE homology domain
ZO	Zonula occludens

Acknowledgements

I would like to thank my supervisor, Vanessa, for her support, patience, and guidance throughout my master's and undergraduate research projects. Thank you to my committee members, Dr. Cal Roskelley and Dr. Katie Marshall, for taking the time to provide valuable insight and feedback. Thank you to all my lab mates for your friendship and help. Thank you for always reading my first drafts and letting me share my cat obsession, Katie C. Duo, I thank you for all the favours and countless little things you helped out with during this "apocalyptic" COVID-19 pandemic. I have to thank our lab alumni Zohreh and Gayathri for helping me early in my project and, Gayathri for continuing to share her expertise with me to this day. I cannot thank **Amelia Hunter** enough for always looking over my data and providing constructive criticism and helping me survive grad school with her humor and baked goods. I also like to thank Murry, our lab research associate, who was willing to teach me new techniques.

Thank you to our grad student BIOL 530 cohort, especially Duo, Delbert, Mizuki, and Mo, who provided scientific insight, giving me the space to vent, and sharing cool scientific findings.

I am very thankful for my family's support. I am forever grateful for my parents' sacrifices, which provided me with this life with democracy and freedoms. To my dear Aunt Mary, thank you for always giving and urging me to take on this challenge. We miss you every day. Thank you to my cousins (Shirley, Johnny, Cindy, Megan, and Avery), thank you for encouraging me every step of the way. I must also thank my best friend of 18 years, Chloe, for always being a shoulder to cry on during this journey. Lastly, I want to thank Landon and our cat Bubbles for their continued support during this degree and pandemic.

To my friends and family, without whom this thesis would not have come to fruition.

CHAPTER 1: Introduction

1.1 Cell adhesion

In multicellular organisms, cells must communicate and cooperate to maintain homeostasis. Cell adhesion is one of the processes that play a fundamental role in tissue homeostasis and developmental processes including epithelial remodeling, cell migration, signal transduction, and wound healing (Janiszewska et al., 2020). By adhering to neighbouring cells and the extracellular matrix (ECM), epithelial cells maintain tissue structure and communicate with each other through signaling. Cell adhesion is accomplished through two modalities - the adhesion between neighbouring cells (cell-cell adhesion via junctions), and adhesion between cells and the ECM (cell-ECM adhesion via focal adhesion complexes) (Ray and Niswander, 2012; Shi et al., 2018). The loss of cell adhesion triggers harmful physiological consequences such as the disruption of epithelial remodeling, which results in delays in wound healing, tissue malformation, and birth defects (Shi et al., 2018). For example, the adhesion and fusion of apposing neural folds in neurulation are facilitated by cell adhesion and epithelial remodeling. Disruptions in neural tube closure result in developmental defects in humans such as anencephaly and spina bifida (Leoni et al., 2015; Pai et al., 2012; Ray & Niswander, 2012).

Cell adhesion is key to the formation of permeability barriers to restrict the flow of ions, pathogens, and molecules between cells in a range of tissues including the epidermis, intestines, and brain (Harden et al., 2016; Harris and Peifer, 2004). Cell adhesion is also implicated in other diseases such as cancer where changes to cell adhesion cause two major hallmarks of cancer – loss of cell-to-cell adhesion and anchorage–independent growth (Janiszewska et al., 2020). This loss of cell adhesion permits uncontrolled cell proliferation and results in the distortion of tissue

structure, enabling the motile and invasive phenotype of malignant cells to detach and migrate to distal organs (Moh and Shen, 2009). As a result, new cancer therapeutics are being developed targeting cell adhesion molecules (Läubli and Borsig, 2019). The study of cell adhesion not only provides a better understanding of developmental processes but also helps researchers develop novel therapies for diseases. The focus of this thesis is a greater understanding of scaffolding protein function and their roles in cell-cell and cell-ECM adhesion complexes using the model system *Drosophila melanogaster*. These adhesion complexes are highly conserved across all animals. This introduction will mainly focus on composition and function of these complexes in *Drosophila* epithelia.

1.2 Cell-ECM interactions

Cellular interactions with the ECM provide structural support to cells and tissues; they regulate cell proliferation, differentiation, migration, and adhesion through cell signaling (Ross, 1998). In both vertebrates and invertebrates, the conserved focal adhesion complexes, composed of multiple adhesion proteins, facilitate the adhesion between cells to the ECM (Brown et al., 2002).

1.2.1 Focal adhesion complex

At the core of focal adhesions are the integrin adhesion complexes - focal adhesion sites characterized by discrete structures where intracellular integrin-associated proteins become highly concentrated (Brown et al., 2002; Dominguez-Gimenez et al., 2007). Integrins are heterodimers, which consist of one α and one β subunit. There are five *Drosophila* α subunits (αPS1-5) and two β subunits (βPS and βν) (Zervas et al., 2001) whereas there are 18 α subunits and 8 β subunits in humans (Hynes, 2002). In the wing disc, the αPS1βPS integrin heterodimer

is expressed primarily on dorsal wing epithelium, while αPS2βPS integrin is found almost exclusively on the ventral epithelium (Brower and Jaffe, 1989; Brown et al., 2000)

Integrin interacts with signalling cell migration-associated components such as Rho family GTPses, focal adhesion kinases, Src kinases, JNK pathways (Harburger and Calderwood, 2009). More importantly, integrin facilitates the adhesion between the cellular cytoskeleton and ECM through an intracellular multiprotein complex—the integrin-cytoskeleton link (Fig 1.1A)(Narasimha and Brown, 2004). The main components of this complex are integrins, talin, vinculin (Vinc), focal adhesion kinase (FAK), integrin-linked-kinase (ILK) and PINCH. Complex members ILK and PINCH are required for integrin's function in strong adhesion (Schotman et al., 2009; Voelzmann et al., 2017; Zervas et al., 2001). FAK and vinculin are not required for integrin function but are harmful when hyperactive (Alatortsev et al., 1997; Grabbe, 2004). For instance, the overexpression of FAK results in phenotypes that mimic those in integrin loss of function as integrin is inhibited from binding to the ECM (Grabbe, 2004). On the other hand, vinculin binds to talin and actin to provide extra mechanical support to the cytoskeletal anchorage (Xu et al., 1998). Hyperactive vinculin ectopically activates talin in the cytoplasm and forms adhesion aggregations that are lethal (Maartens et al., 2016).

A key member of the focal adhesion complex is talin (encoded by the *rhea* gene in *Drosophila*), which is required in most integrin-dependent adhesion functions in stable focal adhesions (Brown et al., 2002; Dominguez-Gimenez et al., 2007; Klapholz and Brown, 2017). talin contains an N-terminal globular head, an extended rod of helical bundles, and an actin-binding motif. talin facilitates the direct linkage between integrins and actin and increases the affinity of integrin for ligands (Klapholz and Brown, 2017; Wang, 2012). At rest, the α and β cytoplasmic tails of integrin are in close proximity in a low-affinity conformation. talin actives

integrin by binding to the integrin β cytoplasmic tail to separate the heterodimer tails, which in turn relieves the low-affinity conformation (Wang, 2012). Talin controls the focal adhesion size in response to force and matrix rigidity, which regulates the strength of integrin-mediated adhesion (Klapholz and Brown, 2017). Mutations in the *Drosophila* talin gene (*rhea*) demonstrated talin is crucial for all integrin adhesive function. For instance, the clustering of talin or βPS integrin at the basal wing imaginal disc is mutually dependent and the loss of either triggers the loss of the basal focal adhesions (Brown et al., 2002). In this thesis, we focused on the basal focal adhesions in the wing imaginal disc. While other focal adhesion complex members are likely present, the localization of talin and βPS integrin as clusters at the basal focal adhesions have been clearly demonstrated in prior works (Brown et al., 2002; Dominguez-Gimenez et al., 2007).

The expression of talin and β-integrin is also observed in the intermediate domain of the columnar epithelia (Fig 1.1 B, Fig 2.1C), the region of the lateral membrane between the apical SJ and basal focal adhesions (Brown et al., 2002; Fristrom et al., 1993). Although their role in the intermediate domain of the wing disc is not well understood, the localization of β-integrin at the lateral membrane has been observed in other tissues such as in follicle cells and amnioserosa/epidermis interface to mediate adhesion (Dinkins et al., 2008; Narasimha and Brown, 2004). It is thought that β-integrin control epithelial cell shape from columnar to cuboidal during wing development by regulating the adhesion of cells to the ECM basally and mediate lateral adhesion between adjacent cells (Dominguez-Gimenez et al., 2007). However, the ligands that engaged in this process at the lateral membrane have not been identified.

Integrin adhesion is critical to maintaining stable attachment between tissue layers such as the formation of the wing blade in the wing imaginal disc. The loss of integrins and integrins-

associated proteins result in blisters due to the separation of the two apposing wing epithelial layers, which affects the trajectory of veins in the wing (Araujo, 2003; Dominguez-Gimenez et al., 2007). Taken together, the focal adhesion complex is critical to development and to cell-ECM adhesion. However, the role of integrin and focal adhesion complex at the lateral membrane is understudied. Thus, the investigation into the role of these lateral focal adhesion complexes may provide further insight into integrin-mediated adhesion.

1.3 Cell-cell junctions

Cell to cell adhesion is mediated by a range of cell adhesion complexes conserved in all animals. These include adherens junctions (AJs), occluding junctions such as tight junctions (TJs) in vertebrates, and the analogous septate junctions (SJs) in invertebrates. Despite some organizational differences, these junctional domains are highly conserved in terms of protein composition and physiological function. Cell-cell junctions consist of both membrane-spanning proteins and intracellular scaffolding that mediate interactions with the cytoskeleton or other intracellular signalling complexes. Given the similarity in function and structure between the vertebrate cellular junction and *Drosophila* septate junction, this makes *Drosophila* an ideal model to study cell junction formation and function *in vivo*.

1.3.1 Adherens junction

Adherens junctions (AJs) are fundamental to basic cell-cell adhesion. In polarized epithelia, vertebrate TJs are found apical to the AJ while the majority of insect SJs are located just basal to the AJ (Fig 1.2 C) (Chen et al., 2018). In *Drosophila*, AJs are positioned at the future boundary of apical and basolateral domains during cellularization (Tepass, 1996). AJs link membrane and cytoskeletal components and establish the apical-basal axis in ectodermal-derived epithelial cells, including imaginal discs. The AJ in mature epithelial cells is the zonula adherens.

Zonula adherens links cells into a continuous sheet by forming belts which segregates the apical from the basal lateral membrane (Rusu and Georgiou, 2020).

Vertebrate and invertebrate AJ share many conserved proteins, such as the classic cadherin family, β-catenin and other catenin proteins. The cadherin/catenin and nectin/afadin complexes are the two main adhesion complexes in AJs, in which conserved interactions and proteins are observed (Harris, 2012). The core cadherin/catenin complex includes DE-cadherin/ (DE-cad, encoded by *shotgun*) and a catenin complex of α-catenin, p120-catenin and β-catenin (*Drosophila* Armadillo (*Arm*), which links the cadherin complex to the actin cytoskeleton (Harris, 2012; Harris and Peifer, 2004). The extracellular homophilic interactions of DE-Cad facilitate the formation of AJs, while the cytoplasmic domain mediates catenin interactions and signalling (Bauer et al., 2006). Similar to the mammalian classical cadherins, calcium-binding changes the conformation of DE-cad and allows for calcium-dependent cell-cell adhesion.

Beyond the catenin family, the cadherin-actin linkage is facilitated by a PDZ (PSD95/Dlg/ZO-1) scaffolding domain interaction. These PDZ interactions in general are interactions between a PDZ domain and a C-terminal PDZ binding motif of a target protein to organize protein complexes (Fanning and Anderson, 1999). In AJ, the PDZ domain of Canoe (Cno), the *Drosophila* homolog of Afadin, directly interacts with the PDZ-binding motif of DE-cad to facilitate AJ-actin linkage. The actomyosin cytoskeleton detaches from AJs in the absence of Cno, and changes epidermal integrity (Sawyer et al., 2009). These interactions highlight the importance of a range of scaffolding proteins including PDZ proteins in junction formation and tissue maintenance.

1.3.2 Occluding Junctions – Tight junctions

Occluding junctions create permeability barriers in a wide range of tissues and include TJs in vertebrates and SJs in invertebrates. TJs are found in various polarized vertebrate tissues, including the intestine, skin, and kidney to establish barriers between compartments (Shi et al., 2018). In the nervous system, TJs are found in the endothelial cells that create the blood-brain barrier (Tsukita et al., 2001), the perineurial cells that form the blood-nerve-barrier (BBB), and at the Nodes of Ranvier in the myelinating glia to block the paracellular flow (Tsukita et al., 2001; Wiley and Ellisman, 1980). TJs appear as multiple "kissing-points" at plasma membrane contacts on transmission electron micrographs (Fig 1.2A) (Farquhar and Palade, 1963). Freeze fracture electron microscope revealed TJs form a meshwork of fibrils by strands of transmembrane particles that likely facilitate barrier formation (Fig 1.2 B) (Chalcroft and Bullivant, 1970).

The TJs are mainly composed of claudin proteins, three MAL and related proteins for vesicle trafficking and membrane link (MARVEL) domain proteins, junctional adhesion molecules (JAMs), and many PDZ proteins like Zonula occludens (ZO-1), MAGI1, and Par-3 (Gonzalez-Mariscal et al., 2016; Zihni et al., 2016).

Major Proteins of Tight junctions

TJs are formed by a core complex of PDZ proteins that are outlined below.

ZO-1 (zona occludens -1) is a key scaffolding protein for the TJ (Willott et al., 1993). All three ZO proteins found at the TJ – ZO-1 , ZO-2, and ZO-3 - belong to the MAGUK family of scaffolding proteins and thus contain PDZ domains (Harden et al., 2016). Barrier dysfunction and tight junction disruption is triggered by the dissociation of ZO-1 from the TJ (Chattopadhyay et al., 2014, 2019).

Claudins are key transmembrane proteins of TJs which connect the transmembrane domains to seal the paracellular space and regulate the interaction between the TJ-associated-MARVEL-proteins (Cording et al., 2013). Most claudins contain a canonical PDZ binding motif at the intracellular C-terminus (Chiba et al., 2008). Interaction between claudin and ZO-1 via the PDZ domain is necessary for TJ formation, and loss of claudin causes severe TJ disruption and death (Arabzadeh et al., 2006; Hamazaki et al., 2002; Rüffer and Gerke, 2004, Furuse et al., 2002).

Occludin, though it is concentrated at TJ, it is not essential for TJ formation as observed in occludin knockout mice (M Furuse et al., 1993; Saitou et al., 2000). Occludin is a MARVEL family protein (Cummins, 2012). MARVEL proteins specialize in membrane apposition events such as vesicular transport and tight junction regulation (Sánchez-Pulido et al., 2002). Expression of an occludin mutant lacking the C-terminal end, which contains a PDZ-binding motif, causes paracellular permeability barrier disruption (Balda et al., 1996).

Junctional adhesion molecules (JAMs), part of the immunoglobulin family, are found at the TJs and the lateral membranes. JAMs are considered type I transmembrane glycoproteins which consists of two extracellular immunoglobulin-like domains, one transmembrane domain, and one cytoplasmic PDZ binding motif (except in JAM-L) (Garrido-Urbani et al., 2014). JAMs are thought to facilitate tight junction assembly through PDZ interactions with scaffolding proteins, such as CAR binding to ZO-1 (Cohen et al., 2001; Hamazaki et al., 2002; Itoh et al., 2001). Overall, PDZ interactions involving important TJ proteins ZO-1, claudins, occludin, and JAMs are essential to TJ formation.

1.3.3 Occluding junctions - Septate junctions

In *Drosophila*, the occluding septate junctions (SJs) function analogous to the vertebrate tight junctions (TJs). The two types of SJs observed are the smooth and pleated SJs which are found

in endoderm-dermal (e.g. midgut) and ectoderm-derived (e.g. epidermis, salivary glands, tracheal system) tissues respectively (Lane and Swales, 1982). The focus of this thesis is on the pleated SJs. Pleated SJs are found basal to the AJ and appear as electron-dense ladder-like septa that span the intermembrane space between cells (Fig 1.3 A) (Tepass and Hartenstein, 1994). More than 20 genes have been identified to contribute to the formation and maintenance of the SJs. There are two groups of proteins that engage in the formation of the SJ - the core complex and the SJ-associated proteins (Fig 1.3 B). The core complex includes Megatrachea, Sinuous, Kune-Kune proteins which are the *Drosophila* homologs of claudins. Other key complex members include cell adhesions proteins, Contactin, Neurexin IV, Lachesin, Neuroglian, the α and β subunits of the Na+/K+ ATPase along with the cytoplasmic scaffolding proteins Coracle and Varicose (Baumgartner et al., 1996; Faivre-Sarrailh, 2004; Fehon et al., 1994; Genova and Fehon, 2003; Llimargas, 2004; Nelson et al., 2010; Wu et al., 2017, 2007). Core SJ proteins form the SJ domain interdependently; mutation in anyone impedes SJ formations and leads to the loss of barrier function. The SJ-associated proteins include the PDZ scaffolding proteins Dlg and Scribbled (Scrib), which regulate the SJ indirectly (Harden et al., 2016). The loss of SJs from the glia and epithelia results in embryonic lethality due to permeability barrier defects, leading to paralysis (Banerjee et al., 2006). Mutations in SJ genes have also been implicated in other developmental defects. For instance, loss of Coracle and Neurexin-IV affect dorsal closure (Baumgartner et al., 1996; Fehon et al., 1994; Perrimon, 1988) and lead to defects in trachea development (Hall and Ward, 2016).

SJs are found in a wide range of tissues including between subperineurial glial cells to establish the blood-nerve-barrier and blood-brain barrier. The vertebrate equivalent of the insect subperineurial SJs are the paranodal junctions (PJs) present at the Node of Ranvier in

myelinating axons of vertebrates. Specifically, the core paranodal junction proteins Paranodin/Caspr, Contactin, and Neurofascin are vertebrate homologs of the SJ proteins NrxIV, Contactin and Neuroglian respectively (Banerjee et al., 2006).

Core proteins of the septate junction

The SJ protein complex contains a range of highly conserved proteins, which are interdependent such that the loss of any one protein leads to the loss of other complex members.

Neurexin IV (NrxIV) is a Neurexin family protein and homologous to the vertebrate Caspr. The localization of NrxIV to the SJ is dependent on other SJ core proteins. NrxIV and Cora associate with core SJ protein ATPα in a complex interdependently with Neuroglian (Baumgartner et al., 1996; Fehon et al., 1994). Mutations in both *coracle (cora)* and *NrxIV* disrupt the paracellular seal as the intermembrane septae are absent from the SJ. Hence, NrxIV is necessary for proper SJ formation and paracellular barrier function (Lamb et al., 1998).

Coracle (cora) is homologous to the vertebrate Band 4.1. It is a cytoplasmic associated SJ protein (Fehon et al., 1994). The amino-terminal end of Coracle interacts directly with the glycophorin C domain of NrxIV to facilitate core SJ protein localization (Ward et al., 1998). The permeability barrier function is disrupted in animals with mutations in Cora, as the septae is lost from the SJ (Genova and Fehon, 2003).

The **Na+/K+ ATPase** consists of an α and β subunit. α and β subunits of interest are ATPα and a Nervana 2 (Nrv2) respectively. Both subunits are required for permeability barrier and SJ formation. Loss of Na+/K+ ATPase causes mislocalization of core SJ proteins (Cora, Nrx IV) and allows dye permeation into the tracheal and salivary gland lumens in Na+/K+ ATPase mutant embryos (Oshima and Fehon, 2011; Paul, 2003).

Neuroglian (Nrg) is an IG domain protein homologous to four vertebrate L1-CAM members – Nr-CAM, L1, CHL1, Neurofascin. Nrg is found in axons, glia, and the epithelia (Bieber et al., 1989; Goossens et al., 2011). Consistent with the role of core SJ proteins, Nrg forms a co-dependent complex with other core SJ proteins, such as Nrv2, ATPα, and Mcr to facilitate SJ formation and paracellular barrier function (Goossens et al., 2011; Hall et al., 2014). The loss of *Nrg* reduces the SJ septa and triggers barrier defects (Genova and Fehon, 2003).

Macroglobulin complement-related (Mcr) belongs to the conserved thioester protein (TEP) family, which includes α-2-macroglobulin (α2M) and complement proteins (Nonaka, 2004). The loss of *Mcr* disrupts the organization of SJs and causes Cora mislocalization. Similarly, mutations in *NrxIV* also cause Mcr mislocalization basolaterally. The paracellular barrier in the embryonic trachea is also disrupted in *Mcr* mutant animals. Furthermore, in *Nrg* mutants, Mcr distribution alters to the lateral membrane as opposed to the apical membrane. A reciprocal alteration to Nrg distribution is observed in *Mcr* mutant suggests that Nrg and Mcr share a unique interdependence (Batz et al., 2014; Hall et al., 2014).

Varicose (Vari), the homolog of Proteins Associated with Lin-7 2 (PALS2), is another MAGUK SJ core protein (Wu et al., 2007). Similar to PALS2, Vari interacts with adhesion proteins, namely the C-terminus of NrxIV, via PDZ interactions (Wu et al., 2007). Consistent with its role as a core SJ protein, mutations in *vari* delocalize SJ proteins NrxIV, FasIII, and Na/K-ATPase basolaterally, while null mutations of *cora*, *Nrv2* and *NrxIV* result in loss of Vari from the SJ. (Wu et al., 2007). Compromised paracellular barrier, disrupted SJ assembly, and severe tracheal defects observed in mutations of *vari* future support its role as an SJ core protein(Moyer and Jacobs, 2008).

Associated proteins of the septate junction:

There are a number of proteins associated with the SJ which are not part of the core complex. In particular, the scaffolding proteins **Discs large (Dlg)** and **Scribbled (Scrib)** are associated with the SJ. Although SJ-associated proteins are not essential for the physical assembly of the permeability barrier, they regulate SJ assembly and function indirectly as loss of Scrib and/or Dlg promotes SJ disruption (Verghese et al., 2012). Both proteins include a number of protein-protein binding domains including PDZ domains engage in many cellular processes such as cell migration, synaptic maturation, cell proliferation, tumor suppression, and establishing tissue polarity (Su et al., 2012). Scrib and Dlg, along with lethal (2) giant larvae (l(2)gl), maintain polarity by preventing the basolateral spread of apical and junctional proteins, while the Par and Crumbs complex antagonizes the apical localization of basolateral polarity proteins (Laprise and Tepass, 2011; Laprise et al., 2009; Tanentzapf and Tepass, 2003). Loss of apical-basal polarity triggers uncontrolled cell proliferation, and epithelia-to mesenchymal transition which promotes cancer development (Verghese et al., 2012).

Dlg1 is conserved with the vertebrate Dlg1 proteins and postsynaptic density protein 95 (PSD-95, also known as synapse-associated protein 90) (Willott et al., 1993). Dlg belongs to the MAGUK superfamily and contains three PDZ (PSD95/Dlg/ZO-1) domains in the N-terminal end, an SRC homolog 3 (SH3) domain, and a guanylate kinase (GUK) domain (Muller et al., 1995; Thomas et al., 1997) (Fig 1.4 B). MAGUK proteins are scaffolding proteins involved in protein complexes that typically regulate cell polarization and adhesion. While the PDZ domains interact with PDZ binding motifs on target proteins facilitating signal transduction; the SH3 domain mediates protein binding through proline-rich motifs (Funke et al., 2005; González-Mariscal et al., 2000). Although the GUK domain does not appear to function as a guanylate

kinase, it is capable of binding to the guanine nucleotide GMP (Hough et al., 1997). Interactions of the GUK domain directly or indirectly coordinate cytoskeletal remodelling and proliferation (Golub et al., 2017; Mathew et al., 2002), and may be involved in the formation of tricellular junctions as discussed below. After epithelial differentiation, the SJ core complex maintains Dlg localization at SJ. For instance, the loss of NrxIV or Cora from the wing imaginal disc triggers the loss of Dlg, while the loss of ATPα from the trachea mislocalizes Dlg (Oshima and Fehon, 2011; Ward et al., 1998). It has not yet been determined how Dlg is recruited to the SJ domain.

Scrib is often associated with Dlg in the polarized epithelia and junctions including the SJ and neuromuscular junction. Scrib has sixteen leucine-rich repeats (LRR) and four PDZ domains that mediate protein-protein interactions (Fig 1.4A). The LRR domain targets l(2)gl to the epithelial membrane, and the PDZ domains function to target Scrib to the SJ domain (Tanentzapf and Tepass, 2003). In mitotic neuroblasts, the LRR domain is necessary and sufficient in targeting Scrib cortical localization, whereas the second PDZ domain (PDZ2) is required for cortical and apical localization (Albertson, 2004; Bilder and Perrimon, 2000), but how Scrib is recruited to the SJ domain is not known.

1.4 Tricellular junctions

In epithelial sheets, three neighbouring cells meet at tricellular contacts. To facilitate the formation of the permeability barrier and cell adhesion, there are unique cell-cell junctions specialized at tricellular contacts to make tricellular junctions. These junctions include tricellular adherens junctions (tAJ), and tricellular tight junctions (tTJ) in vertebrates or tricellular septate junctions (TCJ) in invertebrates (Fig 1.5 D, E). Although junctions at tricellular contacts are essential to permeability barrier formation and bi-cellular occluding junction maintenance, molecular interactions at these junctions are not well understood.

1.4.1 Vertebrate tricellular tight junction (tTJ)

The vertebrate tTJ contains a complex of specifically targeted proteins and two major components are Tricellulin and Angulin-1 (Fig 1.5F). At the tricellular contacts of two neighbouring cells, the apical most TJ strands meet at the right angle and turn basally (Fig 1.5D). Then these TJ strands form connections with the central sealing element to seal the paracellular space (Ikenouchi et al., 2005). The tTJ is defined with the connected TJ strands and the central sealing element which is formed by Angulin. Angulin marks the nascent tTJs and recruits Tricellulin (Fig 1.5 F). Tricellulin is thought to then stabilize the TJ strands as occludin is found concentrated at the ends and intersections of TJ strands (Higashi and Miller, 2017; Masuda et al., 2011).

Tricellulin, also known as MARVEL D2, is a four-span transmembrane protein with cytoplasmic N- and C-terminal ends. Tricellulin, occludin, and MARVEL D3 form the conserved TJ-associated MARVEL protein family (Raleigh et al., 2010). The C-terminal end of Tricellulin is highly conserved with the ELL domain of occludin and interacts with ZO-1 (Riazuddin et al., 2006). Tricellulin is concentrated at the tTJ in almost all epithelial cells and is necessary for the maintenance of TJ morphology and barrier function. Loss of tricellulin increases permeability and disrupts occludin localization at the TJ in cultured epithelial cells (Ikenouchi et al., 2005; Ayala-Torres et al., 2019). In tricellulin deficient mice, the intramembrane particles in strands connecting the TJ and tTJ is disrupted, which triggers loss of mechanosensory cochlear hair cells and subsequent hearing loss (Nayak et al., 2013).

Angulin-1, also known as lipolysis-stimulated lipoprotein receptor (LSR), is a single-pass transmembrane protein with an extracellular Ig-like domain, which potentially mediates cell recognition and adhesion. Angulin-1 is critical in recruiting tricellulin to maintain tTJ and loss of

Angulin-1 decreases the transepithelial electrical resistance in EpH4 cells.(Masuda et al., 2011). Overall, some organization similarities are found between the tTJ and the TCJ as discussed below.

1.4.2 Tricellular junction in *Drosophila*

Tricellular septate junctions (TCJs) form from the convergence of SJs at the tricellular contacts in *Drosophila (*Fig 1.5 A). Similar to the formation of the central sealing element in TJ, SJ strands turn 90° to run basolaterally near the tricellular junction to make a loop (Fig 1.5 E). These loops form three parallel strands around the TCJ known as the limiting strands. The sides of these limiting strands are connected to vertically-stacked triangular structures in the tricellular space known as the diaphragms (Fig 1.5G) (Noirot-Timothée and Noirot, 1980). Although the TCJ is essential to SJ maturation and permeability formation, mechanisms that facilitate TCJ formation and interactions are not well understood (Byri et al., 2015; Harden et al., 2016; Sharifkhodaei et al., 2019).

1.4.3 Proteins in the Tricellular junction of *Drosophila*

To date, only three core TCJ proteins have been described: Gliotactin, M6, and Barkbeetle (also known as Anakonda) (Fig 1.5 C).

Gliotactin (Gli), the first TCJ protein described, is expressed in a wide range of epithelia and in the glia (Auld et al., 1995; Schulte et al., 2003). Gli is a protein in Neuroligin family, and its closest vertebrate homologue is Neuroligin 3 (Gilbert and Auld, 2005). Gli has one transmembrane and one enzymatic inactive extracellular Choline-esterase domain. Intracellularly, Gli contains two conserved tyrosine phosphorylation sites at aa 766 and 790, and a conserved PDZ binding motif (Gilbert and Auld, 2005; Gilbert et al., 2001). Gli associates with Dlg in a complex and concentrates at the TCJ, although this interaction may be independent of

the PDZ-binding motif which does not bind Dlg nor facilitate Gli localization to the TCJ (Schulte et al., 2006a). The localization of Gli is restricted by SJ components and TCJ proteins as discussed below. Loss of Gli is lethal as the SJ septa uncompact and spread the SJ domain basolaterally, causing disruption in the TCJ. This results in leaky paracellular and blood-brain-barriers respectively (Auld et al., 1995; Schulte et al., 2003).

Barkbeetle (Bark), also known as Anakonda (Aka), is a transmembrane protein with a large extracellular triple-repeat domain. Intracellularly, it also contains a PDZ-binding motif at the C terminus. Bark expression is essential for TCJ formation. The loss of Bark causes delocalization of Gli from the TCJ and spreading of core SJ proteins like NrxIV and Nrg basolaterally. This disrupts TCJ and barrier formation (Byri et al., 2015; Hildebrandt et al., 2015). It is thought that the tripartite structure of the extracellular domain of Bark creates the diaphragms in the central canal and recruits Gliotactin to limit SJ septa from the TCJ domain (Byri et al., 2015). This model is similar to the model of tTJ formation in the vertebrate system, where Angulin forms the central element while tricellulin limits the TJ strands (Fig 1.5 F, G).

M6, a glycoprotein belonging to the myelin proteolipid protein (PLP) family, is the most recently described TCJ protein. PLP proteins contain four transmembrane domains and are widely conserved from insects to mammals. The *Drosophila M6* gene and M6 protein are predicted to share a high degree of similarity with mouse M6a, and they might be functionally conserved (Zappia et al., 2011). M6 is necessary for the localization of both Bark and Gli at the TCJ. In the absence of M6, Bark and Gli do not accumulate at the TCJ(Wittek et al., 2020). Similarly, M6 and Gli are mislocalized in the loss of Bark. Taken together, M6 and Bark localize in a mutually dependent manner and act upstream of Gli to accumulate Gli at the TCJ, whereas

Gli functions to stabilize Bark localization at the TCJ(Esmangart de Bournonville and Le Borgne, 2020; Wittek et al., 2020).

It was recently described that the expression of the core SJ proteins and TCJ proteins are essential to prevent the spread of each other basolaterally (Sharifkhodaei et al., 2019). In the loss of these TCJ proteins, long membrane deformations in the interphase of SJ are observed, while core SJ proteins NrxIV and Cora are reduced from the tricellular vertices. On the other hand, the loss of Cora or NrxIV causes the spreading of core TCJ proteins Gli and Bark basolaterally (Esmangart de Bournonville and Le Borgne, 2020; Sharifkhodaei et al., 2019). It is proposed the TCJ act as pillars to anchor the SJ whereas the SJ components restrict the localization of Bark and Gli to the vertices to maintain tissue integrity (Esmangart de Bournonville and Le Borgne, 2020). The understanding the role of TCJ protein other than permeability barrier regulation is limited as well. Recent findings suggest TCJ proteins also engage in other cellular processes for homeostasis and cell organization. For instance, Gli regulates microtubule pulling force and spindle orientation, and intestinal stem cell proliferation (Bosveld et al., 2016; Resnik-Docampo et al., 2017). Overall, gaining a better understanding of TCJ protein function elucidates the formation of junctions, and other important cellular processes.

1.4.4 Scaffolding proteins of the *Drosophila* tricellular SJ

Similar to other cellular junctions, there are a number of scaffolding proteins necessary for TCJ formation, and these proteins are Dlg and Scrib. Dlg, and Scrib are expressed at the SJ and concentrate particularly at the TCJ. At the TCJ, Scrib, Dlg, Bark and Gli closely associate in a mutually dependent complex, and the loss of either Scrib or Dlg disrupts the integrity of this complex (Padash-Barmchi et al., 2013; Schulte et al., 2006a; Sharifkhodaei et al., 2019). The loss of Scrib or Dlg from the TCJ (but not the SJ) lead to the loss of Bark, Gli, and Scrib or Dlg

from the TCJ. Furthermore, the loss of Gli changes the proximity between Bark and Scrib, and Bark and Dlg. These interactions are mediated by the GUK domain of Dlg and PDZ1-2 domains of Scrib (Sharifkhodaei et al., 2019). However, it is not determined whether these are direct or indirect interactions. Overall, these observations suggest that Scrib and Dlg recruit Bark and Gli to the TCJ, and that this complex is mutually dependent for stability at the corners of polarized epithelia. However, the mechanism facilitating the recruitment of Dlg and Scrib to the TCJ is not well understood, and it is one of the main points of this thesis to identify whether a third scaffolding protein Gukholder fulfills this function at the *Drosophila* TCJ.

1.5 Gukholder

Gukholder (Gukh) is a strong candidate for mediating the interaction between Scrib and Dlg at the TCJ. Gukh has multiple roles as a scaffolding protein and contains an N-terminal WAVE homology domain (WHD), Nance Horan Syndrome(NHS) domain, and C-terminal Dlg-binding domain (Fig 1.4 C). The WHD is conserved among WAVE family proteins where WASP and WAVE proteins facilitate the activation Arp2/3 complex for rapid actin assembly. The WHD is critical for direct interaction with HSPC300 and proteins of the Abl interactor (Abi) family, forming the WAVE complex (Bompard and Caron, 2004; Kurisu and Takenawa, 2009). The NHS domain (pfam 15273) is a predicted domain that is highly conserved among Nance Horan Syndrome homologs such as Gukh and mammalian Nance Horan Syndrome proteins. The function of this domain has not been investigated. There are four predicted isoforms of Gukh. While all four predicted *gukh* isoforms contain the WHD, not all isoforms have been verified *in vivo*. Among the four predicted isoforms of Gukh, two of which contain a C-terminal PDZ-binding motif, *gukh-A* and *gukh-C*, the latter is also known as *gukh-L* (Mathew et al., 2002). The highly conserved NHS domain is only found in *gukh-E* and *gukh-A*.

Although the interactions involving this PDZ-binding motif have yet to be investigated, Gukh is known to interact with Dlg in a number of developmental processes. For instance, Gukh is an essential spindle orientation factor in asymmetric cell division of neuroblasts where Gukh binds to the Dlg GUK domain to facilitate the association of Dlg with microtubules (Golub et al., 2017; Qian and Prehoda, 2006). At the *Drosophila* neuromuscular junctions (NMJ), Gukh binds to the GUK domain of Dlg and in turn recruits Scrib to the NMJ. This interaction is mediated by the C-terminal end of Gukh-C (Gukh-L) which does not include the NHS domain (Mathew et al., 2002). Gukh has been identified in both wing and eye imaginal discs (Caria et al., 2018). Gukh plays a role in eye development where the loss of Gukh enhances the small eye phenotype of Scrib and Dlg loss of function (Caria et al., 2018). Gukh mediates the termination of photoreceptors at the optic lobe (Berger et al., 2008). However, the distribution and role of Gukh in polarized epithelia and with respect to the cellular junctions have yet to be examined.

1.5.1 Nance Horan Syndrome (NHS), the vertebrate homolog of Gukholder

Gukh is homologous to the vertebrate protein Nance Horan Syndrome (NHS) (Caria et al., 2018; Katoh and Katoh, 2004) with 30% identity and 63% similarity between *Drosophila* Gukh and human NHS (Fig 1.5 C). Members of this protein family contain a predicted N-terminal WAVE homology domain (WHD) and a C-terminal Nance Horan Syndrome (NHS) domain (Brooks et al., 2010; Mathew et al., 2002). Inherited mutations, mostly missense and small deletions, in NHS cause X-linked eye defects in humans, namely severe congenital cataracts, but also result in distinctive dental anomalies and dysmorphic features (Bixler et al., 2008; Tian et al., 2017). 20 to 30% of the affected males exhibit some levels of intellectual disability (Burdon et al., 2003). Female carriers may experience slight vision impairment (Bixler et al., 2008; Tian et al., 2017). Limited genetic studies have been performed to explain the

pathogenicity of NHS, or the phenotypic heterogeneity observed amongst individuals sharing the same pathogenic variation.

NHS is predicted to have four alternative transcription start sites, and at least five isoforms (Fig 1.6) (Brooks et al., 2010). NHS is expressed broadly including the ocular lens, CNS, epidermis, and kidney (Burdon et al., 2003). Previous studies have shown the causative mutations likely affect the expression of the isoforms which contain exon 1, where WAVE homology domain is encoded. The isoforms of interest are isoforms NHS-1A and NHS-A (Brooks et al., 2010). Premature mutation affects the localization of NHS-A proteins from localizing to the cell contacts. (Sharma et al., 2006, 2008). Though NHS is expressed at tight junctions in MDCK cells (Sharma et al., 2006) and may be concentrated at tTJ (Sharma et al., 2009), the knockdown of NHS did not affect ZO-1 localization *in vitro* (Brooks et al., 2010). The role of NHS in junction formation and cell adhesion processes has not been investigated *in vivo*. Given that little is known about the function of NHS in any cell type, the investigation into the function of Gukh may provide valuable insight into the pathogenesis of NHS.

The NHS WAVE homology domain (WHD) is required for Arp 2/3 localization at cell borders in MTLn3 cells for actin remodelling (Brooks et al., 2010). The Gukh homolog NHS-like-1b genetically interacts with Scrib for proper branchiomotor neuron migration in Zebrafish (Walsh et al., 2011). However, the direct interaction between NHS and the Arp 2/3 complex or Scrib has not been shown, and the role of NHS or Gukh in the formation of intercellular junctions in polarized epithelia has not been determined *in vivo*. It is the aim of this thesis to investigate the *in vivo* function of Gukh in polarized epithelia.

1.6 *Drosophila* as a model system to study cell adhesion

Drosophila melanogaster is a classic model organism ideal for the study of cellular junction formation and development due to its well-studied genome, well-established genetic approaches, and rapid generation times. In this thesis, the model tissue to investigate Gukh function is the developing wing epithelia (wing imaginal disc) in the 3rd instar larvae of *Drosophila*. Imaginal discs are undifferentiated hollow sacs of cells, which differentiate into adult structures during metamorphosis. The wing disc has two different cell layers, the peripodial (squamous) epithelia and the columnar epithelia. While both cell layers contain SJs and TCJs basal to AJs, this study focuses on the columnar epithelia. There are three axes in the 3rd instar wing disc. The dorsal/ventral axis is defined by a stripe of *wingless* expression and by expression of *apterous(ap)* solely in the dorsal compartment, forming the boundary cell lineage (Wolpert, 2003 ,Weihe et al., 2001). In this study, we used the GAL4/UAS gene expression system to drive expression of transgenes in discrete regions of the wing epithelia. (Fig 1.7 B) (Brand and Perrimon, 1993). The promoter of *apterous* is used to drive tissue-specific expression of GAL4 in the dorsal side of the wing disc (Fig 1.7 A). Overall, by using this system we can knockdown or express genes of interest on one side of the wing disc and use the ventral wing disc to serve as the internal control to assess changes to epithelial morphology, junctional integrity and cell survival.

1.7 Hypothesis and Overview

In the *Drosophila* neuromuscular junctions (NMJ) and neuroblasts, Gukh binds to scaffolding protein Dlg to facilitate interaction with Scrib and microtubules respectively (Caria et al., 2018; Golub et al., 2017; Mathew et al., 2002). The interaction between Gukh-Dlg has not been investigated in other cellular junctions. As Dlg and Scrib mediate the localization of TCJ

proteins, I hypothesize that Gukh localizes at TCJs, and that Gukh is a TCJ protein necessary for the recruitment of Scrib along with Dlg to the TCJ.

With immunohistochemistry, I determined the localization of Gukh in the *Drosophila* wing disc. Using RNAi-mediated knockdown and immunohistochemistry, I tested the effect of Gukh, TCJ proteins, and β-integrin knockdowns on Gukh localization. In the knockdown of Gukh, I assessed the change in localization of TCJ proteins and β-integrin, as well as cellular phenotypes.

My results determined that Gukh is localized at the TCJ but does not play a role in TCJ formation. Rather, I found that Gukh localization to the TCJ depends on TCJ proteins. I found Gukh is concentrated in the basal domain flanking the focal adhesions, and that integrin plays a role in recruiting Gukh to this domain (but not vice versa). Gukh is also found in the lateral/intermediate domain and is co-dependently associated with the integrin complex in this region. Loss of Gukh results in a reduction of integrin in this region. Finally, I found that knockdown of Gukh caused dramatic cellular phenotypes including cell delamination, apoptosis, and compensatory proliferation.

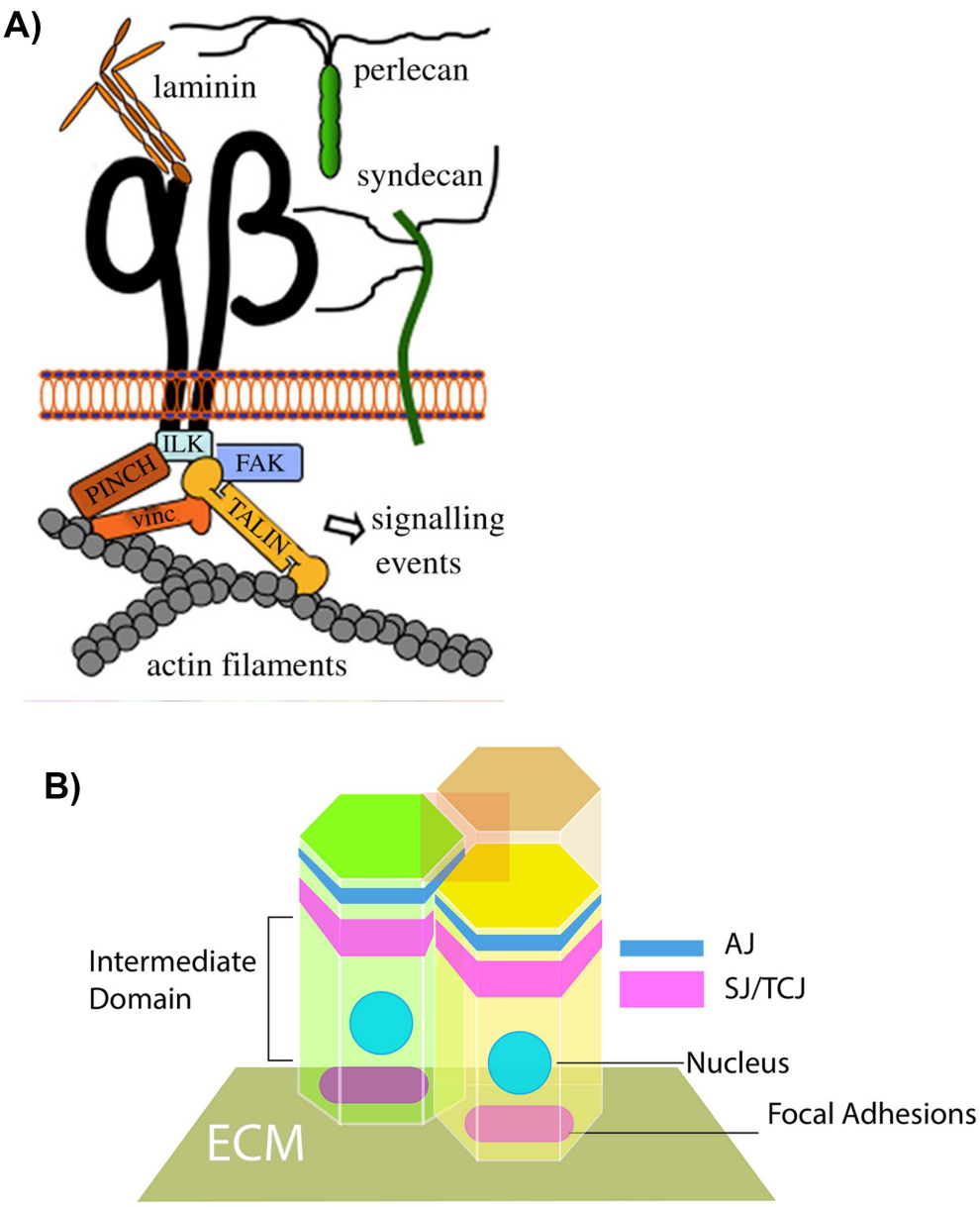

Figure 1.1 The focal adhesion complex is found at the basal side in the wing imaginal disc.
A) Schematic of integrin and integrin-associated components at the focal adhesion complex. Integrin subunits (α and β chain, black) form heterodimers and interact with integrin-linked kinase (ILK, teal), focal adhesion kinase (FAK, blue), vinculin (vinc, orange), and talin (yellow). (Adapted from Thuveson et al., 2019).
B) The focal adhesion complex is found most basally in the wing imaginal disc. The adherens junction (AJ) is most apical followed by the septate junction/tricellular junction (SJ/TCJ) domain.

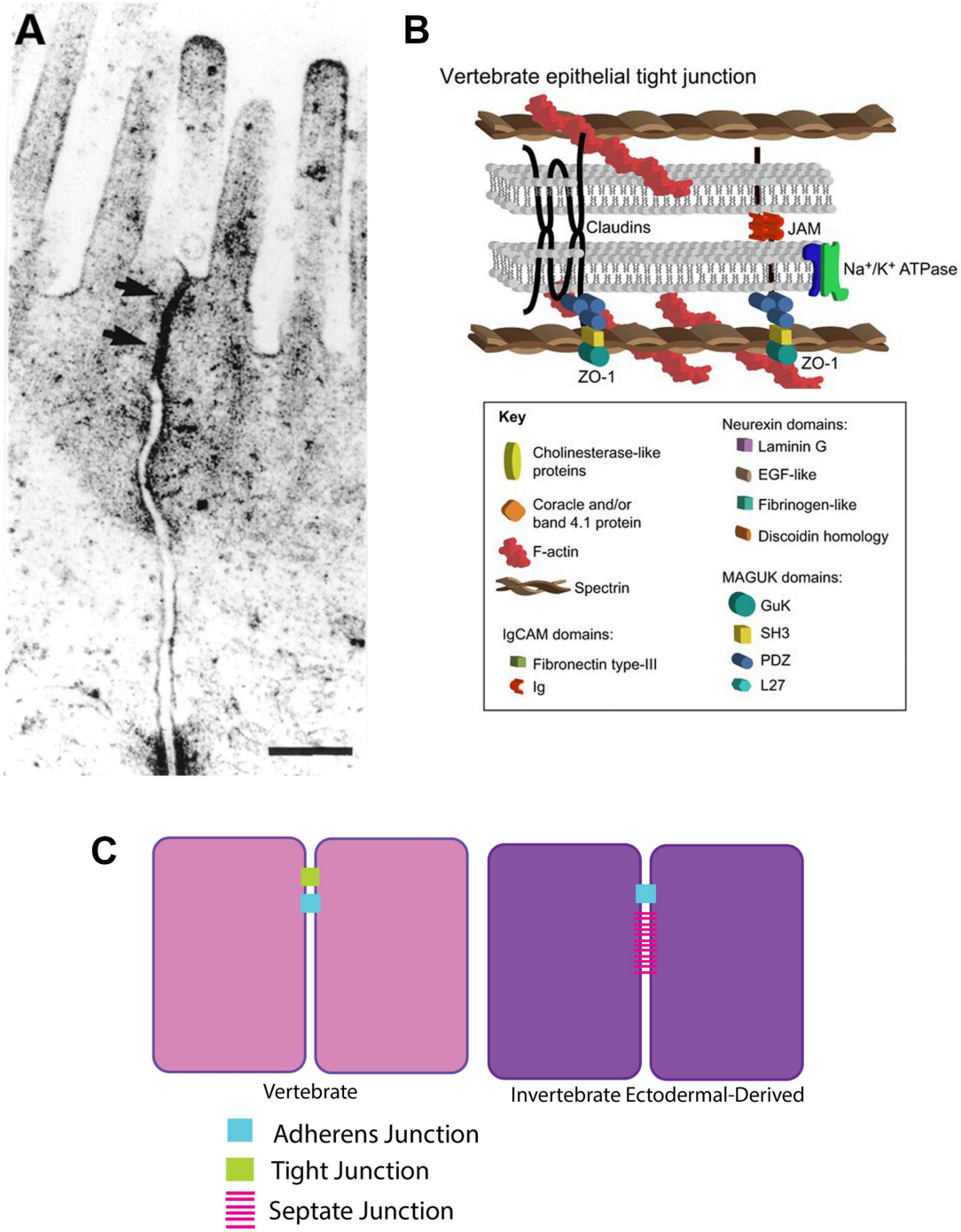

Figure 1.2 The structure and components of the tight junction.
A) TEM of a tight junction (black arrows) in ileal enterocytes. Reproduced with permission (Soderholm, 2002).
B) Components of the tight junction. Adapted from (Harden et al., 2016)
C) The adherens junction (AJ) is found basal to the occluding tight junction (TJ) in vertebrates and apical to the occluding septate junction (SJ) in invertebrates.

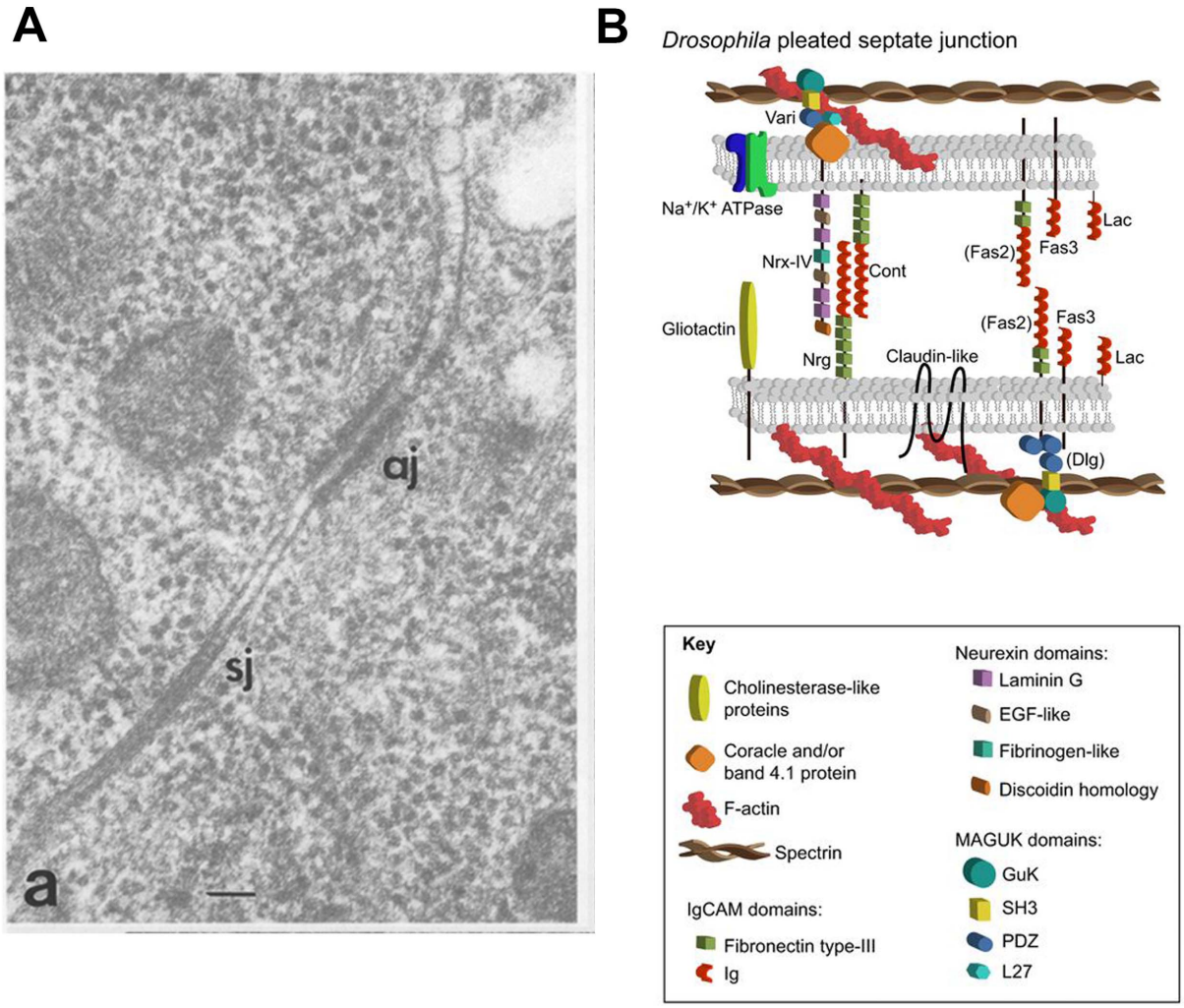

Figure 1.3 The structure and components of the septate junction (SJ).
A) TEM of the SJ. The SJ is found basal to the adherens junction (AJ) (Woods et al., 1996).
B) Some proteins of the septate junction are similar to those in the tight junction such as claudin and claudin-like proteins(Harden et al., 2016). ZO-1 and Dlg are MAGUK proteins found in the TJ and SJ respectively.

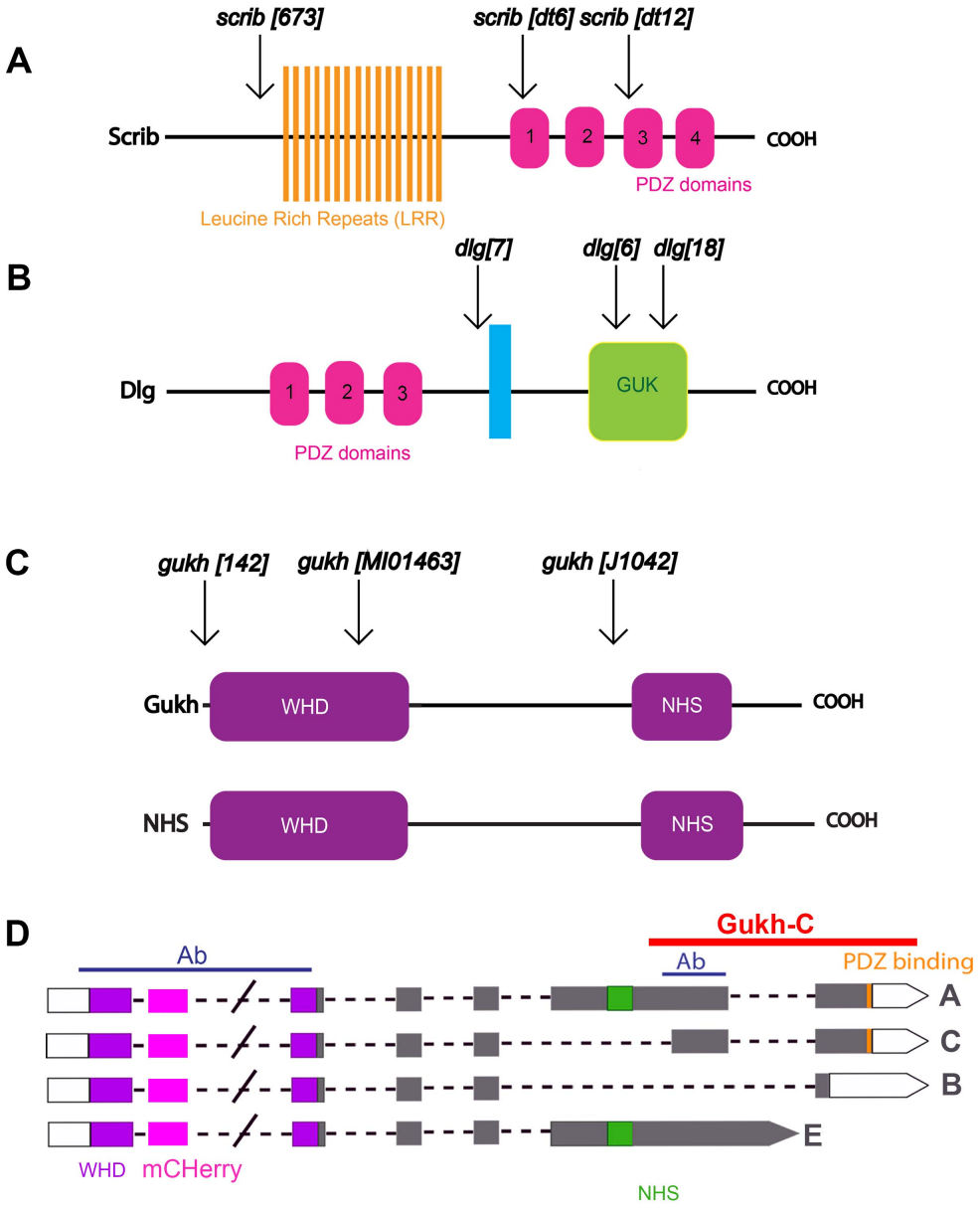

Figure 1.4 Schematic of Discs large, Scribble and Gukholder. Not drawn to scale.
A) Scrib has sixteen leucine-rich repeats (LRR) and four PDZ domains
B) Dlg has three PDZ domain, a SH3 domain and a GUK domain,
C) Gukh and Nance Horan Syndrome both contain a 5' WAVE homology domain (WHD) and a 3' NHS domain. WHD and NHS share ~30% identity and 63 % similarity.
D) Gukh has four predicted isoforms. Predicted isoforms A and C have a C-terminal PDZ binding motif. The Gukh-C terminal domain (red line) facilitates Dlg and Scrib interaction through Dlg GUK domain and Scrib PDZ2 domain. Isoform C, also known as isoform L, has been shown (Mathew et al., 2002)

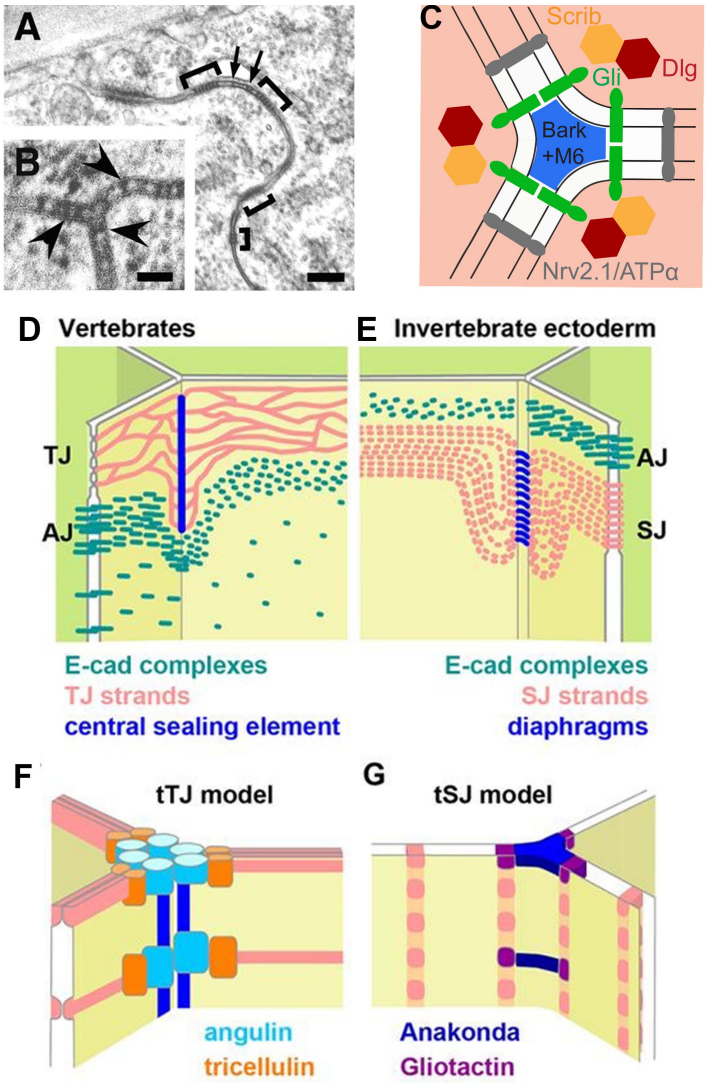

Figure 1.5 The structure and components of the tricellular septate junction (TCJ) and the vertebrate tricellular tight junction (tTJ).

TEM of stage 17 embryos epidermis shows A) the septa of pleated septate junction (arrows) and B) the septa are present at the bicellular contacts around the tricellular junction (Schulte et al., 2003)

C) Scrib and Dlg recruit Bark and Gli to the TCJ. M6 and Bark localize to the TCJ in a mutually dependent manner, and recruit Gli.

D-G) The vertebrate tricellular tight and the tricellular septate junction share organizational similarities (adapted from Higashi & Miller, 2017).

D) The vertebrate tricellular tight junction contains a central sealing element while E) the invertebrate tricellular septate junction seals the tricellular space with diaphragms. Both junctions are found the contact point of three neighbouring cells and are the sites where occluding junction strands intersect with the tricellular contacts perpendicularly.

F) In vertebrates, Angulin forms the central sealing element and Tricellulin interact with the TJ strands.

G) In *Drosophila*, Bark/Aka forms diaphragms to seal the paracellular space and recruits Gli to the TCJ to limit the SJ strands from the TCJ domain.

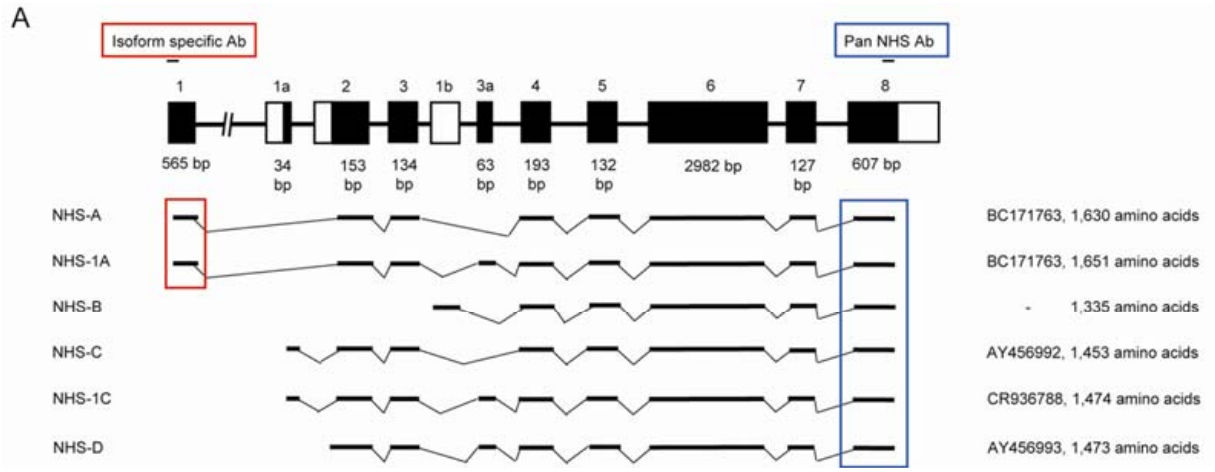

Figure 1.6 Genomic structure of the NHS gene with predicted isoforms.

A) There are four predicted start sites and the accession numbers and predicted number of amino acids for each isoform are given on the right. Of interest, NHS-A and NHS-1A include exon 1 which has been implicated in NHS (adapted from Brooks et al., 2010).

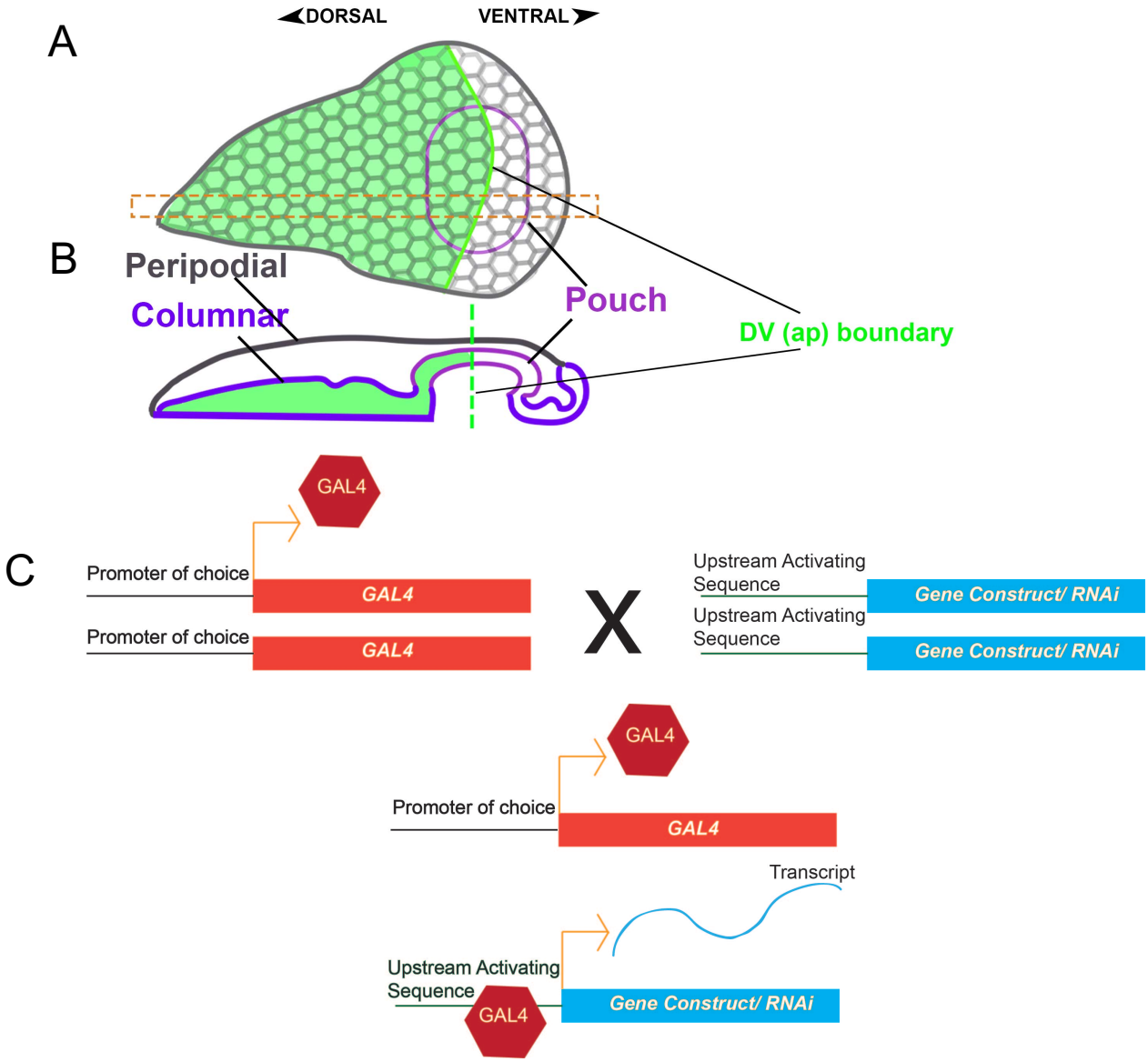

Figure 1.7 the GAL4 UAS system in the wing imaginal disc
A) Schematic of the wing imaginal disc en-face. Apterous-GAL4 is expressed on the dorsal side of the columnar epithelia in the wing disc (green cells) as such the ventral side of the wing disc serves as an internal control. The dorsoventral boundaries are marked by the green lines.

B) Schematic of a cross-section of the wing disc along the anterior-posterior axis as indicated by the orange box in A). The wing imaginal discs is formed by two layers of epithelia, the peripodial (squamosal) and columnar epithelia. Cells expressing *ap-GAL4* are indicated by the green cells.

C) The GAL4/UAS system. GAL4 is a yeast transcription factor that binds to the upstream activating sequence (UAS) upstream of the construct of interest.

CHAPTER 2: Gukholder is not necessary for tricellular junction formation but mediates the localization of integrin to the developing wing epithelia

2.1 Introduction

Cell adhesion is essential for establishing and resolving cell contacts during tissue development and tissue maintenance in multicellular organisms. During development, cell adhesion facilitates epithelial remodelling through cell shape changes, cell migration and signal transduction for adhesion of cells to the extracellular matrix (cell-ECM) are the two modules of adhesion. In polarized epithelia, cell-cell adhesion is mediated by intercellular junctions such as the adherens junctions (AJs), septate junctions (SJs) in insects, or tight junctions (TJs) in vertebrates and cell-ECM adhesion is mediated by the basal integrin, focal adhesion complex (FAC). Another set of junctions that form in polarized epithelia at the corners of cells are the tricellular tight or septate junctions. The tricellular tight or septate junction is created at the convergence of three TJs or SJs and play keys roles in maintaining epithelial barrier integrity (Harden et al., 2016; Higashi and Miller, 2017).

Scaffolding proteins play important roles in mediating junction formation and the membrane associate guanylate kinase (MAGUK) proteins play critical and conserved roles in multiple junctions. MAGUK proteins are characterized by PDZ, SH3, and GUK domains (González-Mariscal et al., 2000; reviewed in Harden et al., 2016). Discs large 1 (Dlg) and ZO-1 are representative MAGUK proteins in the septate junctions (SJ) and tight junctions (TJs) respectively (Hough et al., 1997; Stevenson et al. 1986; D. F. Woods et al., 1996; Daniel F. Woods & Bryant, 1991). Dlg is also a key component of the tricellular septate junction (Schulte et al., 2003, 2006b; Sharifkhodaei et al., 2019). Dlg along with another scaffolding protein Scribble (Scrib), an LRR PDZ domain protein, are key to recruiting the transmembrane proteins Anakonda/Bark Beetle and Gliotactin to the TCJ (Sharifkhodaei et al., 2019). Anakonda/Bark is

thought to create the diaphragms that fill the extracellular space of the TCJ (Byri et al., 2015) and Gliotactin is thought to link the TCJ to the neighbouring SJs (Schulte et al., 2003; Sharifkhodaei et al., 2019. While it clear that Dlg and Scrib play a critical role at the TCJ it is unclear how these proteins interact and are recruited to the TCJ.

Gukholder (Gukh) is a strong candidate for mediating the interaction between Scrib and Dlg at the TCJ. Gukh has multiple roles as a scaffolding protein. For instance, Gukh is an essential spindle orientation factor in asymmetric cell division of neuroblasts. Following phosphorylation of Dlg by aPKC, Gukh binds to the Dlg GUK domain to facilitate the association of Dlg with microtubules (Golub et al., 2017; Qian and Prehoda, 2006). At the *Drosophila* neuromuscular junctions (NMJ), Gukh C-terminal Dlg-binding domain binds to the GUK domain of Dlg and in turn recruits Scrib to the NMJ (Mathew et al., 2002). While the interaction at the NMJ is mediated by the PDZ2 of Scrib, *in vitro* finding suggest that both PDZ1 and PDZ2 are capable of binding to Gukh (Caria et al., 2018). Furthermore, it is unknown whether the PDZ-binding motif of Gukh found in two of the four predicted isoforms engages in PDZ interactions. Gukh has been identified in both wing and eye imaginal discs (Caria et al., 2018). Gukh plays a role in eye development where the loss of Gukh enhances the small eye phenotype of Scrib and Dlg loss of function (Caria et al., 2018). However, the distribution and role of Gukh in polarized epithelia have yet to be examined.

Gukh is homologous to the vertebrate protein Nance Horan Syndrome (NHS) (Caria et al., 2018; Katoh and Katoh, 2004) with 30% identity and 67% similarity between *Drosophila* Gukh and human NHS. Members of this protein family contain a predicted N-terminal WAVE homology domain (WHD) and a C-terminal Nance Horan Syndrome (NHS) domain (Brooks et al., 2010; Mathew et al., 2002). Inherited mutations in NHS cause X-linked eye defects namely

severe congenital cataracts but also result in distinctive dental anomalies, and dysmorphic features, and mental retardation (Bixler et al., 2008; Tian et al., 2017). Little is known about the function of NHS in any cell type, though NHS is expressed at tight junctions in MDCK cells (Sharma et al., 2006) and maybe concentrated at tricellular TJs (Sharma et al., 2009). The NHS WAVE homology domain is required for Arp 2/3 localization at cell borders in MTLn3 cells for actin remodelling (Brooks et al., 2010). However, the role of NHS or Gukh in the formation of intercellular junctions in polarized epithelia has not been determined.

We investigated the distribution and function of Gukh in the polarized epithelia of the *Drosophila* wing imaginal disc. We determined that Gukh is expressed in three distinct regions of the columnar epithelia. Gukh is localized along with Dlg and Scrib at the TCJ and is recruited to this junction by the TCJ proteins. Gukh is concentrated in the basal domain flanking the focal adhesion complex and is recruited to the basal domain by the beta subunit of integrin (β-integrin). Finally, Gukh is concentrated in the intermediate/lateral domain and co-localizes with β-integrin and talin and the knockdown of Gukh altered the distribution of β-integrin in the intermediate/lateral domain and vice versa. Overall knockdown of Gukh resulted in disruption of the epithelia with extensive JNK-mediated apoptosis, cell delamination, and compensatory proliferation. Our findings suggest that Gukh is recruited to distinct junctional domains in the wing imaginal disc by two independent processes, and Gukh mediates localization of β-integrin to the lateral domain of columnar epithelia.

2.2 Materials and Methods

2.2.1Fly stocks and crosses

The following *Drosophila* stocks were obtained from the Vienna *Drosophila* RNAi Center (VDRC): UAS-Bark-RNAi (v52608, v1077348), UAS-Dlg-RNAi (v44134,v44136),

UAS-Scrib-RNAi (v105414), UAS-NrxIV (v8353,v108128), UAS-Cora-RNAi (v9787,9788), UAS-Nrv2-RNAi (v2660), UAS-Mcr-RNAi (v2785,v100197), UAS-Gli-RNAi (v107258, v37115) UAS-Gukh-RNAi (v330523). The following *Drosophila* stocks were obtained from the Bloomington *Drosophila* Stock Center (BDRC): Df (3R) Exel6182 (BI:7661) gukh[J1024], Gukh-RNAi (BI:42486, 55858), ap-GAL4 (BI: 3041), UAS-mCD8GFP (BI: 5130), UAS-Bsk.DN (BI: 6409), Scrib::GFP (BI:59082), rhea::mCherry (BI:39648). *Bark[L200*], Bark::GFP (Byri et al. 2015); UAS-Gukh full length and UAS-Gukh-Cter (Mathew et al., 2002) were obtained from cited researchers. UAS-NLS-GFP was a gift from Dr. Douglas Allan. Gukh::mCherry was generated by MiMIC cassette exchange at *gukh [MI01463] by* Genetivision (Nagarkar-Jaiswal et al., 2015; Venken et al., 2011).

To avoid early lethality, RNAi, crosses with ap-GAL4; Gukh::mCherry were performed at 18°C for 48 hours before transferring to 29°C, with the exception of Gukh-RNAi. ap-GAL4; Gukh::mCherry was crossed with Gukh-RNAi at 18°C for 72 hours before transferring to 29°C. All other RNAi crosses were performed at 29°C. ap-GAL4; Gukh::mCherry crossed to *w[1118]* was the control except where specified. Cellular phenotypes were verified across two RNAis. To test for complementarity the Gukh::mCherry line was crossed to *gukh*[*J1024*] or Df(3R)Exel6182 and percentage of adult progeny was determined

2.2.2 Immunofluorescence labelling

Third instar larvae were dissected and inverted inside-out in 1XPBS and fixed with 4% paraformaldehyde for 15-20 minutes. Inverted head samples were washed in PBST (PBS +0.1% TritonX-100) and blocked in PBS + 2% normal goat serum (block solution) overnight at 4 °C. Primary antibodies and secondary antibodies were incubated in block solution overnight and for

two hours respectively. 3 × 20 min room temperature washes with PBST were performed following antibody incubations. Vectashield (Vector Labs) was used to clear samples overnight before discs were fine-dissected and mounted. The following cited antibodies were used at the stated dilutions: mouse anti-Gli IF6.3 (1:50) (Auld et al. 1995), rabbit anti-Gli (1:500) (Sharifkhodaei et al., 2019), rabbit anti-Gukh-N (1:300) and anti-Gukh-C (1:500)(Mathew et al., 2002), rat anti-Mcr (1:300) (Hall et al., 2014). The following commercially available antibodies were used: rabbit anti-Nrv2 (1:500; Sigma-Aldrich), rabbit anti-phosphoHistone3 (1:300; Novus Biologicals, CA), chicken anti-mCherry (1:500 ; Abcam), rabbit anti-GFP (1:300; Life Technologies), rat anti-tubulin (1:50; Millipore), rabbit anti-Dcp-1 (1:500; Cell Signaling Technology). The following antibodies were obtained from the Developmental Studies Hybridoma Bank (DSHB): mouse anti-Dlg 4F3 (1:200; Parnas et al.,2001); mouse anti- *β*PS (1:10; D. L. Brower et al., 1984); rat anti-DE-Cadherin (1:50;Oda et al., 1994). The following secondary antibodies (abcam) were used at 1:300, goat anti-rabbit (Alexa Fluor 488, 568 or 647), goat anti-mouse (Alexa Fluor 488 or 647), goat anti-chicken (Alexa Fluor 568 or 647), goat anti-rat (Alexa Fluor 488 or 647).

2.2.3 Imaging

CoolSnap HQ digital camera captured 0.2 µm step z-stacks using a DeltaVision Spectris microscope (Applied Precision, Cytiva) with either a 60× oil-immersion lens (NA 1.4) or 20x air lens (0.4NA). SoftWorx 690 (Applied Precision) software version 6.1.3 was applied to create side projections and deconvolve 60× z-stacks using a point spread function generated from a 0.2 µm bead conjugated with Alexa Fluor 568 (Molecular Probes) mounted in Vectashield (Vector

Labs). Tiff files were imported and compiled into figures with Photoshop CS and Illustrator CS (Adobe Creative Suite).

2.2.4 Data and statistical analysis

ImageJ was utilized to process side projections with four channels and to measure intensities along a line in the XY plane for intensity profiling. The intensity of a given channel was measured relative to the signal and was not corrected for background. Intensities measured were graphed by Excel (Microsoft Office 365). The line tool in ImageJ was used to measure the distance of spread of GFP-marked delaminated cells into the ventral half of the wing disc compared to the overall distance of the ventral half. To quantify for the reduction of β-integrin in Bsk-DN; Gukh-RNAi, the mean intensity of β-integrin at the intermediate domain was measured on the dorsal and ventral side of the disc in ImageJ across the consistent 400 px area. The ratio of dorsal/ventral intensity was compared against control discs with the student's T-test. Mean, SD, and statistical analyses of data sets were computed using Prism 6.0 (GraphPad). The ratio of distance travelled by GFP-positive cells over the length of the ventral side of the disc was determined with one-way ANOVA with Tukey post-hoc comparison. As a measure of mitosis using ImageJ the number of phosphoHistone3 positive cells were counted in a constant sized region of interest from the apterous and non-apterous side and plotted as a ratio. The student's T-test was performed to compare the ratio of mitotic cells on the dorsal (experiemanl) and the ventral (control) side of the wing disc. In all graphs the SD is indicated and the P values are represented as: * $p<0.05$; ** $p<0.01$; *** $p<0.001$; **** $p<0.0001$. n = the number of wing imaginal discs quantified.

2.3 Results

2.3.1 Gukh distributes across adhesion domains in the wing imaginal disc

To assess the distribution of Gukh we made use of a Gukh protein endogenously tagged with mCherry (Supplemental Fig. 2.1A). We used a recombinase-mediated cassette exchange (RMCE) to insert the mCherry tag into *gukh [MI01463]* at a Minos cassette (MiMIC) site (Venken et al., 2011). The site of insertion is at the first intron creating cherry insertion that flanks the predicted WAVE homology domain (WHD) at the N-terminus end (Supplemental Fig. 2.1A). This insertion does not disrupt function as the line is homozygous viable and complements *gukh* alleles *gukh [J1024]* (100% of expected), and a deficiency Df(3R)Exel6182 (33% of expected). Using Gukh::mCherry, we investigated the localization of Gukh in the columnar epithelia of 3rd instar wing imaginal disc. We used E-Cadherin (Ecad) and beta-integrin (βPS) to mark the apical adherens junctions and the basal focal adhesion complexes respectively. Gukh localized at the apical domain, immediately basal to the AJs (Fig 2.1A). At the intermediate domain that forms the lateral side of the epithelia between the SJ and basal integrin-complex, we found that puncta of Gukh and β-integrin co-localize in puncta distributed around the cell periphery (Fig. 2.1B,C; yellow arrows). On the most basal side of the epithelium, Gukh was concentrated in puncta that flanked but did not co-localize with β-integrin labeled focal adhesions (Brown et al., 2002) (Fig. 2.1D,E magenta arrows). This distribution is more apparent in the side projections (Fig. 2.1F) with Gukh strongly localized immediately basal to Ecad localization (Fig 1F'; magenta arrow), likely within the SJ, and at the level of the integrin complex (Fig 1F', F'''; yellow arrow). We tested Gukh distribution at the SJ (Fig. 2.1G) and found Gukh co-localizes with the SJ markers Scrib and Dlg (Fig 1G'; magenta arrow). We verified the localization of Gukh::mCherry with antibodies raised against the N-terminal and C-

terminal region (Supplemental Fig. 2.1A) and the distribution of Gukh::mCh was consistent with both antibodies (Supplemental Fig1. C-I). Overall, we concluded that Gukh was associated with multiple levels of the epithelium and localized to a range of junctional domains.

Gukh has been identified as a microtubule associate protein and plays a role in spindle orientation in neuroblast asymmetric cell division (Golub et al., 2017; Qian and Prehoda, 2006). Consistent with an association with microtubules, we observed Gukh co-localized with the mitotic spindle in dividing wing disc epithelia (Supplemental Fig. 2.2C; yellow arrows). However Gukh was not associated with microtubules in interphase cells including the overlay squamous peripodial cells (Supplemental Fig. 2.2A), the apical microtubule cap in the columnar epithelia (Supplemental Fig. 2.2B) or the microtubules in the intermediate and basal domains (Supplemental Fig. 2.2D, E). In the intermediate domain, the Gukh puncta were found adjacent to the microtubules that span the epithelia from apical to basal in this region (Supplemental Fig. 2.2D'; yellow arrows).

We wondered if Gukh is also found in junctional domains in other larval tissues beyond the previously identified expression at the larval NMJ. In other tissues, Gukh is coexpressed with Scrib in photoreceptors (Supplemental Fig. 2.3A; yellow arrows) and the surrounding support cells (Supplemental Fig. 2.3A; magenta arrows). In the squamous peripodial layer of the imaginal discs, Gukh was localized to the SJ (Supplemental Fig. 2.3B; magenta arrows) but not concentrated at the TCJ with Gliotactin (Supplemental Fig. 2.3B; yellow arrows) but was localized with Gliotactin and Dlg in the salivary gland (Supplemental Fig. 2.3C; yellow arrows). In the trachea, Gukh was distributed along the SJ offset from Dlg (Supplemental Fig. 2.3D; yellow arrows) at the dorsal truck junction, but not at the tracheal TCJ (Supplemental Fig. 2.3E; yellow arrows). Weak Gukh localization was observed around Dlg at the bicellular SJ domain

(Supplemental Fig. 2.3E', E'''; magenta arrows). Overall our observations suggest that Gukh is expressed in many tissues with a consistent association with SJ proteins.

2.3.2 Gukh co-localizes with TCJ proteins

Overall Gukh strongly associated with the SJ domain and appeared to be concentrated at the cell corners in the columnar epithelia. To further investigate the distribution of Gukh at the SJ and the TCJ, we immunolabeled with the TCJ proteins Bark, Gli, Dlg and Scrib in conjunction with Gukh::mCh. We found that Gukh was coexpressed with Scrib and Dlg at the SJ and concentrated with Scrib and Dlg at the TCJ (Fig. 2.2A,B; yellow arrows). Rather than a tight association at the SJ, we observed that Gukh appeared as a collection of puncta at the SJ, and was less concentrated at the TCJ than Scrib and Dlg. When the relative fluorescence intensity was sampled, Scrib, Dlg and Gukh intensities peaked at identical regions suggesting they were expressed in similar pattern (Fig 2E,E'; matching arrows). Similarly, Gukh co-localized with Gli and Bark::GFP at the TCJ (Fig 2C,D; yellow arrows) and the peaks of Gukh fluorescence coincided with the concentrations of Gli and Bark at the TCJ (Fig 2F; matching arrows). Intriguingly in the peripodial epithelia, a squamous epithelium covering the columnar epithelia of the wing disc, Gukh was expressed at the corner of cells but did not co-localize with the distinct concentrations of Gli (Supplemental Fig 3B). Taken together, our data showed that Gukh localizes to the TCJ and SJ in the columnar epithelia of the wing imaginal disc.

2.3.3 TCJ proteins and β-integrin recruit Gukh

To test the interaction between Gukh and the different junctional domains, we performed RNAi-mediated knockdowns using the apterous-Gal4 driver to knockdown expression in the dorsal side of the wing columnar epithelia such that the ventral side serves as the internal control. To test the recruitment of Gukh to the TCJ, we knocked down the core TCJ proteins, Bark and

Gli. As expected, Gli was lost from the TCJ in Bark-RNAi (Byri et al., 2015; Sharifkhodaei et al., 2019) (Fig. 2.3A",B",C"). Gukh was reduced and its recruitment to the SJ and TCJ was disrupted in Bark knockdown (Fig. 2.3A',B',C'). The relative intensity of Gukh became dispersed throughout the cells and appeared to distribute independent of Dlg expression (Fig. 2.3 B", C"). Since Dlg was mostly retained at the SJ (Fig. 2.3A", B", C"), this suggests the loss of Gukh was not due to changes in Dlg.

In Gli-RNAi (Supplemental Fig. 2.4A-C), Gli expression was lost from the TCJ (Supplemental Fig. 2.4A", B",C") and Gukh was no longer concentrated at the SJ or the TCJ (Supplemental Fig. 2.4A', B' C'). We observed that Gukh appeared occasionally associated with remnants of Gli at the TCJ in the knockdown of Gli or Bark (Supplemental Fig. 2.4B',B"; yellow arrows). The localization of Gukh in the intermediate and basal domains was unaffected in the knockdowns of Bark (Fig. 2.3C'; yellow arrow) or Gli (Supplemental Fig. 2.4C'; yellow arrow). Our findings suggest that Bark and Gli are both necessary to recruit Gukh to the SJ and TCJ.

To investigate how Gukh is recruited to the basal domain, we tested whether the integrin-complex plays a role in recruiting Gukh. We performed RNAi-mediated knockdown of myospheroid (mys) (Fig. 2.3D-G), the gene that encodes the β-integrin subunit. In the knockdown of mys, β-integrin was lost throughout the epithelium (Fig. 2.3D''',E''',F''',G'''), and tissue integrity was affected as expected (Dominguez-Gimenez et al., 2007). Loss of β-integrin resulted in the loss of Gukh from the intermediate (Fig. 2.3F) and basal domains (Fig. 2.3G) while the co-localization of Gukh with the SJ and TCJ was unaffected (Fig. 2.3D,H'; yellows arrows). This suggests that β-integrin is necessary for the recruitment of Gukh in the intermediate and basal domains only, and the recruitment of Gukh to the TCJ is independent of this interaction.

2.3.4 Scrib and Dlg recruit Gukh to the SJ and TCJ

As Scrib and Dlg form complexes at the neuromuscular junction (NMJ) and TCJ (Mathew et al., 2002; Sharifkhodaei et al., 2019), we wondered if their interaction is facilitated by Gukh at the TCJ. We first tested the effect of RNAi-mediated knockdown of Scrib on Gukh localization with ap-GAL4 in the dorsal side of the wing disc. To limit the disruption to epithelial polarity, we used temperature shifts (see Materials and Methods) to limit the time of Scrib knockdown and to reduce Scrib and Dlg localization from the SJs and most TCJs without disrupting polarity (Sharifkhodaei et al., 2019). We used Dlg and Gli immunolabeling to verify the degree of Scrib knockdown. Gukh was downregulated and diffused across the SJ and TCJ in Scrib-RNAi (Fig4A-D) as were Gli and Dlg as expected (Fig 4A-D). This was reflected by the decrease in the maximum relative intensity of Gukh across the dorsal wing epithelium (Fig 4D). We observed instances where Dlg was retained at the TCJ but lost in the SJ (Sharifkhodaei et al., 2019). In these cases, Gukh was not present at the SJ (Fig 4B; yellow arrows) but Gukh appeared associated with Dlg remnants. To confirm these findings, we then performed RNAi-mediated knockdown of Dlg. We observed that the loss of Dlg resulted in the disruption of Gukh localization to the SJ and TCJ (Fig. 2.4E-G). Similar to our observations in the Bark and Gli knockdowns, we noted the knockdown of Dlg and Scrib did not affect the localization of Gukh basally (Fig. 2.4C'G', G': yellow arrows; Supplemental Fig. 2.4 D, E). Overall, our findings suggest that the TCJ protein complex is required to recruit and stabilize Gukh at the TCJ and the SJ.

2.3.5 Gukh localizes to the TCJ independent of SJ proteins

To further investigate the relationship between the SJ and Gukh, we knocked down core SJ proteins, Macroglobulin Complement-Related protein (Mcr), Neurexin IV (Nrx IV) (Fig. 2.5),

and Coracle (Cora) (data not shown) with ap-GAL4. Mcr-RNAi led to loss of Mcr from the dorsal side of the wing disc and Gukh was downregulated from the level of the SJ (Fig 5B'). As expected, the loss of Mcr resulted in the basolateral spread of Gli (Sharifkhodaei et al., 2019) (Fig 5B''). Although the recruitment of Gukh to the SJ was reduced, Gukh was still localized at the TCJ (Fig. 2.5B'C'; yellow arrows) and retained the association with Gli (Fig. 2.5D',D": yellow arrows). These findings were corroborated with NrxIV-RNAi (Fig. 2.5E-G) and Cora-RNAi. With NrxIV knockdown, Gukh and Gli spread basolaterally (Fig. 2.5G',G": yellow arrows) while Gukh and Cora was downregulated at the SJ level (Fig. 2.5E',E''',E',F''',G',G'''). Overall Gukh maintained its association with Gli at the TCJ even in the absence of core SJ proteins. Our findings suggest that while SJ proteins stabilize Gukh to the SJ, the localization of Gukh to the TCJ is independent of its localization to the SJ.

2.3.6 The loss of Gukh triggers cell delamination, JNK-mediated apoptosis and migration

To test the role of Gukh within the columnar epithelia, we knocked down Gukh on the dorsal side of the wing imaginal disc using Gukh-RNAi. Efficacy of the RNAi was verified with the loss of Gukh::mCherry (Supplemental Fig. 2.5A) and we used two independent RNAi lines to verify observed phenotypes. Membrane bound GFP (mCD8::GFP) was co-expressed to better understand the cellular phenotypes in the loss of Gukh. Control were apterous-Gal4 driving mCD8::GFP crossed to w[1118] (Fig. 2.6A-C). Expression of Gukh-RNAi affected the general appearance of the wing disc so while the epithelium appeared intact, it was undulated with extensive tissue folds (Fig. 2.6D) and we observed extensive pyknotic nuclei in the basal domain. Knockdown of Gukh resulted in the basal delamination of GFP-positive cells, and the displacement of GFP-positive cells (dotted yellow line) across the apterous boundary (dotted white line) into the basal domain of the ventral side (Fig 6D, E). To test whether the Gukh

knockdown cells were apoptotic, we immunolabeled for Death Caspase-1 (Dcp-1) and found Gukh-RNAi increased Dcp-1 expression particularly in the wing pouch (Fig. 2.6D') and this corresponded to the GFP labelled cells (Fig. 2.6D"). In the side projections (Fig. 2.5E), the Dcp-1, GFP positive cells clearly delaminated towards the basal side and crossed from the apterous boundary (dotted white line) into the ventral non apterous side (yellow dotted line). To quantify the movement of GFP labeled Gukh-RNAi cells into the ventral side, we measured the migration distance as a ratio of the distance of the ventral half of the wing disc (Padash-Barmchi et al., 2010) (Fig. 2.6I). The Gukh-RNAi cells moved on average 44.6% of the way across the ventral half (Fig. 2.6J), a significant difference compared to control ($p<0.0001$). Apoptosis is often accompanied by compensatory proliferation (Fan and Bergmann, 2008), and to test for increase in mitosis we immunolabeled with phospho-Histone3. We observed mitosis was increased in the Gukh knockdown the apterous side in comparison to the ventral side control (Fig 6F') and this increase was significant compared to control (Fig. 2.6K; $p=0.0016$). To test whether apoptosis was triggered by JNK signalling in the loss of Gukh, we co-expressed Gukh-RNAi and Bsk-DN, the dominant-negative form of *Drosophila* JNK (Basket). We analyzed Dcp-1 immunolabeling and the degree of migration of the GFP cells into the ventral half of the wing disc. Immunolabeling of Dcp-1 (Fig. 2.6G',H') and cell migration (Fig. 2.6G",H") was suppressed by Bsk-DN. When quantified (Fig. 2.6J), Bsk-DN significantly suppressed the movement of GFP-labelled cells into the ventral half of the wing compared to Gukh-RNAi expression alone ($p<0.0001$) and was not significantly different from control. Overall, our findings suggest that the loss of Gukh triggers JNK-mediated apoptosis leading to cell delamination and movement of cells into the ventral side of the wing disc.

2.3.7 Loss of Gukh does not affect SJs, TCJs but reduces β-integrin in the intermediate domain

The loss of Gukh had strong effects on epithelial integrity and so we next tested if loss of Gukh affected any of the junctional domains. At the apical side, Ecad localization was unaffected and the AJ appeared intact in Gukh-RNAi (data not shown). The localization of SJ proteins Nervana 2.1 (Nrv2.1) and Coracle (Cora) at the SJ were unaffected (Supplemental Fig. 2.5D). Gukh knockdown did not affect the localization of Gli, Dlg or Scrib to the TCJ (Supplemental Fig. 2.5D-F). We next focused on the distribution of integrin in the intermediate and basal focal adhesions. β-integrin appeared to be reduced within intermediate domain in Gukh-RNAi (Fig 7A) and we observed a concentration of β-integrin just apical to the delaminated cells (marked with GFP) (Fig. 2.7A, A',C,C'; magenta arrows). On the non-apterous side the focal adhesion complex was similarly found above the delaminated GFP cells that had spread into the ventral side of the disc (Fig. 2.7A'; yellow arrow) and were found in the normal basal distribution further away from the GFP cells (Fig. 2.7B'; yellow arrow). Side projections (Fig. 2.7C) confirmed that focal adhesions appear to form basally but were displaced above the delaminated cells (Fig. 2.7C'; magenta arrow, Fig. 2.7D, D', Fig. 2.7D"). Due to the disruption of the epithelia in Gukh-RNAi assessing the distribution of β-integrin in the intermediate domain was difficult and thus it was necessary to block JNK-mediated apoptosis with Bsk-DN. In Gukh-RNAi and Bsk-DN, we observed intact β-integrin concentrations at focal adhesions in the basal domain (Fig. 2.7F',G'; magenta arrows) that matched the focal adhesions on the control non-apterous side (Fig. 2.7F'; yellow arrow). Surprisingly we detected the presence of delaminated Gukh-RNAi cells marked with GFP interspersed with the columnar epithelia that were rounded up and did not express β-integrin (Fig. 2.7F'; asterisk) suggesting loss of Gukh can lead to the

delamination of cells independent of JNK (Fig. 2.7H"). Within the intermediate domain the β-integrin levels were reduced compared to the control side significantly ($p<0.001$) (Fig 7E', I). Thus while Gukh-RNAi is not necessary for the formation of the basal focal adhesions, it is required for the concentration of β-integrin within the intermediate domain.

2.3.8 β-integrin and talin distribution in the intermediate domain require Gukh

To better understand the role of Gukh and focal adhesions within the intermediate domain, we investigated the distribution of focal adhesion proteins, talin and β-integrin, with respect to Gukh. We found talin and β-integrin co-localized in puncta at the cell membrane in the intermediate domain (Fig. 2.8A; yellow arrows). At the basal side of the epithelium, talin and β-integrin co-localized into clusters forming basal focal adhesions (Fig. 2.8 B; yellow arrows) as previously observed (Brown et al., 2002). Integrin subunits have been shown to enrich on either side of the DV axis (Brower and Jaffe, 1989; Brower et al., 1984; Dominguez-Gimenez et al., 2007). We noted β-integrin and talin are more enriched on the ventral and dorsal side respectively (Fig. 2.8) We found that Gukh, talin and β-integrin colocaize at the intermediate domain (Figure 2.8 C; magenta arrows), while the colocalization of talin and β-integrin could be found independent of Gukh (Figure 2.8 C; yellow arrows). Similarly, we observed that Gukh and β-integrin colocalized with an alpha subunit of Laminin, an ECM ligand for integrin, at the intermediate domain (Figure 2.8 D; yellow arrows), and enriched basally (Fig. 2.8F; yellow arrow). Our data suggested a reciprocal association of β-integrin and Gukh in the intermediate domain and to test this interaction further we expressed a Gukh transgene that expresses the last 392 amino acids of the C-terminal end (Gukh-C) (Supplemental Fig. 2.1A). The overexpression of Gukh-C can act in a dominant-negative manner (Caria et al., 2018) and this transgene contains the Dlg-binding domain (Mathew et al., 2002) but lacks the NHS and N-terminal WHD. The

overexpression of eGFP::Gukh-C using apterous-Gal4 resulted in the loss of Gukh::mCh from the apical (Fig. 2.8 G' ; yellow arrows) and intermediate domains (Fig. 2.8 H'; yellow arrows) but not from the basal domain (Fig 2.8 I'; yellow arrows). Consistent with our results with Gukh-RNAi, β-integrin was reduced from the intermediate domain characterized by the loss of the strong puncta (Fig 2.8 H'''; magenta arrow). The concentration of β-integrin to basal focal adhesions (Fig 2.8 I'''; magenta arrows) were unaffected suggesting normal FAC formation. Our data suggests that the C-terminal GUK-binding is able to compete with a normal binding interaction to interfere with the recruit of β-integrin and Gukh itself to the intermediate domain.

2.4 Discussion

2.4.1 TCJ proteins recruit Gukh

We found Gukh is co-localized with TCJ proteins Bark and Gli, and co-localizes with Dlg and Scrib at the SJ and TCJ. Although the localization of Gukh at the TCJ is dependent on these TCJ proteins, Gukh is not necessary for the formation of either the TCJ or the SJ. Since Scrib localization to the TCJ was unaffected in the loss of Gukh, this suggest that contrary to the NMJ, Gukh does not play a role in recruiting Scrib to Dlg in the wing imaginal disc (Fig 2.8 J). At the NMJ, the Gukh C-terminus binds to Dlg GUK domain and recruits Scrib via its PDZ2 domain (Mathew et al., 2002). The mechanism that recruits Dlg and Scrib to the TCJ remains unresolved. Furthermore, we found that Gukh appears to flank the TCJ at the interface of the TCJ and SJ, and this is most apparent in the periopodial cells (Supplemental Fig. 2.3). This suggest that Gukh marks a subdomain of the TCJ and does not contribute to its formation, but potentially coordinates interactions with the SJ. Further the recruitment of Gukh to the SJ and the TCJ appears to be independent as loss of the SJ proteins lead to a loss of Gukh from the SJ but not from the TCJ suggesting that Gukh may interact with protein complexes in both domains.

2.4.2 Cell death in the loss of Gukh

Our results suggest Gukh does not play a critical role in TCJ and FAC stability and formation, but that Gukh is necessary for cell survival. Loss of Gukh triggers JNK-mediated apoptosis, compensatory proliferation and cell delamination. However, when JNK was blocked, cells still delaminated basally, albeit to a lesser extent. A number of mechanisms could result in apoptosis and cell delamination. For instance, the loss of intercellular cell adhesion proteins such as cadherins can lead to delamination. Contrarily, none of the junctional complexes were affected by the reduction of Gukh. Another mechanism is cell competition, where mutant cells are eliminated by neighbouring wild type cells, such as *scrib* or *dlg* mutant clones which are actively eliminated from the epithelium by neighbouring cells (Brumby, 2003; Ohsawa et al., 2011). While it is still not clear the mechanism, the possibility that the observed apoptosis is triggered by cell competition warrants further study.

2.4.3 Gukh and focal adhesions

We found Gukh encircles the basal FACs where integrins and talin concentrate. The loss of Gukh does not affect basal FAC formation, while integrins are necessary to recruit Gukh to the basal FAC domain. Of interest, we observed focal adhesion-like structures characterized by the co-localization of integrin, talin and Gukh in the intermediate domain as observed previously (Brown et al., 2002). Our results suggest that their interaction is interdependent as the loss of β-integrin results in the reduction of Gukh from the intermediate domain and vice versa. In support of this possibility, the overexpression of the C-terminal domain of Gukh (Mathew et al., 2002) reduced β-integrin and Gukh itself in the intermediate domain. As the C-terminal construct contains the GUK-binding domain, the overabundance of the Gukh C-terminal domain may

outcompete protein-protein interactions in the intermediate domain. The function of this conserved region has not yet been established, however there are a number of potential GUK domain proteins that could interact with Gukh through this domain. Dlg is a clear possibility but we do not favour a role for Dlg in this region as we observed that Dlg does not localize at the level of the focal adhesion complex (data not shown) suggesting that other GUK domain proteins may mediate the localization of this potential complex.

The function of the integrin/talin complex and Gukh in the intermediate domain is also still an open question. Previous works suggest that disc cells may secrete extracellular matrix basolaterally (Dominguez-Gimenez et al., 2007; Fristrom et al., 1993). Given integrins function to adhere amnioserosa cells laterally (Narasimha and Brown, 2004), we propose that talin and β-integrin co-localize to form FAC-like structures in the intermediate domain, and that Gukh plays a role in either the function of the complex or the localization to this domain. Alternatively, there is a possibility that these proteins are found concentrated within trafficking vesicles as previously observed (Bhuin and Roy, 2011). However, we observed that the Gukh-positive puncta do not co-localize with alpha-tubulin in the intermediate domain suggesting that these do not represent trafficking vesicles. Overall, we propose a model where there are three populations of β-integrin in the wing disc. Intermediately, β-integrin co-localizes with talin and ECM components such as laminin to mediate adhesion at the lateral membrane. β-integrin can be found independent of Gukh in vesicles for trafficking and recycling. Basally, β-integrin forms FAC for cell-ECM adhesion, and indirectly localizes Gukh for signaling or for other unexplored functions (Fig 2.8 K).

2.4.4 Other potential roles of Gukh

Some potential roles for Gukh in the *Drosophila* epithelia are suggested by observations on vertebrate NHS. Gukh is the predicted homolog of NHS, and we found that distribution of Gukh

and NHS are similar. NHS co-localizes with ZO-1 at the tricellular contacts in MDCK cells, and distributes basolaterally in a pattern comparable to Gukh distribution in the intermediate and basal domains (Sharma et al., 2006, 2009). Similar to the loss of Gukh, the loss of NHS does not affect the formation of TJ as measured by the localization of ZO-1 (Brooks et al., 2010). However, NHS also co-localizes with integrins and knockdown of NHS results in increased cell spreading while overexpression of NHS inhibits lamellipod formation (Brooks et al., 2010; Sharma et al., 2009). NHS also co-localizes with Lasp-1 (Lim, actin, and SH3 domain protein 1) at focal adhesions. Lasp-1 is a scaffolding protein found in adhesion junctions such as focal adhesions and at the leading edges of lamellipodia. Lasp-1 binds to proline-rich domains of cytoskeleton proteins - most notably zyxin, which scaffolds focal adhesions (Chew, 2002; Orth et al., 2015). The *Drosophila* homolog of Lasp-1, Lasp, also engages in adhesion processes. For instance, in early germ cells Lasp-1 co-localizes with integrins, and anchors the male stem cell niche to the apical tip of the testis in an integrin-dependent manner (Lee et al., 2008). This suggests Gukh and integrins may associate in the intermediate domain to stabilize actin dynamics. This hypothesis is further supported by the presence of a highly conserved WHD in Gukh, and this domain has been more thoroughly investigated in the vertebrate NHS homologue. This domain is necessary for Arp 2/3 localization at cell borders of migrating cells for actin remodelling (Brooks et al., 2010). The NHS protein family is postulated to be a member of the WAVE/SCAR protein complex, which includes HSPC300 and proteins of the Abl interactor (Abi) family (Bompard and Caron, 2004; Kurisu and Takenawa, 2009). The loss of NHS results in the upregulation of HSPC 300 and Abi (Brooks et al., 2010). Overall, NHS may be responsible for controlling rearrangement of the actin cytoskeleton, where loss of NHS results in excessive cell spreading and lamellipod formation. Given these observations, the loss of Gukh

could lead to changes in the underlying cytoskeleton of the columnar epithelia and subsequently to the observed apoptosis and changes to the distribution of integrin complexes in the intermediate domain. Further experiments that test this model will provide insight into the molecular functions of Gukh and the NHS protein family *in vivo*.

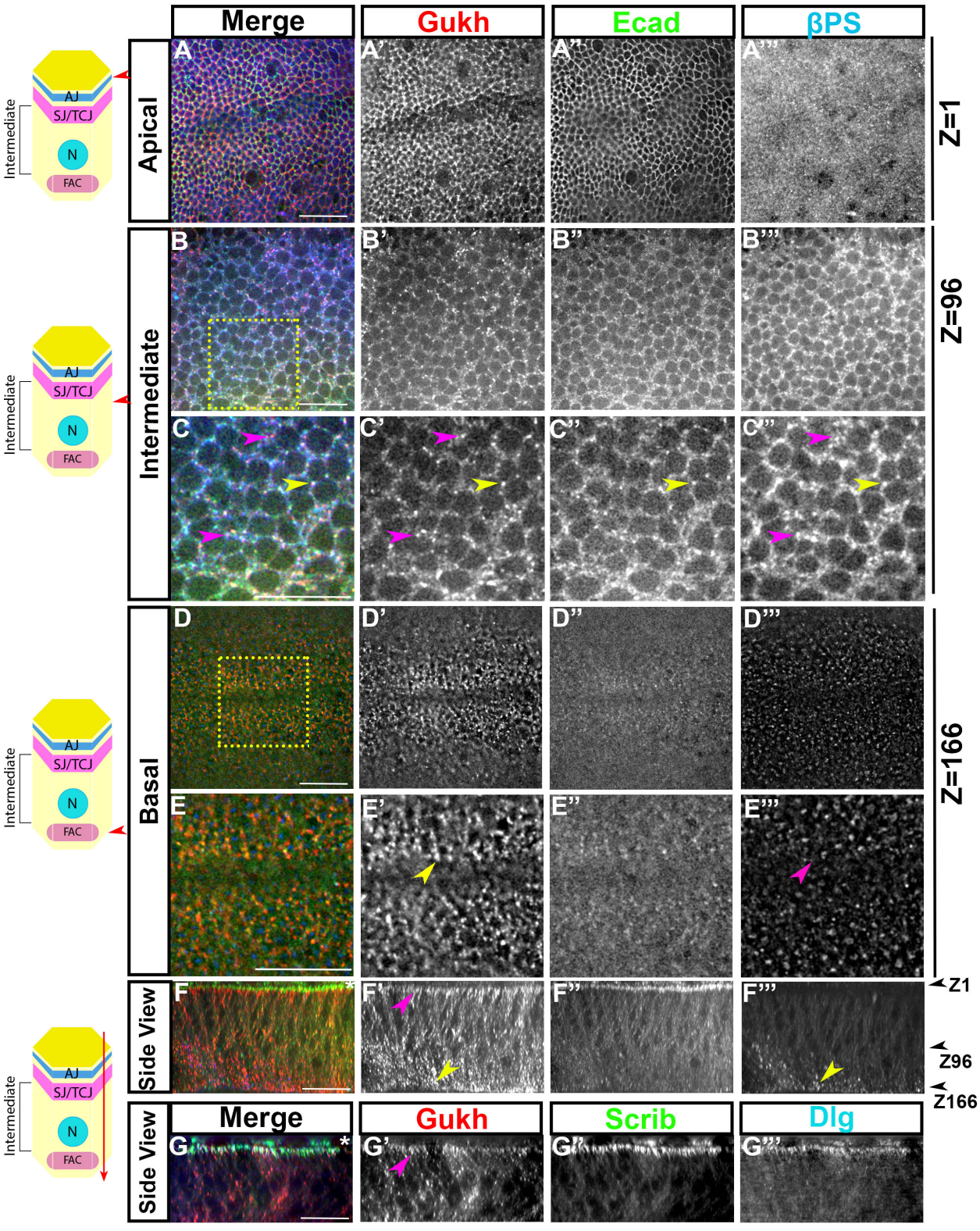
Merge
Gukh
Ecad
βPS
Apical
Intermediate
Basal
Side View
Side View
Merge
Gukh
Scrib
Dlg
A
A'
A''
A'''
B
B'
B''
B'''
C
C'
C''
C'''
D
D'
D''
D'''
E
E'
E''
E'''
F
F'
F''
F'''
G
G'
G''
G'''
Z=1
Z=96
Z=166
Z1
Z96
Z166
Intermediate
AJ
SJ/TCJ
N
FAC

Figure 2.1. Gukh is expressed throughout the wing imaginal disc.

A-F) Gukh::mCherry (mCherry, red) localization at the apical, intermediate and basal domain of a third-instar *Drosophila* wing imaginal disc. The adherens junction and basal integrin domain are marked by immunolabeling for E-cadherin (Ecad, green), and integrin β-subunit (βPS, blue) respectively.

The relative region from which the Z slice was sampled is shown by the cartoon on the left.

A) **Apical domain**: Z=1. Gukh::mCherry localize immediately basal to Ecad.
B-C) **Intermediate domain**: Z=96. Gukh::mCherry (B',C') Ecad (B",B") and βPS (B''',C''') form puncta. Gukh::mCherry and βPS puncta co-localize at cell contacts, magenta arrows. All three proteins are found in common puncta, yellow arrows. C) A 2× digital magnification of the area enclosed by the yellow box in B.
D-E) **Basal domain**: Z=166. Gukh::mCherry (D',E'; yellow arrow) distribution flanks but does not overlap the concentrated regions of βPS marking the basal focal adhesion. (D''',E'''; magenta arrow). E) A 2× digital enhancement of the area enclosed by the yellow dotted box in D.
F) Side views of the wing disc epithelium apical at the top (Z=1) and basal at the bottom (Z=166). Gukh::cherry (F') is concentrated at the apical (magenta arrow) and basal domains (yellow arrows).
G) Side view of a third-instar wing imaginal discs expressing Gukh::mCherry (red) and SJ proteins Scrib::GFP (green) and immunolabeled for Dlg (blue). Gukh co-localizes Scribble and Dlg at the level of the septate junction (magenta arrow).
Each panel represents a single Z projection. Asterisk marks the peripodial epithelia in the side views. Scale bars: 15 μm.

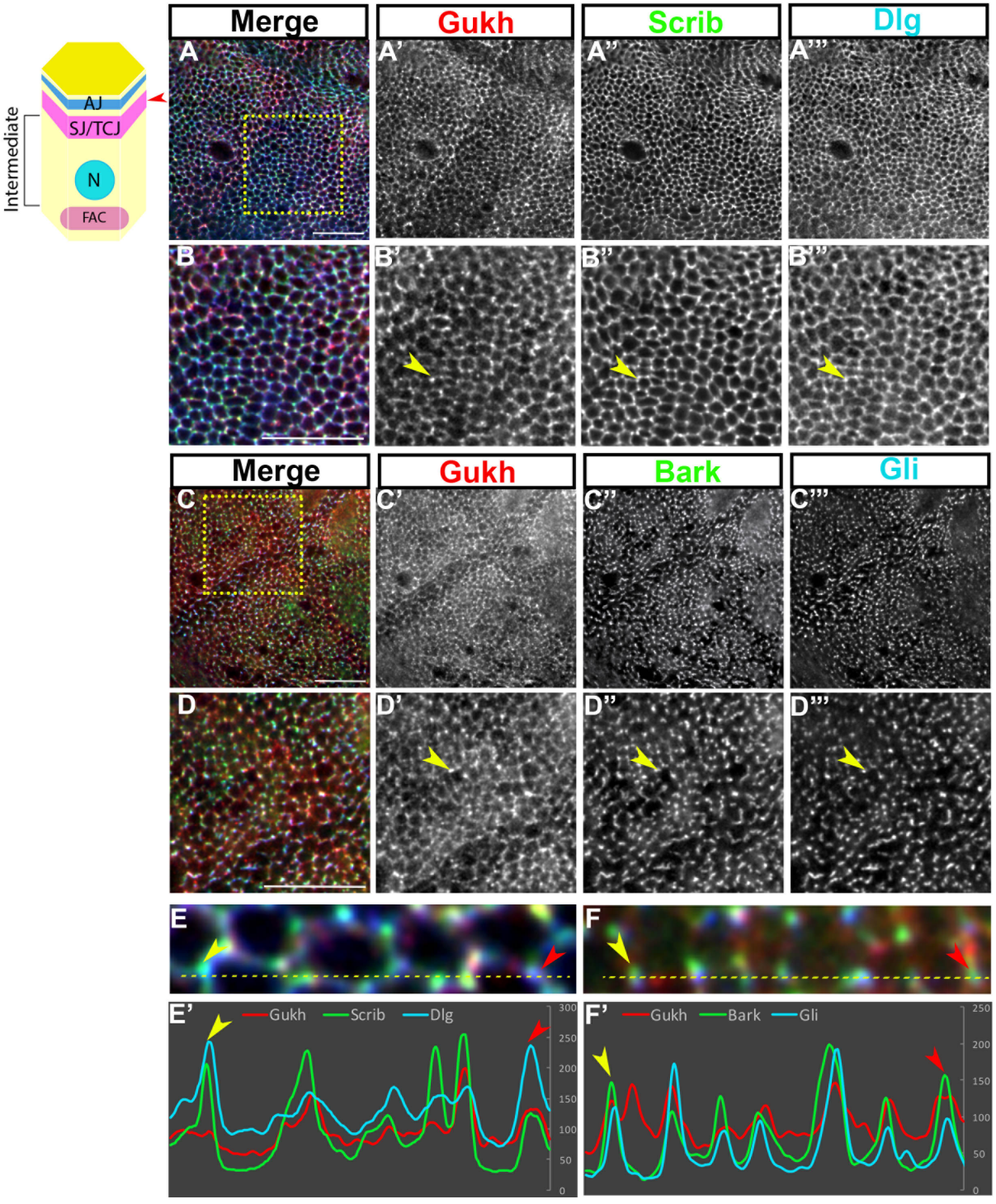
Intermediate
AJ
SJ/TCJ
N
FAC
Merge
Gukh
Scrib
Dlg
A
A'
A''
A'''
B
B'
B''
B'''
Merge
Gukh
Bark
Gli
C
C'
C''
C'''
D
D'
D''
D'''
E
F
E'
Gukh
Scrib
Dlg
300
250
200
150
100
50
0
F'
Gukh
Bark
Gli
250
200
150
100
50
0

Figure 2.2. Gukh co-localizes with Scribble, Discs-large, Bark-beetle and Gliotactin at the tricellular junction (TCJ).
The relative region from which the Z slice was sampled is shown on the cartoon on the left.

A-B) Gukh::mCherry (red, A',B') co-localizes with Scrib::GFP (green, A'',B'') and anti-Dlg (blue, A''',B''') at both the septate junctions and the TCJ (yellow arrows). B) A 2× digital magnification of the area enclosed by the yellow dotted box in A.
C-D) Gukh::mCherry (red, C',D') co-localizes with Bark::GFP (green, C'',D'') and anti-Gli (blue, C''',D''') at the TCJ (yellow arrows). D) 2× digital magnification of the area enclosed by the yellow dotted box in C.
E, E'): Gukh, Scrib and Dlg. E) Digitally magnified panel (2×) of Gukh::mCherry (red), Scrib::GFP (green) and Dlg (blue) immunolabeling The yellow dotted line corresponds to area where the relative intensity profiles (E') were measured from. Gukh, Scrib::GFP and Dlg have similar intensity profiles (E'). Yellow and red arrows indicate the TCJs and the matching intensity peaks.
F, F') Gukh, Bark and Gli. F) Digitally magnified panel (2×) of Gukh::mCherry (red), Bark::GFP (green) and Gli (blue) immunolabeling The yellow dotted line corresponds to area where the relative intensity profiles were measured from. The intensity profiles of Bark, Gli, and Gukh peak simultaneously at the TCJ. Yellow and red arrows indicate the TCJs and the matching intensity peaks.
Each enface panel represents a Z projection. Scale bars: 15 μm.

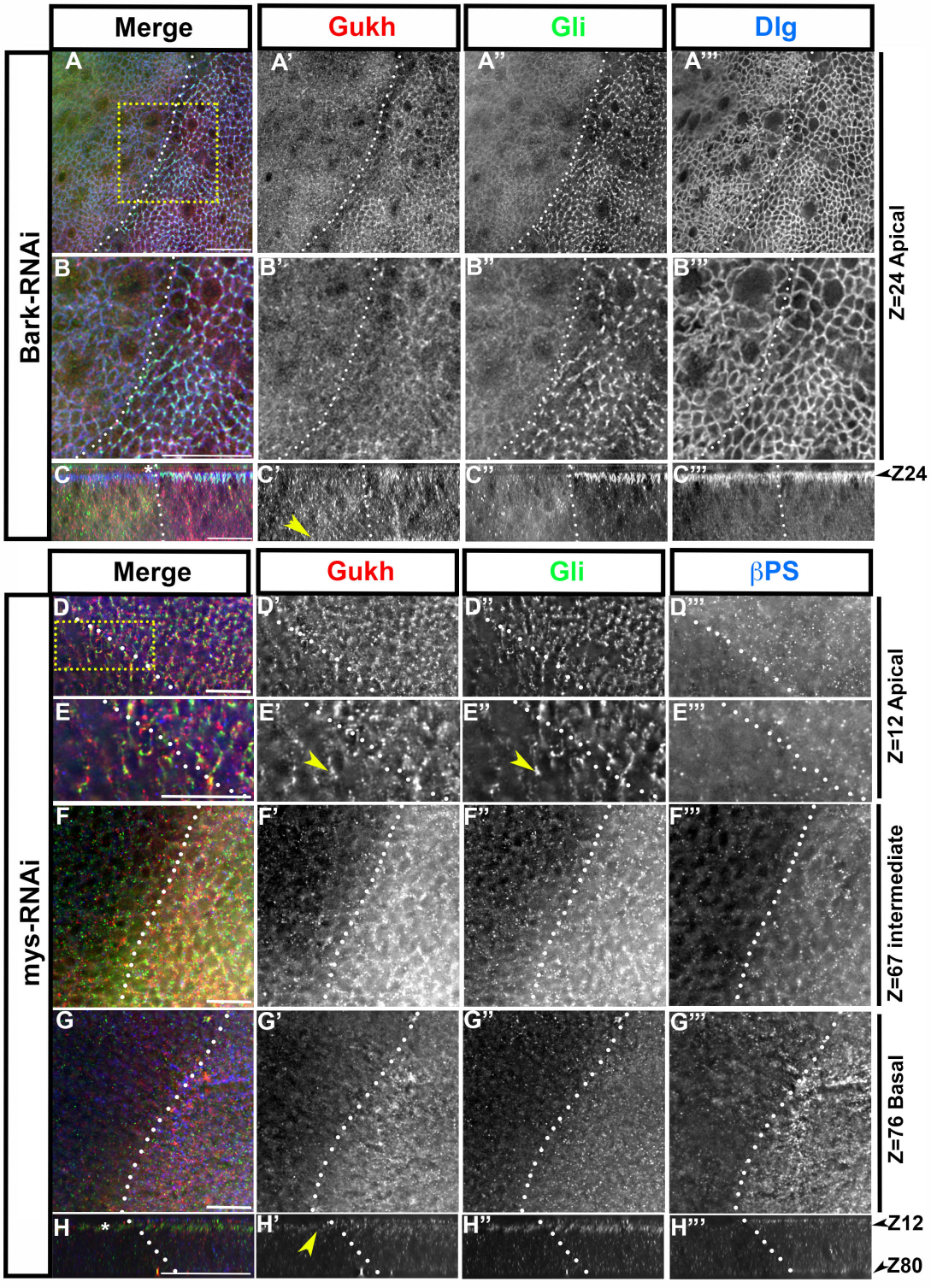
Merge
Gukh
Gli
Dlg
Bark-RNAi
A
A'
A''
A'''
B
B'
B''
B'''
C
C'
C''
C'''
Z=24 Apical
Z24
Merge
Gukh
Gli
βPS
mys-RNAi
D
D'
D''
D'''
E
E'
E''
E'''
F
F'
F''
F'''
G
G'
G''
G'''
H
H'
H''
H'''
Z=12 Apical
Z=67 intermediate
Z=76 Basal
Z12
Z80

Figure 2.3: Knockdown of Bark delocalizes Gukh from the TCJ and SJ while knockdown of β-integrin delocalizes Gukh from the intermediate and basal domain.

Apterous-GAL4 was used to drive RNAi expression on the dorsal side of the wing imaginal disc, with the dorsal side oriented to the left of each panel. White dotted lines indicate the apterous (dorsal-ventral) expression boundary. Each enface panel represents a single Z projection. Asterisks on side views mark the peripodial epithelia (B,E). Scale bars: 15 μm.

A-C) Bark-RNAi. Gukh::mCherry (red) and immunolabeling for Gli (green) and Dlg (blue),
A-B) Z=24. Loss of Bark leads to the bicellular spread of Gli (green, A'',B") and disrupts Gukh (red, A',B') concentration at the TCJ and SJ. B) A 2× digital magnification of the area enclosed by the yellow dotted box in A.
C) Side view of A. Bark knockdown causes spreading of Dlg (blue, C"') basolaterally and reduces the expression of Gukh (red, C') and Gli (green, C'') at the level of TCJ. However the basal localization of Gukh is not affected (C', yellow arrow)

D-G) mys-RNAi. Gukh::mCherry (red) and immunolabeling for Gli (green) and βPS (blue).
D-E) Apical domain, Z=12. Mys-RNAi to knockdown the integrin β-subunit does not affect Gli (green, D'',E") and Gukh (red, D',E') co-localization to TCJ. Gukh concentrates with Gli puncta at the TCJ (yellow arrows).
E) 2× digital magnification of the area enclosed by the yellow dotted box in D.
F) Intermediate domain, Z=67.
G) Basal domain, Z=76. Gukh expression (red, F') is lost from the basal domain in the loss of mys immunolabeled with the βPS antibody (blue, F''').
H) Side view of F. Mys-RNAi downregulates intermediate and basal Gukh (red, H') expression level but not from the level of SJ (H', yellow arrow)

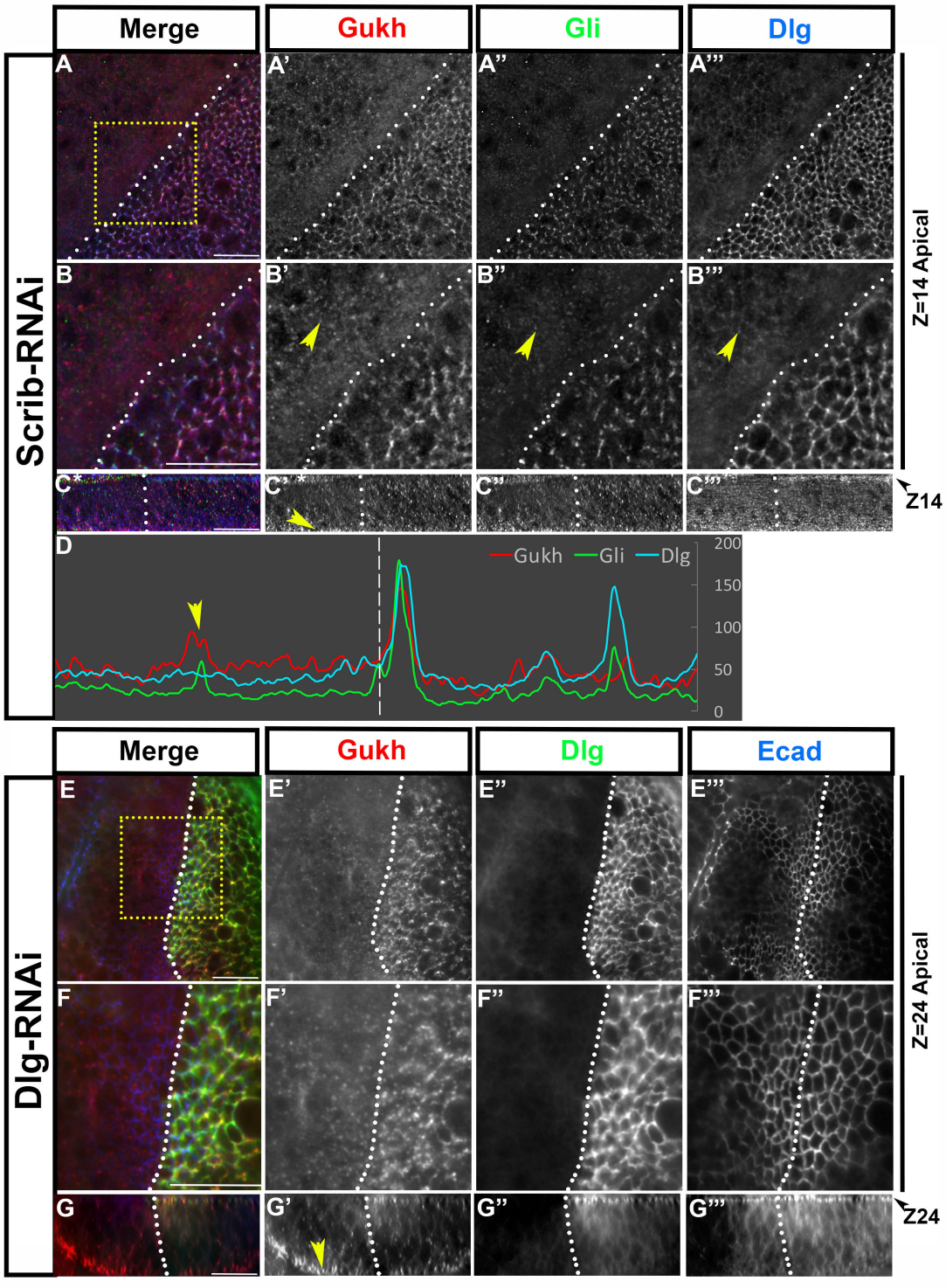
Merge
Gukh
Gli
Dlg
Ecad
Scrib-RNAi
Dlg-RNAi
A
A'
A''
A'''
B
B'
B''
B'''
C*
C'*
C''
C'''
D
Gukh
Gli
Dlg
200
150
100
50
0
E
E'
E''
E'''
F
F'
F''
F'''
G
G'
G''
G'''
Z=14 Apical
Z14
Z=24 Apical
Z24

Figure 2.4. Gukh delocalization from the septate and tricellular junction in Scrib and Dlg knockdown.

Apterous-GAL4 drives RNAi on the dorsal side of the *Drosophila* wing imaginal disc. White dotted lines indicate the apterous (dorsal-ventral) expression boundary with with the dorsal side oriented to the left of each panel..Each enface panel represents a single Z projection. Asterisks on the side views mark the peripodial epithelia. Scale bars: 15 μm. Gukh::mCherry signal enhanced by anti-mCherry (red). Gli, Dlg and Ecad immunostained.

A-D) Scrib-RNAi. Gukh::mCherry (red) with immunolabeling for Gli (green) and Dlg (blue).
A-B) Apical Z=14. Knockdown of Scrib causes downregulation of Gukh (red, A',B'), Gli (green, A'',B") and Dlg (blue, A''',B''') expression.
B) 2× digital magnification of the area enclosed by the yellow dotted box in A). Yellow arrows indicate Gukh retained by residual Dlg and Gli.
C) Side view of A. Scrib-RNAi causes delocalization of Gukh (red, C'), Gli (green, C'') and Dlg (blue, C''') from the level of the SJ but Gukh is retained at the basal domain (yellow arrow).
D) Fluorescence intensity profiles in Scrib-RNAi background. White dashed lines mark the apterous boundary with the apterous side to the left. Gukh signal is reduced in the knockdown of Scrib. The yellow arrow indicates where Gukh coincides with Gli remnants.
E-G) Dlg-RNAi. Gukh::mCherry (red) with immunolabeling for Dlg (green) and Ecad (blue).
E) Apical Z=24. Dlg knockdown causes loss of Gukh (red, E',F') and Dlg (green, E'',F") expression from the TCJ.
F) 2× digital magnification of the area enclosed by the yellow dotted box in E.
G) Side view of E. Dlg-RNAi causes loss of Gukh (red, G') and Dlg (green, G'') from the level of the SJ, while Ecad remains localized to the adherens junction. Gukh basal distribution is unaffected by Dlg-RNAi (G' yellow arrow).

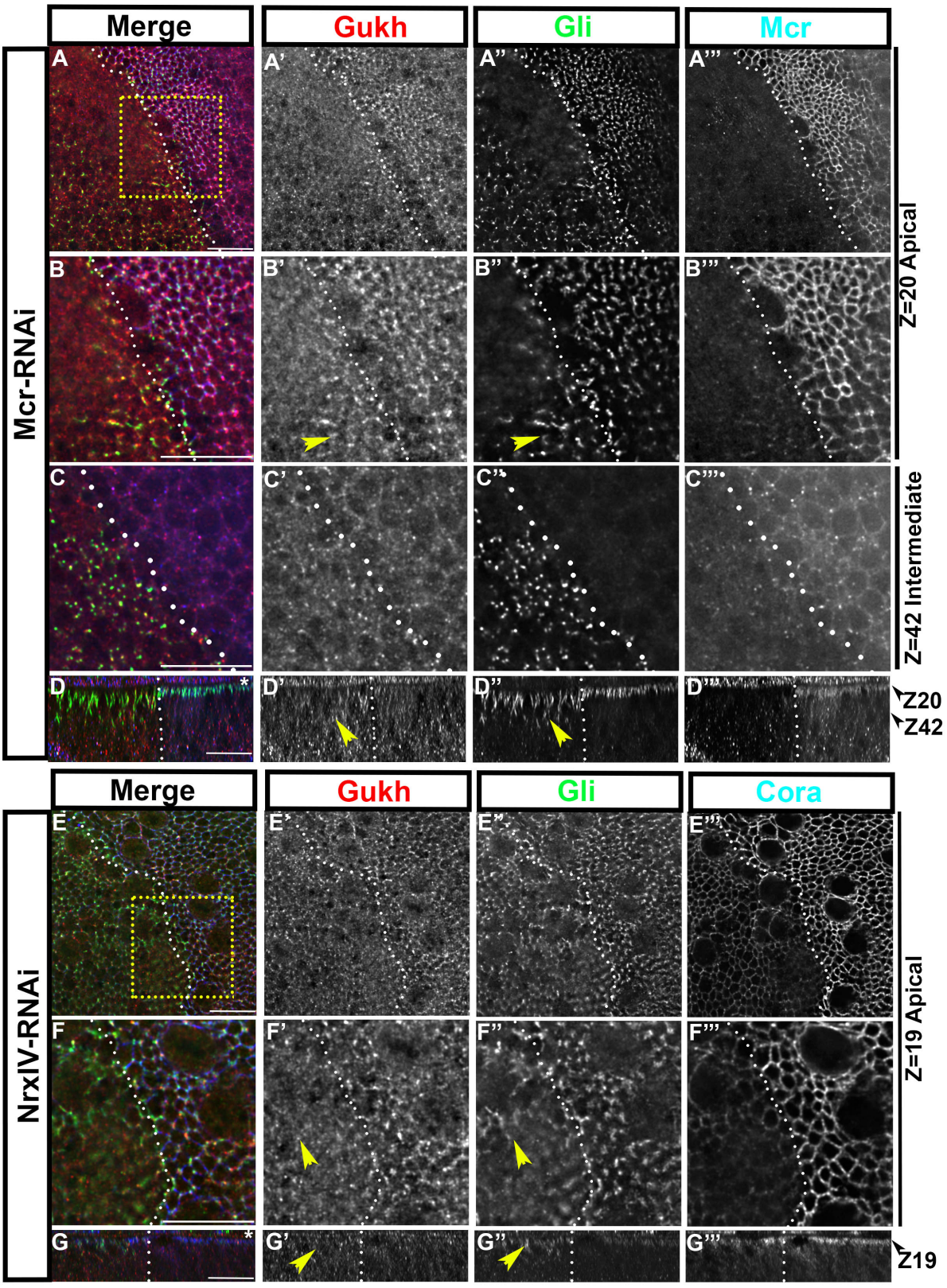
Merge
Gukh
Gli
Mcr
Mcr-RNAi
A
A'
A''
A'''
B
B'
B''
B'''
C
C'
C''
C'''
D
D'
D''
D'''
*
Z=20 Apical
Z=42 Intermediate
Z20
Z42
Merge
Gukh
Gli
Cora
NrxIV-RNAi
E
E'
E''
E'''
F
F'
F''
F'''
G
G'
G''
G'''
*
Z=19 Apical
Z19

Figure 2.5. Knockdown of septate junction proteins Mcr and NrxIV causes delocalization of Gukh from the SJ.

Using apterous-GAL4, RNAi expression was driven on the dorsal side of the wing imaginal disc. White dotted lines indicate the apterous (dorsal-ventral) expression boundary with the dorsal side oriented to the left of each panel. Each panel represents a single Z-projection. Asterisks on the side views mark the peripodial epithelia. Scale bars: 15 μm.

A-D) Mcr-RNAi: Gukh::mCherry (red) with Gli (green) and Mcr (blue) immunolabeling.
A) Apical Z=20 Knockdown of Mcr with Mcr-RNAi (A’’’,B’’’,C’’’) causes delocalization of Gukh (red, A’) from the SJ at the level of SJ/TCJ.
B) A 2× digital magnification of the area enclosed by the yellow dotted box in A. Gukh (red, B’) is retained along with Gli (green, B’’) at the TCJ (yellow arrows).
C: Intermediate Z=42. A 2× digital magnification from the intermediate level of the epithelia. Gukh (red, C’) is normally distributed and co-localizes with the Gli (green, C”) as the TCJ spreads basolaterally (yellow arrows).
D: Side view of A. Mcr-RNAi downregulates Mcr (blue, D’’’). Yellow arrows show the co-spread of Gli (green, D’’) and Gukh (red, D’) basolaterally.

E-G) NrxIV-RNAi: Gukh::mCherry (red) with Gli (green) and Cora (blue) immunolabeling.
E) Apical Z=19. Knockdown of NrxIV causes downregulation of Cora (blue, E’’’) and delocalization of Gukh (red, E’) from the SJ.
F) A 2× digital magnification of the area enclosed by the yellow dotted box in E. Gukh (red, F’) is retained with Gli (green, F’’) at the TCJ (yellow arrows).
G) Side view of E. NrxIV-RNAi causes downregulation of Cora (blue, G”’). Yellow arrows show the co-spread of Gli (green, G’’) and Gukh (red, G’) basolaterally.

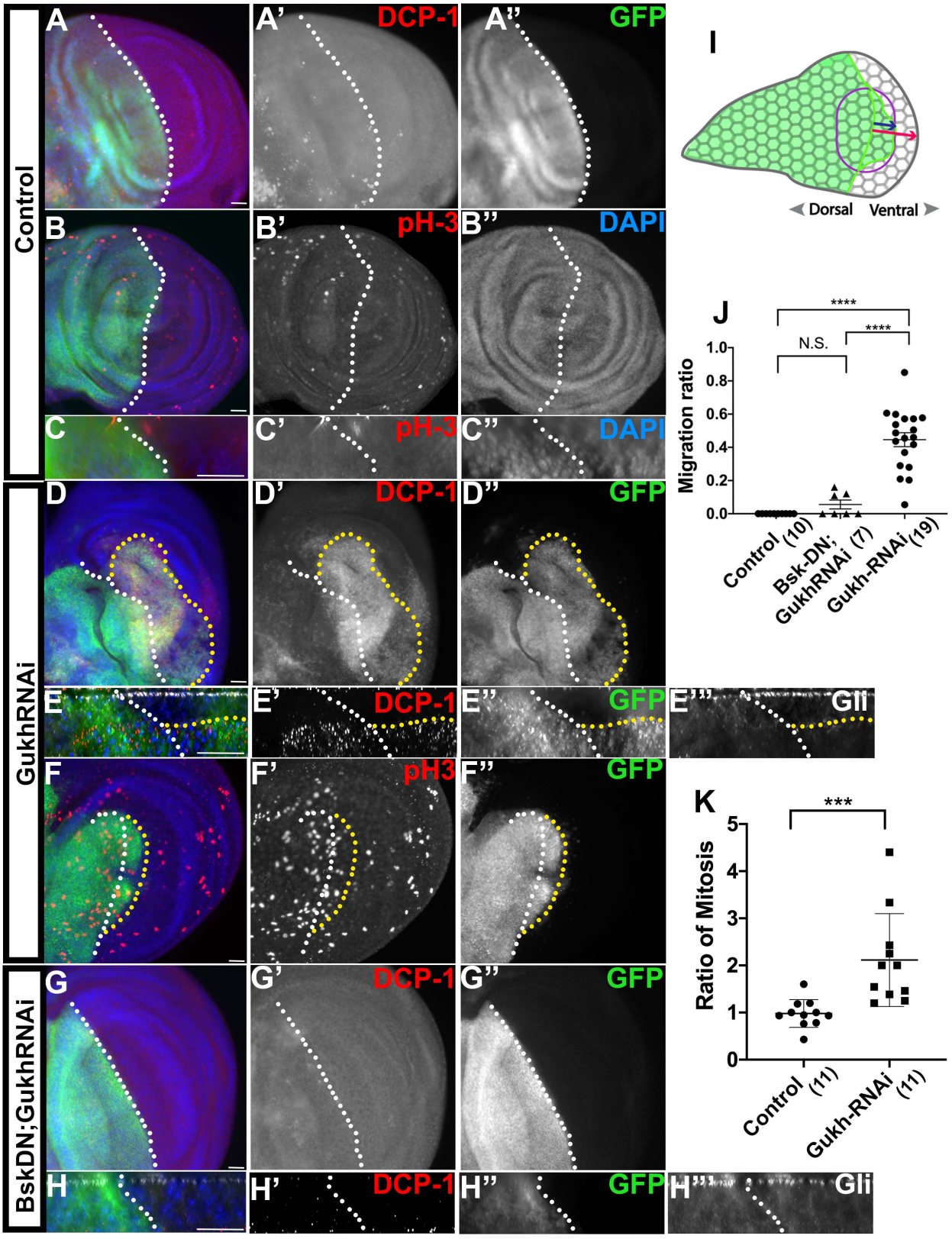
Control
A
A'
DCP-1
A''
GFP
B
B'
pH-3
B''
DAPI
C
C'
pH-3
C''
DAPI
GukhRNAi
D
D'
DCP-1
D''
GFP
E
E'
DCP-1
E''
GFP
E'''
Gli
F
F'
pH3
F''
GFP
BskDN;GukhRNAi
G
G'
DCP-1
G''
GFP
H
H'
DCP-1
H''
GFP
H'''
Gli
I
Dorsal
Ventral
J
****
****
N.S.
Migration ratio
1.0
0.8
0.6
0.4
0.2
0.0
Control (10)
Bsk-DN; GukhRNAi (7)
Gukh-RNAi (19)
K
***
Ratio of Mitosis
5
4
3
2
1
0
Control (11)
Gukh-RNAi (11)

Figure 2.6. Gukh knockdown triggers JNK-dependent apoptosis and cell delamination.

Apterous-GAL4 driven expression of the mCD8::GFP alone (A-C), Gukh-RNAi (D-F) or BskDN+Gukh-RNAi (G,H). The white dotted line marks the apterous boundary with the dorsal side oriented to the left. The yellow dotted line marks the spread of GFP labeled into the ventral half of the wing pouch. Each panel represents a Z-projection. Scale bars: 15 μm.

A-C) Control imaginal disc. apterous-GAL4 driven mCD8::GFP alone (green) immunolabeled for cleaved death caspase-1 (DCP-1) (red, A'), phospho-histone 3 (pH3) (red, B',C') and DAPI (blue, B",C"). GFP expressing cells are restricted to the wing dorsal side with background levels of DCP-1and pH3.
C) Side view of B across the apterous boundary.

D-F) Gukh-RNAi. Membranes marked by mCD8::GFP (green, D", E", F") immunolabeled for DCP-1 (red, D',E'), phospho-histone 3 (pH3) (red, F') with Gli (white, E''') to mark the apical side. GFP, Gukh-RNAi cells (green, D'') cross the apterous boundary (white dots) into the basal domain of ventral side (yellow dots) with upregulation of DCP-1 (red, D').
E) Side view of D. GFP marks the delaminated cells (green, E''). DCP-1 expression (red, C') is upregulated and restricted to the basal side.

G-H) BskDN, Gukh-RNAi. Membranes marked by mCD8::GFP (green, G") immunolabeled for DCP-1 (red, G'H') with Gli (white, E''') to mark the apical side. Expression of BSK-DN with Gukh-RNAi suppressed the delamination and migration of GFP cells (green, G", H") and the upregulation of DCP-1 (red, G',H')

I) Cartoon of the wing imaginal disc with the apterous expression pattern (green). The measurement of GFP cell movement was quantified by the distance from the apterous boundary (blue arrow) as a ratio of length of the ventral side (red arrow).

J) The migration ratio of GFP positive cells in control, BskDN;Gukh-RNAi, and Gukh-RNAi. Control is apterous-Gal4 driving mCD8::GFP. The mean plus SD is shown with **** $p<0.0001$; n.s. not significant. Number of wing discs quantified indicated in brackets.

K) The ratio of mitotic cells (labeled with pH3) on the dorsal side over the ventral side quantified of control or Gukh-RNAi. Control is apterous-Gal4 driving mCD8::GFP. The mean plus SD is shown with *** $p<0.001$. Number of wing discs quantified indicated in brackets.

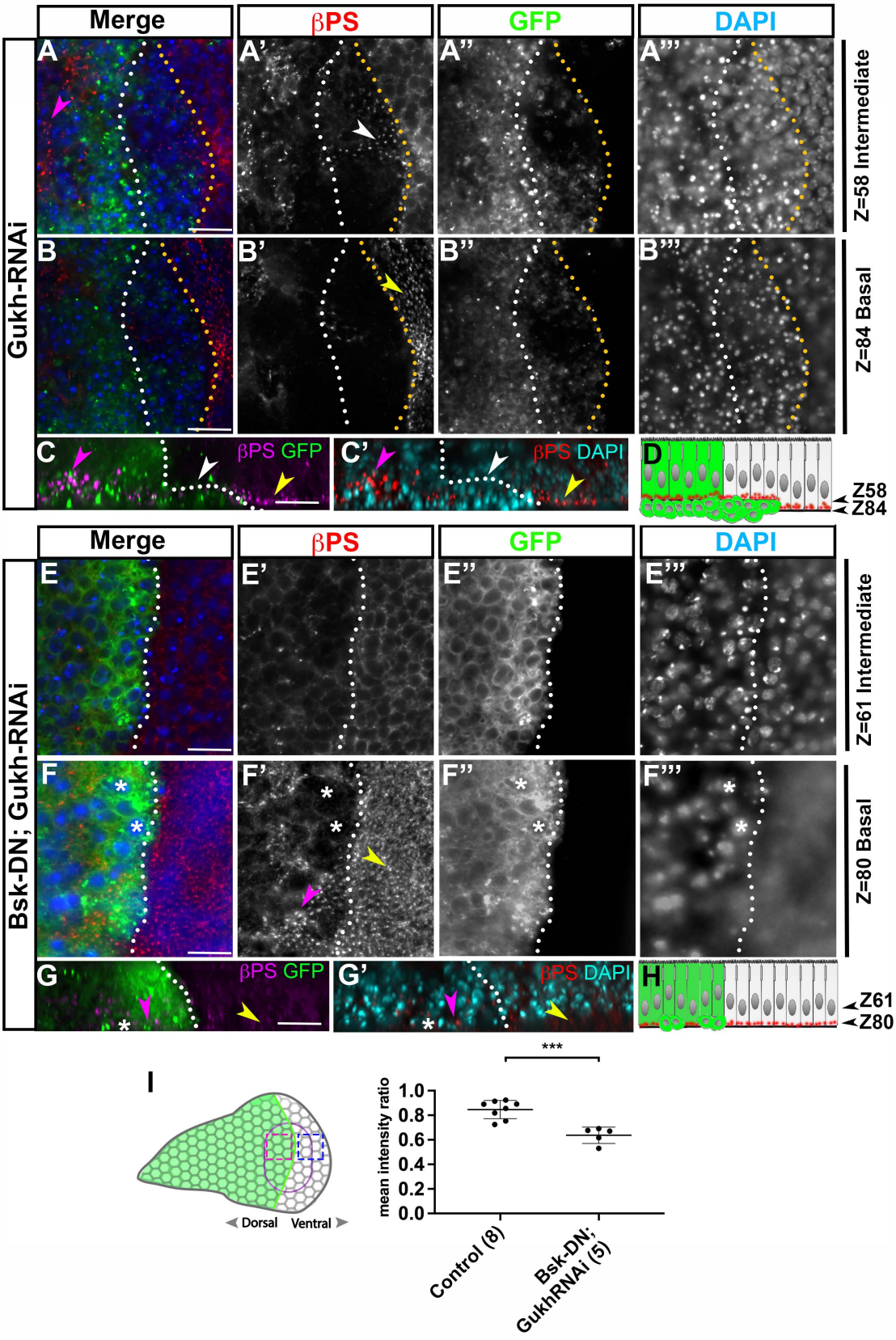
Merge
βPS
GFP
DAPI
Gukh-RNAi
A
A'
A''
A'''
Z=58 Intermediate
B
B'
B''
B'''
Z=84 Basal
C
βPS GFP
C'
βPS DAPI
D
Z58
Z84
Bsk-DN; Gukh-RNAi
E
E'
E''
E'''
Z=61 Intermediate
F
F'
F''
F'''
Z=80 Basal
G
βPS GFP
G'
βPS DAPI
H
Z61
Z80
I
Dorsal
Ventral
***
mean intensity ratio
1.0
0.8
0.6
0.4
0.2
0.0
Control (8)
Bsk-DN; GukhRNAi (5)

Figure 2.7. Gukh knockdown disrupts β-integrin (βPS) localization in the intermediate domain.

Apterous-GAL4, marked by mCD8-GFP expression driving Gukh-RNAi in the wing disc dorsal side (A-D) or Gukh-RNAi + BSK-DN (E-H). Each en face panel represents a single Z-projection. The white dotted line marks the apterous boundary with the dorsal side oriented to the left. The yellow dotted line marks the outer edge of GFP labeled cells that have crossed into the ventral wing pouch. Scale bars: 15 μm.

A-C) Gukh-RNAi. mCD8::GFP (green, A", B") immunolabeled with βPS (red, A',B') and stained with DAPI (blue, A''',B''').
A) Intermediate domain. Z=58. Focal adhesions positive for β-integrin (red, A') on the dorsal side (magneta arrow) and ventral side (white arrow) appear in this domain due to the presence of the underlying deliminated mCD8::GFP positive cells (green, A").
B) Basal domain. Z=84. Focal adhesions positive for β-integrin (red, B') at found at the basal domain on the ventral side (yellow arrow) beyond the edge to the GFP positive cells (dashed yellow line).
C) Side view of A-B across the apterous boundary. The location of β-integrin positive focal adhesions (magenta, C; red, C') above the delaminated cells marked with mCD8::GFP (green, C) and DAPI (cyan, C') is indicated on the dorsal side (magenta arrows) and on the ventral side (white arrows). β-integrin positive focal adhesions are at the expect basal plane beyond the GFP cells on the ventral side (yellow arrows).
D) Cartoon of the side view with mCD::GFP labelled cells (green) and β-integrin positive focal adhesions (red) and the corresponding Z planes indicated.

D-G) Bsk-DN, Gukh-RNAi. mCD8::GFP (green, E", F") immunolabeled with βPS (red, E',F') and stained with DAPI (blue, E''',F'''). There is reduced cell delamination and no spread of mCD8::GFP positive cells into the ventral side.
E) Intermediate domain. Z=61. β-integrin (red, E') expression is reduced in the intermediate domain. GFP-positive cells remain restricted to the wing dorsal side (green, E'').
F) Basal domain. Z=80. Focal adhesions positive for β-integrin (red, F') at found at the basal domain on the dorsal side (magenta arrow) and the ventral side (yellow arrow). mCD::GFP-positive cells remain restricted to the wing dorsal side (green, F''). Delaminated cells positive for mCD8::GFP are indicated with an asterisk.
G) Side view of E-F across the apterous boundary. The location of β-integrin positive focal adhesions (magenta, G; red, G') in the basal plane are indicated on the dorsal side (magenta arrows) and on the ventral side (yellow arrows). Delaminated mCD8::GFP positive cells (green, G) marked with DAPI (cyan, G') are marked with asterisks.
H) Cartoon of the side view with mCD8::GFP labelled cells (green) and β-integrin positive focal adhesions (red) and the corresponding Z planes indicated.
I) In control discs or Bsk-DN,Gukh-RNAi discs, the ratio of mean intensity level of β-integrin is quantified in the intermediate domain. The ratio of intensity is calculated by the intensity on the dorsal side (magenta box on schematic) over the ventral side (blue box on schematic). The mean and SD are shown. $p<0.001$. Number of wing discs quantified indicated in brackets.

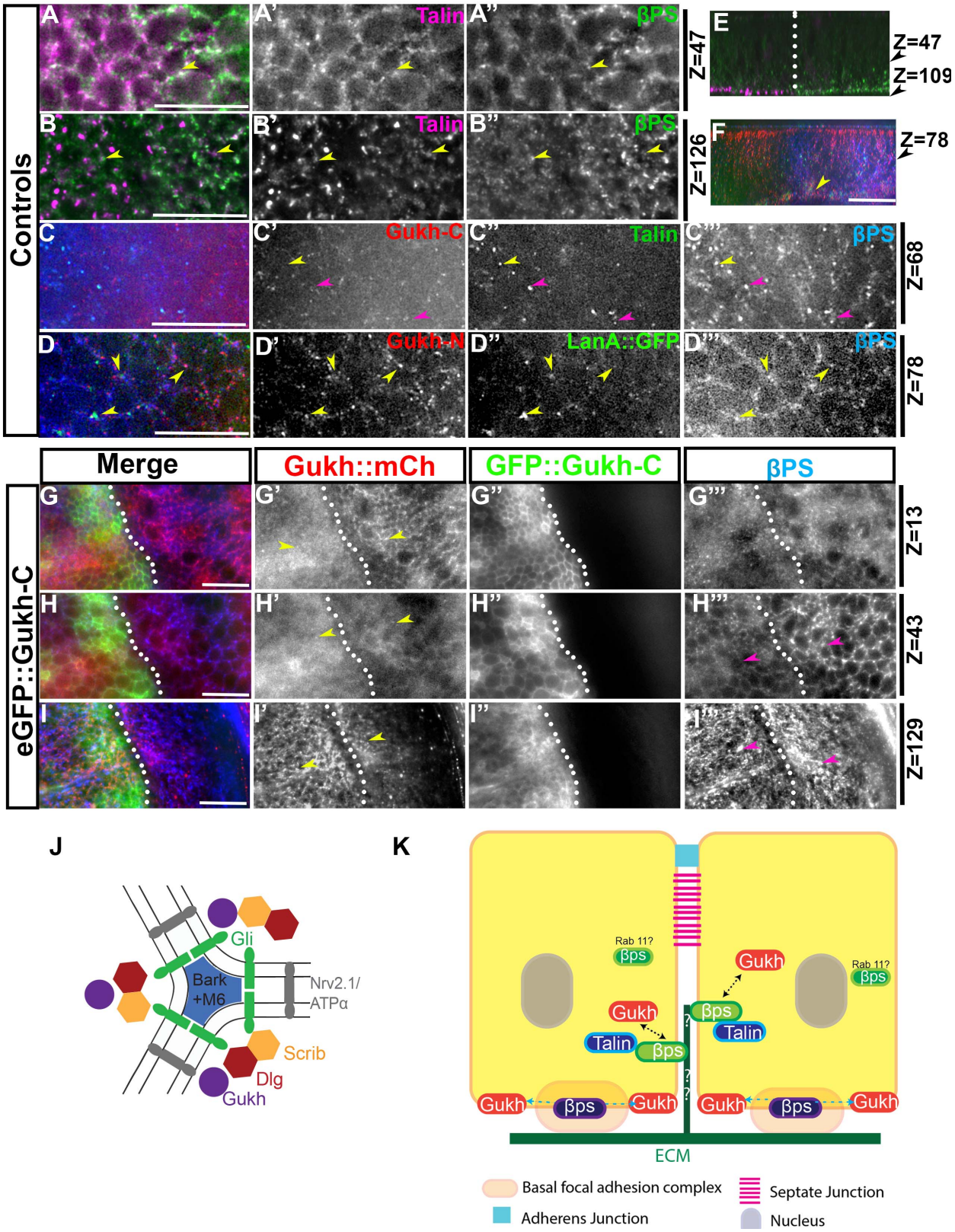
Controls
A
A'
Talin
A''
βPS
E
Z=47
Z=47
Z=109
B
B'
Talin
B''
βPS
Z=126
F
Z=78
C
C'
Gukh-C
C''
Talin
C'''
βPS
Z=68
D
D'
Gukh-N
D''
LanA::GFP
D'''
βPS
Z=78
eGFP::Gukh-C
Merge
Gukh::mCh
GFP::Gukh-C
βPS
G
G'
G''
G'''
Z=13
H
H'
H''
H'''
Z=43
I
I'
I''
I'''
Z=129
J
Gli
Bark
+M6
Nrv2.1/
ATPα
Scrib
Dlg
Gukh
K
Rab 11?
βps
Gukh
Talin
ECM
Basal focal adhesion complex
Adherens Junction
Septate Junction
Nucleus

Figure 2.8. Gukh-C overexpression reduces β-integrin in the intermediate domain.
Talin::mCherry discs were stained with βPS (A-B,E), or stained with Gukh-C and βPS (C) antibodies. LamininA::GFP discs were stained with βPS and Gukh-N antibodies (D, F) Apterous-GAL4, drives eGFP::Gukh-C construct (G-I) in the wing disc dorsal side (oriented to the left of each panel).
Model of Gukh at the TCJ (J) , and at the intermediate, and basal domains (K).
Each en-face panel represents a single Z-projectionn. The white dotted line marks the apterous boundary with the dorsal side oriented to the left.

A-B) talin::mCherry (magenta, A', B') immunolabeled with βPS (red, A',B')
A) Intermediate domain. Z=47. Focal adhesions sites positive for β-integrin (green, A'') and talin (magenta, A') at the cell contacts (yellow arrows).
B) Basal domain. Z=126. Focal adhesions positive for β-integrin (green, B'') and talin (magenta, B') found basally.
C) Intermediate domain. Z=78. Gukh-C (red, C'), talin::mCherry (green, C'') and βPS (blue, C''') colocalize (magenta arrows) in puncta, but colocalization of talin and βPS can be found independent of Gukh-C (yellow arrow).
D) Intermediate domain. Z=68. Gukh-N (red, D'), LanA::GFP (green, D'') and βPS (blue, D''') colocalize (yellow arrows) in puncta.
E) Side view of A-B across the apterous boundary. Talin (magenta) is enriched on the dorsal side; β-integrin (green) is enriched on the ventral side.
F) Side view of F across the apterous boundary. Gukh-N (red, F'), LanA::GFP (green, F'') and βPS (blue,F) enriched basally as expected (yellow arrow).

G-I) GFP::Gukh-C; Gukh::mCherry (red, G',H', I') immunolabeled with βPS (blue, F'",G"',H").
G) Apical domain. Z=13. Gukh::mCherry (red, G') reduced (yellow arrows) in the overexpression of eGFP::Gukh-C (green, G'').
H) Intermediate domain. Z=43. β-integrin (blue, G''' magenta arrow) and Gukh (red, G' yellow arrows) reduced from the intermediate domain.
I) Basal domain. Z=129. Gukh (red, I' yellow arrows) and β-integrin (blue, H''' magenta arrows) levels unaffected at the focal adhesions.

J) Gukh colocalizes at the TCJ with TCJ proteins but does not function in a triparte with Dlg and Scrib as observed in the NMJ.
K) We propose there are three populations of β-integrin can be found. Basal β-integrin at the FAC localizes Gukh that flanks the FAC. β-integrin and Gukh localize at the lateral membrane in FAC-like sites interdependently. β-integrin found intracellular are recycled by Rab 11.

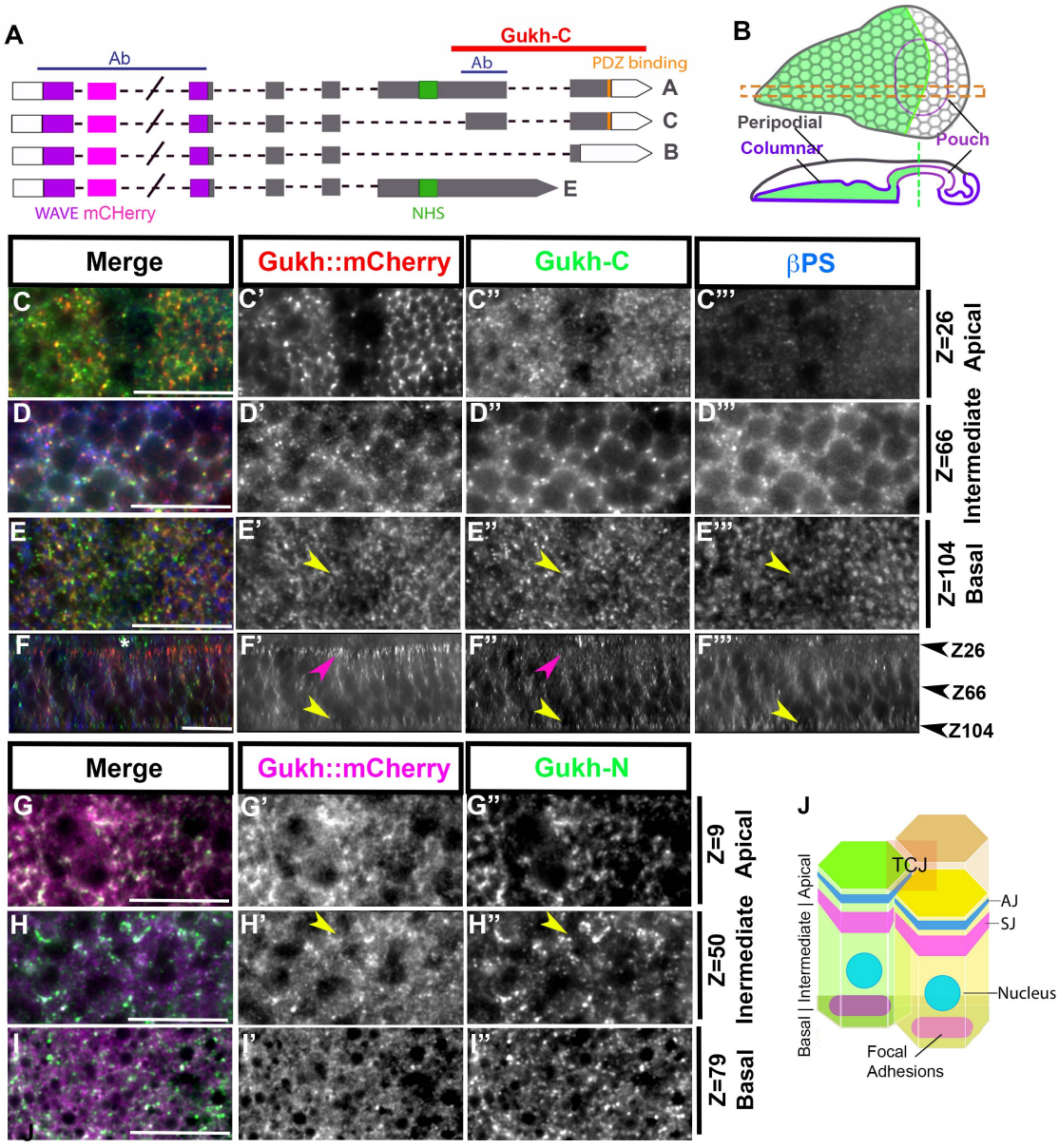
A
Ab
Gukh-C
Ab
PDZ binding
A
C
B
E
WAVE mCHerry
NHS
B
Peripodial
Columnar
Pouch
Merge
Gukh::mCherry
Gukh-C
βPS
C
C'
C''
C'''
Z=26 Apical
D
D'
D''
D'''
Z=66 Intermediate
E
E'
E''
E'''
Z=104 Basal
F
F'
F''
F'''
Z26
Z66
Z104
Merge
Gukh::mCherry
Gukh-N
G
G'
G''
Z=9 Apical
H
H'
H''
Z=50 Inermediate
I
I'
I''
Z=79 Basal
J
TCJ
AJ
SJ
Nucleus
Basal | Intermediate | Apical
Focal Adhesions

Supplemental Figure 2.1. Gukh::mCherry localization verified by immunolabeling with Gukh antibodies.

A) Schematic of the Gukh gene (exons/introns) for the four predicted Gukh protein isoforms. Isoform C corresponds to Gukh-L in Mathew et al., 2002. Indicated are: WAVE homology domain (purple), NHS (green), PDZ-binding motif (orange), mCherry tag (pink), antibodies (blue), the Gukh-C construct (red).

B) Cartoon of the third-instar wing imaginal discs. apterous-GAL4 expression, represented by green cells, is restricted to the dorsal side of the columnar epithelia. The wing pouch is indicated (purple) on the en face view. The apterous (dorsoventral) boundary is indicated by dashed green line on the side view of the wing pouch from a view along the dashed red lines. The peripodial epithelia is apical to the columnar epithelia

C-I) Wing imaginal discs with Gukh::mCherry (red) were immunolabeled using antibodies raised against the Gukh C-terminal domain (Gukh-C) (C-F) and the N-terminus (Gukh-N) (G-I). Each enface panel represents a Z-projection. Scale bars: 15 μm. Asterisks marks the peripodial epithelia in the side view (F)
Enface sections at the apical level (C, G), intermediate level (D, H) and basal level (E, I) of the columnar epithelium are shown with the corresponding Z number. Distribution of Gukh::mCherry is the same as with the C-terminal and N-terminal antibodies across all the levels.

J) Cartoon of the columnar epithelia in 3D at the convergence of three cells with the apical, intermediate and basal domains indicated along with the placement of the SJ, TCJ, AJ and focal adhesions.

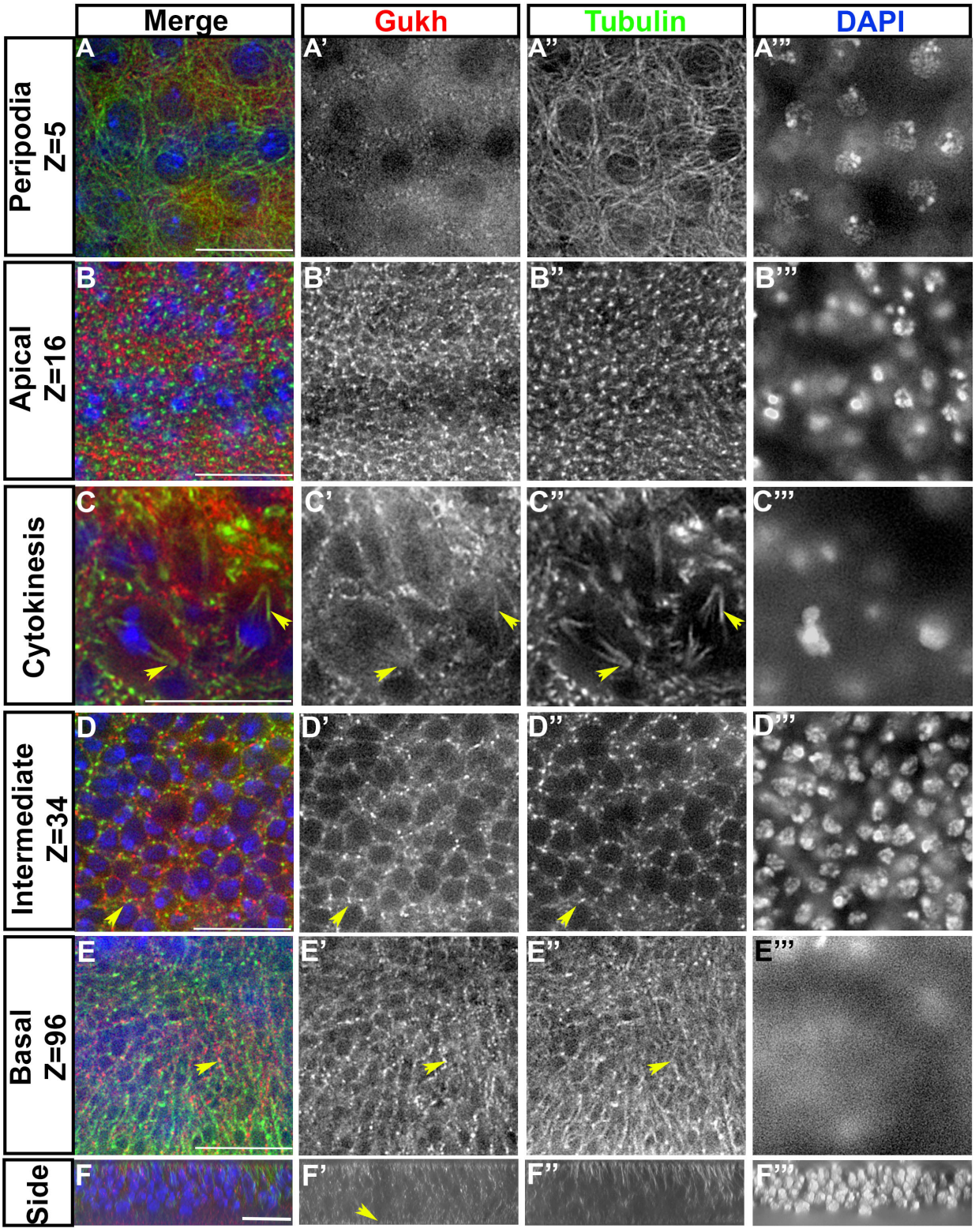
Merge
Gukh
Tubulin
DAPI
Peripodia Z=5
Apical Z=16
Cytokinesis
Intermediate Z=34
Basal Z=96
Side
A
A'
A''
A'''
B
B'
B''
B'''
C
C'
C''
C'''
D
D'
D''
D'''
E
E'
E''
E'''
F
F'
F''
F'''

Supplemental Figure 2.2. Gukh distribution is independent of microtubules in interphase cells.

Gukh::mCherry localization at the peripodial and columnar epithelia (apical, intermediate and basal) relative to immunolabeled alpha-tubulin (green), and DAPI (blue)..Each en face panel represents a Z-projection digitally magnified 2× except 3×in C. Scale bars: 15 μm.
A) Peripodia: Z=5. Gukh puncta do not co-localize with the microtubules in these squamous epithelia.
B) Apical domain: Z=16. Gukh does not co-localize with concentrated aggregations of alpha-tubulin.
C) Apical domain: Z=16. 3X digital magnification of a mitotic cell in B. Gukh co-localizes with tubulin during cytokinesis (yellow arrow).
D) Intermediate domain: Z=34. Gukh puncta are distinct from the microtubules, which run parallel to the longitudinal axis of the cell in this domain.
E) Basal domain: Z=96. Expression of Gukh and tubulin do not overlap.
F) Side view. Gukh localizes strongly to apical and basal domain (arrows).

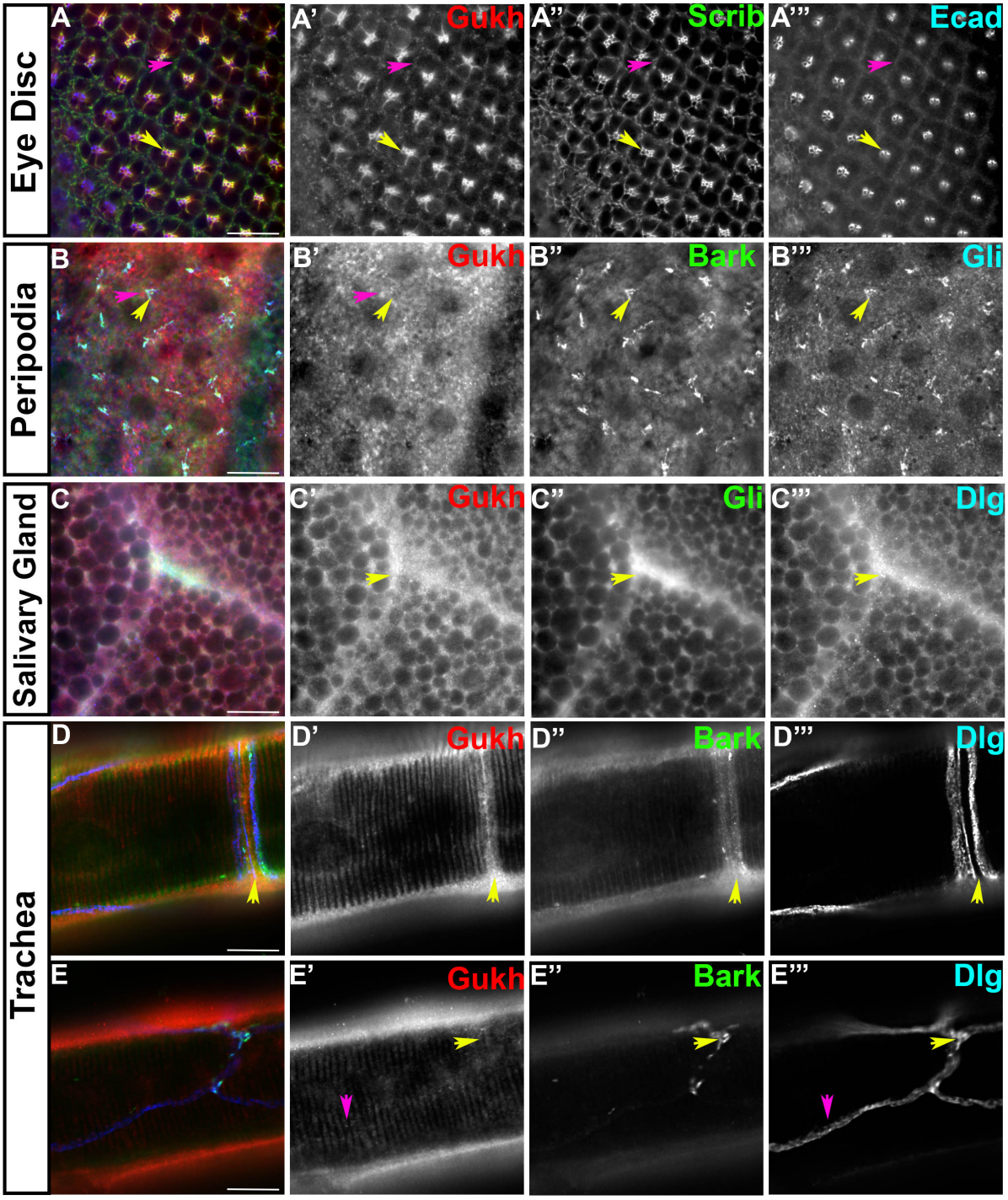
Eye Disc
A
A'
Gukh
A''
Scrib
A'''
Ecad
Peripodia
B
B'
Gukh
B''
Bark
B'''
Gli
Salivary Gland
C
C'
Gukh
C''
Gli
C'''
Dlg
Trachea
D
D'
Gukh
D''
Bark
D'''
Dlg
E
E'
Gukh
E''
Bark
E'''
Dlg

Supplemental Figure 2.3. Gukh::mCherry localizes to junctional domains in a range of other tissues in the 3rd instar *Drosophila* larva.

Each panel represents a single Z slice. Scale bars: 15 μm.

A) Eye imaginal disc. Gukh::mCherry (red, A') co-localizes with Scrib::GFP (green, A'') in the eye photoreceptors marked by the adherens junctions and anti-Ecad (blue, A''''). Gukh is also distributed with Scrib in the support cells surrounding the photoreceptors.

B) Peripodial epithelia. Gukh::mCherry (red, B') at the SJ and flanks (magenta arrows) but does not overlap with the TCJ (yellow arrows) immunolabeled with Bark:: GFP (green, B'') and Gli (blue, B''').

C) Salivary gland. Gukh::mCherry (red, C') co-localizes with immunolabeled Gli (green, C'') and Dlg (blue, C''').

D-E) Trachea. Gukh::mCherry (red, D',E'), Bark (green, D'',E") and Dlg (blue D''', E''') are expressed around the tracheal branch junction. Gukh is not concentrated at the tracheal TCJ (yellow arrows) and is weakly expressed around the bicellular junction (pink arrows).

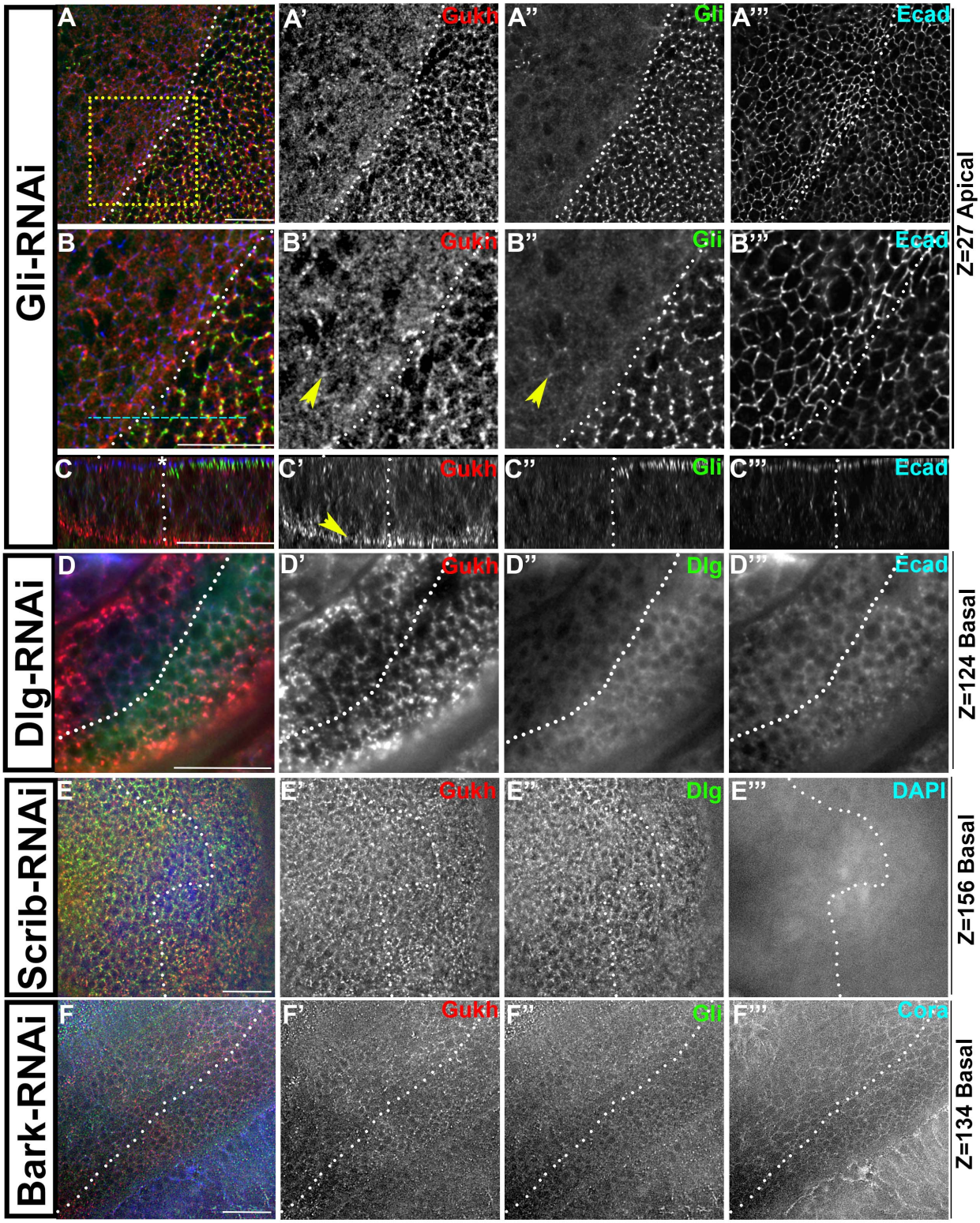
Gli-RNAi
Dlg-RNAi
Scrib-RNAi
Bark-RNAi
A
A'
Gukh
A''
Gli
A'''
Ecad
B
B'
Gukh
B''
Gli
B'''
Ecad
Z=27 Apical
C
C'
Gukh
C''
Gli
C'''
Ecad
D
D'
Gukh
D''
Dlg
D'''
Ecad
Z=124 Basal
E
E'
Gukh
E''
Dlg
E'''
DAPI
Z=156 Basal
F
F'
Gukh
F''
Gli
F'''
Cora
Z=134 Basal

Supplemental Figure 2.4. Loss of Gli affects Gukh at the TCJ but not basal domain.

Apterous-GAL4 driving RNAi on the dorsal side of the wing imaginal disc. White dotted lines indicate the apterous (dorsal-ventral) expression boundary, with the dorsal side oriented to the left of each panel. Each panel represents a single Z slice. Scale bars: 15 μm.

A-D) Gli-RNAi. Gli-RNAi downregulates Gli (green, A'',B", C") on the apterous side and Gukh (red, A', B', C') is reduced at the SJ and the TCJ. The adherens junctions are marked with Ecad (blue, A''', B''', C''').
B) A 2× digital magnification of the yellow dotted box in A. Gukh is retained when Gli remnants are observed (yellow arrows).
C) Side view of A. Gli-RNAi downregulates apical Gukh at the SJ level but Gukh at the basal domain (yellow arrow) is not affected.
D) Dlg-RNAi. Dlg RNAi downregulates Dlg (green D'') on the apterous side but basal localization of Gukh (red, D') is unaffected (Z=124).
E) Scrib-RNAi. At the basal domain (Z=155) knockdown of Scrib does not affect the distribution of Dlg (green, E") or Gukh (red, E') compared to the control non-apterous side.
F) Bark-RNAi. At the basal domain (Z=134) knockdown of Bark does not affect the distribution of Gukh (red, F') or Cora (blue, F''') compared to the control non-apterous side. Gli (green, F") is not expressed in this domain.

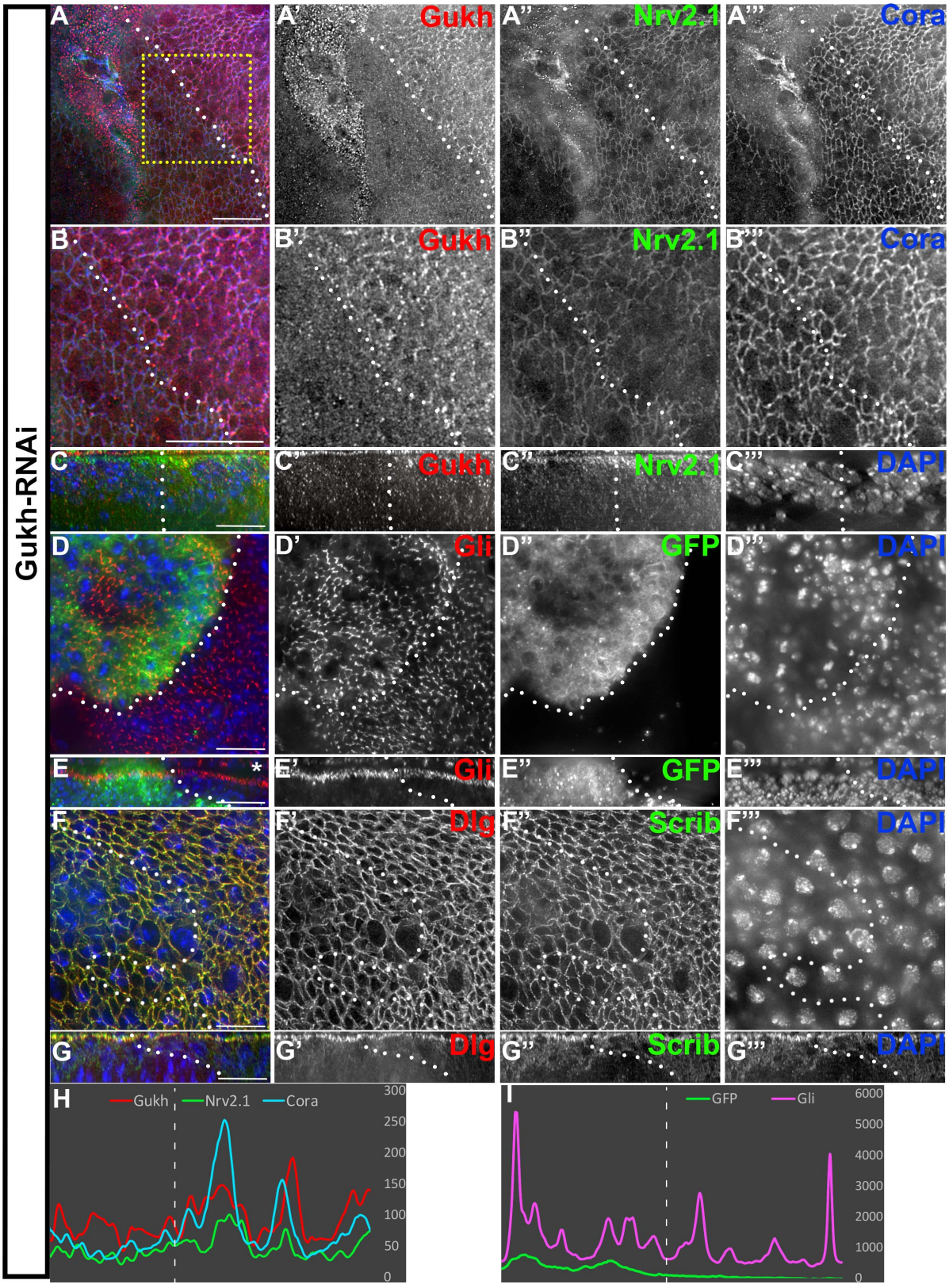
Gukh-RNAi
A
A'
Gukh
A''
Nrv2.1
A'''
Cora
B
B'
Gukh
B''
Nrv2.1
B'''
Cora
C
C'
Gukh
C''
Nrv2.1
C'''
DAPI
D
D'
Gli
D''
GFP
D'''
DAPI
E
*
E'
Gli
E''
GFP
E'''
DAPI
F
F'
Dlg
F''
Scrib
F'''
DAPI
G
G'
Dlg
G''
Scrib
G'''
DAPI
H
Gukh
Nrv2.1
Cora
300
250
200
150
100
50
0
I
GFP
Gli
6000
5000
4000
3000
2000
1000
0

Supplemental Figure 2.5. Knockdown of Gukh does not affect the localization of TCJ proteins, Gli, Dlg and Scrib.

Apterous-GAL4 drives Gukh-RNAi on the dorsal side of the wing imaginal disc. White dotted lines indicate the apterous (dorsal-ventral) expression boundary with the dorsal side oriented to the left of each panel. Each panel represents a single Z slice. Scale bars: 15 μm.

A-C) Knockdown of Gukh does not affect SJ proteins. Gukh::mCherry is (red, A', B',C') is reduced on the apterous side while the SJ proteins Nrv2.1 (green, A'', B", C") and Cora (blue, A''', B''') remain at the SJ. A region of the wing disc illustrating the unevenness of the epithelia with the Gukh-RNAi is marked with an asterisk. B) 2× digital magnification of the area enclosed by the yellow dotted box in A. C) Side view of A.

D-E) Apterous-GAL4 drives Gukh-RNAi and mcd8-GFP in the dorsal side. Gli (green, D') localization to the TCJ is not affected by knockdown of Gukh.
E: Side view of A. Gukh-RNAi does not affect Gli localization to the apical domain (red, E') but causes cell migration basally (green, D'). Nrv2.1 is slightly downregulated (green, B'').
F: Gukh-RNAi is driven by apterous-GAL4 on the wing dorsal side. The apterous boundary was determined by GAL4 staining (data not shown). Dlg (green, F'') and Scrib (blue, F''') localize and express normally at the SJ and TCJ.
G: Side view of F. Gukh-RNAi does not affect Dlg (green, F'') and Scrib (blue, G'') localization to the apical domain.
H: The relative fluorescence intensity profiles of A. White dashed lines mark the apterous boundary with the apterous side to the left of the line. In Gukh-RNAi, Gukh (red), Nrv2.1 (green), Cora (blue) intensity signal is reduced.
I: The relative fluorescence intensity profiles of D. White dashed lines mark the apterous boundary with the apterous side to the left of the line. In Gukh-RNAi, Gli intensity levels and pattern of peaks are unchanged.

CHAPTER 3. Summary and Future Directions

The focus of this thesis was to determine if the Gukh scaffolding protein was present and necessary for tricellular junction formation and function. Given the role of Gukh in other tissues in mediating the distribution of Dlg and Scrib, our original hypothesis was that Gukh was necessary at the TCJ to localize Scrib and Dlg. We found Gukh distributed at many junctional domains such as the septate junctions and tricellular junctions, and at focal adhesions in the intermediate and basal domains. However, loss of Gukh did not disrupt these junctional domains with the exception of the intermediate domain focal adhesions. Conversely, the loss of these domains resulted in the loss of Gukh but independently of each other. Finally, the loss of Gukh triggered JNK-mediated apoptosis and cell delamination.

These findings did not support the hypothesis that Gukh is a TCJ protein and instead suggest that it is essential in other cellular mechanisms, namely the adhesion at the intermediate domain in a polarized epithelium. The function of the integrin/talin complex and Gukh in the intermediate domain remains unknown. While focal adhesions have been observed in the lateral membrane/intermediate domain in the wing disc and other tissues (Brower and Jaffe, 1989; Brown et al., 2000), the function and formation of these focal adhesion sites is not well understood. Overall, we propose talin and β-integrin co-localize to form FAC-like structures in the intermediate domain and that Gukh plays a role in either the function of the complex or the localization to this domain. Further investigation is needed to better understand the role of Gukh and also the FAC structures in the intermediate domain.

3.1 Future directions – Testing Gukh isoforms, interactions and domain function

The discussion in Chapter 2 presents a detailed discussion of the results obtained in this thesis. The following section provides some potential future directions for the next stages of this

research project. While *gukh* is predicted to have one transcription start site and all four predicted isoforms contain the WHD, not all isoforms have been verified *in vivo*. Among the four predicted isoforms of Gukh, two of which contain a C-terminal PDZ-binding motif, including isoform C. The Cherry-tagged Gukh used in this thesis labels all predicted isoforms and therefore it is not clear if all isoforms are expressed in the wing epithelium or distributed within the epithelium in the same pattern. While we noted some subtle differences in the intensity levels between the immunolabeling with Gukh-C antibody and Gukh::mCh, but not Gukh-N, at the apical and basal domains (data not shown), further investigation is needed to draw concrete conclusions. To detect which isoforms are expressed within the wing disc, we attempted western blot analysis on proteins isolated from the wing imaginal disc. Preliminary findings using Gukh::mCherry wing disc lysate and anti-mCherry antibody showed five distinct bands (data not shown). While two of these bands (~100 kDA and ~230 kDA) were around the predicted protein sizes (~110 kDA and ~200kDA), some other bands were at unpredicted sizes (~50kDA, ~150kDA, ~260kDA). Furthermore, lysate from Gukh::mCherry brain lobes showed bands from different sizes. This suggests that post-translational modification, or tissue-specific isoform expression may be at play. Due the limited quantity of Gukh antibodies, we propose to generate antibodies raised against the domains of Gukh, specifically the WHD, the NHS and C-terminal Dlg binding domains, to further investigate which isoforms are differentially expressed in future western blot analyses.

Gukh has multiple roles as a scaffolding protein and contains an N-terminal WAVE homology domain (WHD), NHS domain, and C-terminal Dlg-binding domain. However, the protein interactions mediated by these domains or their functions have not been determined in the wing epithelium. The C-terminal half of Gukh contains the NHS and Dlg-binding domains

and there is evidence that this part of Gukh plays roles in a range of developmental processes including mediating the termination of photoreceptors at the optic lobe (Berger et al., 2008), facilitating the associate of Dlg and Scrib (Caria et al., 2018; Mathew et al., 2002) and regulating the interaction of Dlg in neuroblast division (Golub et al., 2017; Qian and Prehoda, 2006). In Chapter 2, we determined that the C-terminal domain of Gukh was sufficient to block the normal recruitment of integrin to the lateral membrane, again suggesting that this region mediates protein-protein interactions. The role of the WHD in the Gukh N-terminal half has not been studied either. To better understand the function, specific mutations in different domains of Gukh can be introduced in future experiments using the CRISPR-Cas9 genome editing system (Gratz et al., 2015). We propose to create precise deletions of the WHD, NHS and Dlg-binding domains to investigate the function of each domain independently. The change in protein distribution can be assessed in trans-heterozygous mutants by tagging mutant proteins with a fluorescent tag or using newly generated antibodies. If the loss of WHD changes the distribution of Gukh to the cell contacts, this would lend support to the hypothesis the pathogenesis of NHS is likely due to the mislocalization of NHS proteins resulting from the loss of WHD (Huang et al., 2006; Sharma et al., 2009).

Furthermore, we propose to test the potential interaction between PDZ proteins and Gukh. As two of the predicted isoforms of *gukh* contain a PDZ-binding motif, and Gukh has been shown to interact with PDZ proteins Dlg and Scrib, it is likely that Gukh localizes to the junctions to scaffold PDZ proteins like Varicose, and Canoe. Using antibodies to immunolabel candidate PDZ proteins, we can assess whether the loss of Gukh affects the expression and localization of PDZ proteins in Gukh RNAi-mediated knockdown, or in *gukh* mutants lacking the PDZ binding motif.

In the developing *Drosophila* wing epithelia, WAVE complexes are found at the focal adhesion complex (FAC) with talin and integrins, and function to stabilize integrin junctions (Gohl et al., 2010). However, the potential role of Gukh at the FAC has not been explored. The *gukh* WHD is highly conserved with the vertebrate *NHS* WHD which is conserved among WAVE family proteins. WAVE proteins facilitate the activation Arp2/3 complex for rapid actin assembly (Kurisu and Takenawa, 2009), in which the WHD is critical for forming the WAVE complex (Bompard and Caron, 2004; Kurisu and Takenawa, 2009). Thus there is the possibility that Gukh may mediate cytoskeleton dynamics through the WHD domain. The NHS protein family is postulated to be a member of the WAVE/SCAR protein complex with Haematopoietic stem/progenitor cell protein 300 (HSPC300) and proteins of the Abl interactor (Abi) family (Brooks et al., 2010). Loss of NHS triggers the upregulation of HSPC 300 and Abi (Brooks et al., 2010) leading to a model where NHS is responsible for controlling rearrangement of the actin cytoskeleton. We could use the CRISPR mutants described above to further investigate the interactions mediated by the WHD at focal adhesions and with actin cytoskeleton. We propose to first test whether the WHD in Gukh also functions in a WAVE/SCAR protein complex with *Drosophila* Abelson interacting proteins (dAbi) and HSPC 300, both of which are functionally conserved with the human orthologs (Juang and Hoffmann, 1999; Qurashi et al., 2007). We propose to perform RNAi-mediated knockdown targeting the WHD of Gukh, then investigate whether levels of Abi and HSPC 300 are affected. Next, to determine whether a direct interaction is involved, an immunoprecipitation can be performed. Alternatively, to investigate the interaction between these proteins spatially in the tissue, a proximity ligation assay (PLA) can be perform in a similar manner as previously described in our system (Sharifkhodaei et al., 2019). By assaying the distribution of actin (using life-act::GFP) and the distribution of Arp2/3 complex

in the knockdown of Gukh, we can confirm whether Gukh plays a role in the WAVE/SCAR complex. Using the above approach, the interaction between Gukh and *Drosophila* Lasp can also be investigated. It has been noted that NHS co-localizes with Lasp-1 in the vertebrate dynamic focal adhesion complex *in* Caco-2 cells (Brooks et al., 2010). We predict that these experiments would elucidate whether Gukh is localized at the TCJ and around the basal focal adhesion complex for WAVE/SCAR complex and/or the focal adhesion complex function.

3.2 Future directions - Testing normal and mutant human NHS function in the *Drosophila* model

We predict our findings would be translatable to the vertebrate system where Gukh is homologous to the vertebrate protein NHS (Caria et al., 2018; Katoh and Katoh, 2004) with 30% identity and 63% similarity between *Drosophila* Gukh and human NHS. While the distribution of NHS in cultured epithelia suggests an association with TJs or potentially focal adhesions, the role of NHS *in vivo* has not been determined. At least four transcription start sites of the human NHS genes have been predicted (Fig 1.6). Of interest are the transcription of NHS-A and NHS-1A which are initiated from exon 1 encoding the N-terminal WHD (Brooks et al., 2010; Sharma et al., 2009). Although NHS-A and NHS-1A are expressed in the developing eye and brain of the mouse (Sharma et al., 2009), NHS-A is known to associate with the cell membrane with ZO-1 in Madin Darby Canine Kidney (MDCK) epithelial cells and in neonatal rat lens; whereas isoforms lacking exon 1 are found in non-epithelial tissues and the cell cytoplasm (Brooks et al., 2010; Sharma et al., 2006, 2009). RT-PCR from human lens, retina, and brain tissue, further demonstrate that exon 3a is alternatively spliced from exon 1 transcripts (Sharma et al., 2009). Loss of function mutations of *NHS* are predicted to affect isoforms NHS-A and NHS-1A in humans. In *Xcat* mouse, the introduction of a late insertion mutation into mouse NHS gene

disrupts the expression of *Nhs1*, equivalent of *NHS-A*, and results in cataracts (Huang et al., 2006). Nhs exon1 has been implicated to mediate the localization of NHS1 to the cytoplasm *in vitro* (Huang et al., 2006). Thus, it is hypothesized that NHS-A is responsible for the congenital cataracts, and the splice variations may contribute to the phenotypic pleiotropy observed in affected individuals. (Brooks et al., 2010). This hypothesis can be tested in future experiments in the *Drosophila* system. We propose to test NHS function by expressing the human NHS isoforms and in the wing disc epithelia. If the key protein domains are sufficiently conserved, the expression of *NHS* may rescue the gukh-RNAi or *gukh* mutant phenotypes in the wing disc. Thus, JNK-mediated cell death, cell migration and cell delamination could be rescued.

Although previous vertebrate studies postulated that NHS may be caused by tight junction dysregulation as NHS protein co-localizes with ZO-1 (Ling et al., 2019; Sharma et al., 2009), the knockdown of NHS in MTLn3 cells does not affect ZO-1 localization. Our findings are congruent with the alternative hypothesis that NHS is not caused by occluding junction dysregulation. We found that the loss of Gukh did not affect junction formation, but disrupted the localization of integrins in the lateral domain. This suggests that a model wherein disruption to cell adhesion causes NHS. In humans, the dysregulation of integrins have been correlated with cataract formation. Generally, cataractous lenses expresses integrin α2, α3, α6, β1subunits normally but α5, β2 subunits ectopically (Wederell and de Iongh, 2006). Assuming NHS and Gukh is functionally conserved, we predicted the knockdown of Gukh in the eye imaginal disc would also disrupt the expression of integrin subunits resulting in eye defects.

To date, around 50 human families have been described with mutations in the *NHS* gene (Ling et al., 2019). The investigation into the cellular mechanism which causes NHS is challenging in humans given the alternative transcription start sites and broad expression of NHS

(Burdon et al., 2003). Previous studies have shown the causative mutation likely affects the expression of the N-terminus isoform NHS-A, (Sharma et al., 2006, 2008). Some premature mutation affects the localization of NHS proteins from the cytoplasm to the cell contacts but the functional consequence or the mechanisms underlying these changes are not understood. To better understand and predict the pathogenicity of mutations, we propose using our system to test whether mutations at conserved amino acids result in disrupted protein function. First, we would test whether *Drosophila* Gukh and human NHS are conserved functionally by expressing NHS in *gukh* null mutants. If the *gukh* mutant phenotype can be restored by the NHS expression, we can then express mutant variants of human NHS in *gukh* null mutant. Furthermore, we can predict the pathogenicity of variants by mapping the sequence human *NHS* mutations to corresponding location on the *gukh* and correlating those to the observed effect on the development of the visual system. Overall, we predict these experiments would provide valuable insight to the pathogenicity of NHS and provide a better understanding of the cellular mechanism that underlies the congenital cataracts and phenotypic pleiotropy of NHS.

References

Alatortsev, V.E., Kramerova, I.A., Frolov, M.V., Lavrov, S.A., and Westphal, E.D. (1997). *Vinculin* gene is non-essential in *Drosophila melanogaster*. FEBS Letters *413*, 197–201.

Albertson, R. (2004). Scribble protein domain mapping reveals a multistep localization mechanism and domains necessary for establishing cortical polarity. Journal of Cell Science *117*, 6061–6070.

Arabzadeh, A., Troy, T.-C., and Turksen, K. (2006). Role of the Cldn6 Cytoplasmic Tail Domain in Membrane Targeting and Epidermal Differentiation In Vivo. MCB *26*, 5876–5887.

Araujo, H. (2003). Integrins modulate Sog activity in the *Drosophila* wing. Development *130*, 3851–3864.

Ayala-Torres, C., Krug, S.M., Schulzke, J.D., Rosenthal, R., and Fromm, M. (2019). Tricellulin Effect on Paracellular Water Transport. IJMS *20*, 5700.

Balda, M.S., Whitney, J.A., Flores, C., González, S., Cereijido, M., and Matter, K. (1996). Functional dissociation of paracellular permeability and transepithelial electrical resistance and disruption of the apical-basolateral intramembrane diffusion barrier by expression of a mutant tight junction membrane protein. Journal of Cell Biology *134*, 1031–1049.

Banerjee, S. (2006). Axonal Ensheathment and Septate Junction Formation in the Peripheral Nervous System of *Drosophila*. Journal of Neuroscience *26*, 3319–3329.

Batz, T., Forster, D., and Luschnig, S. (2014). The transmembrane protein Macroglobulin complement-related is essential for septate junction formation and epithelial barrier function in *Drosophila*. Development *141*, 899–908.

Bauer, R., Weimbs, A., Lechner, H., and Hoch, M. (2006). *D* E-Cadherin, a Core Component of the Adherens Junction Complex Modifies Subcellular Localization of the *Drosophila* Gap Junction Protein Innexin2. Cell Communication & Adhesion *13*, 103–114.

Berger, J., Senti, K.-A., Senti, G., Newsome, T.P., Åsling, B., Dickson, B.J., and Suzuki, T. (2008). Systematic Identification of Genes that Regulate Neuronal Wiring in the *Drosophila* Visual System. PLoS Genet *4*, e1000085.

Bhat, A.A., Uppada, S., Achkar, I.W., Hashem, S., Yadav, S.K., Shanmugakonar, M., Al-Naemi, H.A., Haris, M., and Uddin, S. (2019). Tight Junction Proteins and Signaling Pathways in Cancer and Inflammation: A Functional Crosstalk. Front. Physiol. *9*, 1942.

Bieber, A.J., Snow, P.M., Hortsch, M., Patel, N.H., Jacobs, J.R., Traquina, Z.R., Schilling, J., and Goodman, C.S. (1989). *Drosophila* neuroglian: A member of the immunoglobulin superfamily with extensive homology to the vertebrate neural adhesion molecule L1. Cell *59*, 447–460.

Bilder, D., and Perrimon, N. (2000). Localization of apical epithelial determinants by the basolateral PDZ protein Scribble. Nature *403*, 676–680.

Bixler, D., Higgins, M., and Hartsfield, J. (2008). The Nance-Horan syndrome: a rare X-linked ocular-dental trait with expression in heterozygous females. Clinical Genetics *26*, 30–35.

Bliss, K.T., Chu, M., Jones-Weinert, C.M., and Gregorio, C.C. (2013). Investigating lasp-2 in cell adhesion: new binding partners and roles in motility. MBoC *24*, 995–1006.

Bompard, G., and Caron, E. (2004). Regulation of WASP/WAVE proteins: making a long story short. J. Cell Biol. *166*, 957–962.

Bonello, T.T., Choi, W., and Peifer, M. (2019). Scribble and Discs-large direct initial assembly and positioning of adherens junctions during the establishment of apical-basal polarity. Development *146*, dev180976.

Bosveld, F., Markova, O., Guirao, B., Martin, C., Wang, Z., Pierre, A., Balakireva, M., Gaugue, I., Ainslie, A., Christophorou, N., et al. (2016). Epithelial tricellular junctions act as interphase cell shape sensors to orient mitosis. Nature *530*, 495–498.

Brand, A.H., and Perrimon, N. (1993). Targeted gene expression as a means of altering cell fates and generating dominant phenotypes. Development *118*, 401–415.

Brooks, S.P., Coccia, M., Tang, H.R., Kanuga, N., Machesky, L.M., Bailly, M., Cheetham, M.E., and Hardcastle, A.J. (2010). The Nance–Horan syndrome protein encodes a functional WAVE homology domain (WHD) and is important for co-ordinating actin remodelling and maintaining cell morphology. Human Molecular Genetics *19*, 2421–2432.

Brower, D.L., and Jaffe, S.M. (1989). Requirement for integrins during *Drosophila* wing development. Nature *342*, 285–287.

Brower, D.L., Wilcox, M., Piovant, M., Smith, R.J., and Reger, L.A. (1984). Related cell-surface antigens expressed with positional specificity in *Drosophila* imaginal discs. Proceedings of the National Academy of Sciences *81*, 7485–7489.

Brown, N.H., Gregory, S.L., and Martin-Bermudo, M.D. (2000). Integrins as Mediators of Morphogenesis in *Drosophila*. Developmental Biology *223*, 1–16.
Brown, N.H., Gregory, S.L., Rickoll, W.L., Fessler, L.I., Prout, M., White, R.A.H., and Fristrom, J.W. (2002). Talin Is Essential for Integrin Function in *Drosophila*. Developmental Cell *3*, 569–579.
Brumby, A.M. (2003). scribble mutants cooperate with oncogenic Ras or Notch to cause neoplastic overgrowth in *Drosophila*. The EMBO Journal *22*, 5769–5779.
Burdon, K.P., McKay, J.D., Sale, M.M., Russell-Eggitt, I.M., Mackey, D.A., Wirth, M.G., Elder, J.E., Nicoll, A., Clarke, M.P., FitzGerald, L.M., et al. (2003). Mutations in a Novel Gene, NHS, Cause the Pleiotropic Effects of Nance-Horan Syndrome, Including Severe Congenital Cataract, Dental Anomalies, and Mental Retardation. The American Journal of Human Genetics *73*, 1120–1130.
Butt, E., and Raman, D. (2018). New Frontiers for the Cytoskeletal Protein LASP1. Front. Oncol. *8*, 391.
Caria, S., Magtoto, C.M., Samiei, T., Portela, M., Lim, K.Y.B., How, J.Y., Stewart, B.Z., Humbert, P.O., Richardson, H.E., and Kvansakul, M. (2018). *Drosophila melanogaster* Guk-holder interacts with the Scribbled PDZ1 domain and regulates epithelial development with Scribbled and Discs Large. J. Biol. Chem. *293*, 4519–4531.
Chalcroft, J.P., and Bullivant, S. (1970). AN INTERPRETATION OF LIVER CELL MEMBRANE AND JUNCTION STRUCTURE BASED ON OBSERVATION OF FREEZE-FRACTURE REPLICAS OF BOTH SIDES OF THE FRACTURE. Journal of Cell Biology *47*, 49–60.
Chattopadhyay, R., Dyukova, E., Singh, N.K., Ohba, M., Mobley, J.A., and Rao, G.N. (2014). Vascular Endothelial Tight Junctions and Barrier Function Are Disrupted by 15(*S*)-Hydroxyeicosatetraenoic Acid Partly via Protein Kinase Cϵ-mediated Zona Occludens-1 Phosphorylation at Threonine 770/772. J. Biol. Chem. *289*, 3148–3163.
Chattopadhyay, R., Dyukova, E., Singh, N.K., Ohba, M., Mobley, J.A., and Rao, G.N. (2019). Correction: Vascular endothelial tight junctions and barrier function are disrupted by 15(*S*)-hydroxyeicosatetraenoic acid partly via protein kinase C ϵ-mediated zona occludens-1 phosphorylation at threonine 770/772. J. Biol. Chem. *294*, 3311–3311.

Chen, J., Sayadian, A.-C., Lowe, N., Lovegrove, H.E., and St Johnston, D. (2018). An alternative mode of epithelial polarity in the *Drosophila* midgut. PLoS Biol *16*, e3000041.
Chew, C.S. (2002). Lasp-1 binds to non-muscle F-actin in vitro and is localized within multiple sites of dynamic actin assembly in vivo. Journal of Cell Science *115*, 4787–4799.
Chiba, H., Osanai, M., Murata, M., Kojima, T., and Sawada, N. (2008). Transmembrane proteins of tight junctions. Biochimica et Biophysica Acta (BBA) - Biomembranes *1778*, 588–600.
Cohen, B., McGuffin, M.E., Pfeifle, C., Segal, D., and Cohen, S.M. (1992). apterous, a gene required for imaginal disc development in *Drosophila* encodes a member of the LIM family of developmental regulatory proteins. Genes & Development *6*, 715–729.
Cohen, B., Simcox, A.A., and Cohen, S.M. (1993). Allocation of the thoracic imaginal primordia in the *Drosophila* embryo. Development *117*, 597–608.
Cohen, C.J., Shieh, J.T.C., Pickles, R.J., Okegawa, T., Hsieh, J.-T., and Bergelson, J.M. (2001). The coxsackievirus and adenovirus receptor is a transmembrane component of the tight junction. Proceedings of the National Academy of Sciences *98*, 15191–15196.
Cording, J., Berg, J., Kading, N., Bellmann, C., Tscheik, C., Westphal, J.K., Milatz, S., Gunzel, D., Wolburg, H., Piontek, J., et al. (2013). In tight junctions, claudins regulate the interactions between occludin, tricellulin and marvelD3, which, inversely, modulate claudin oligomerization. Journal of Cell Science *126*, 554–564.
Cummins, P.M. (2012). Occludin: One Protein, Many Forms. Molecular and Cellular Biology *32*, 242–250.
Dinkins, M.B., Fratto, V.M., and LeMosy, E.K. (2008). Integrin alpha chains exhibit distinct temporal and spatial localization patterns in epithelial cells of the *Drosophila* ovary. Dev. Dyn. *237*, 3927–3939.
Dominguez-Gimenez, P., Brown, N.H., and Martin-Bermudo, M.D. (2007). Integrin-ECM interactions regulate the changes in cell shape driving the morphogenesis of the *Drosophila* wing epithelium. Journal of Cell Science *120*, 1061–1071.
Esmangart de Bournonville, T., and Le Borgne, R. (2020). Interplay between Anakonda, Gliotactin, and M6 for Tricellular Junction Assembly and Anchoring of Septate Junctions in *Drosophila* Epithelium. Current Biology *30*, 4245-4253.e4.

Faivre-Sarrailh, C. (2004). *Drosophila* contactin, a homolog of vertebrate contactin, is required for septate junction organization and paracellular barrier function. Development *131*, 4931–4942.

Fan, Y., and Bergmann, A. (2008). Apoptosis-induced compensatory proliferation. The Cell is dead. Long live the Cell! Trends in Cell Biology *18*, 467–473.

Fanning, A.S., and Anderson, J.M. (1999). PDZ domains: fundamental building blocks in the organization of protein complexes at the plasma membrane. J. Clin. Invest. *103*, 767–772.

Farquhar, M.G., and Palade, G.E. (1963). JUNCTIONAL COMPLEXES IN VARIOUS EPITHELIA. Journal of Cell Biology *17*, 375–412.

Fehon, R.G., Dawson, I.A., and Artavanis-Tsakonas, S. (1994). A *Drosophila* homologue of membrane-skeleton protein 4.1 is associated with septate junctions and is encoded by the coracle gene. Development *120*, 545–557.

Fristrom, D., Wilcox, M., and Fristrom, J. (1993). The distribution of PS integrins, laminin A and F-actin during key stages in *Drosophila* wing development. Development *117*, 509–523.

Funke, L., Dakoji, S., and Bredt, D.S. (2005). MEMBRANE-ASSOCIATED GUANYLATE KINASES REGULATE ADHESION AND PLASTICITY AT CELL JUNCTIONS. Annu. Rev. Biochem. *74*, 219–245.

Furuse, M., Hirase, T., Itoh, M., Nagafuchi, A., Yonemura, S., Tsukita, S., and Tsukita, S. (1993). Occludin: a novel integral membrane protein localizing at tight junctions. Journal of Cell Biology *123*, 1777–1788.

Furuse, M., Hata, M., Furuse, K., Yoshida, Y., Haratake, A., Sugitani, Y., Noda, T., Kubo, A., and Tsukita, S. (2002). Claudin-based tight junctions are crucial for the mammalian epidermal barrier. Journal of Cell Biology *156*, 1099–1111.

Fuse, N., Hirose, S., and Hayashi, S. (1994). Diploidy of *Drosophila* imaginal cells is maintained by a transcriptional repressor encoded by escargot. Genes & Development *8*, 2270–2281.

Garrido-Urbani, S., Bradfield, P.F., and Imhof, B.A. (2014). Tight junction dynamics: the role of junctional adhesion molecules (JAMs). Cell Tissue Res *355*, 701–715.

Genova, J.L., and Fehon, R.G. (2003). Neuroglian, Gliotactin, and the Na+/K+ ATPase are essential for septate junction function in *Drosophila*. Journal of Cell Biology *161*, 979–989.

Gilbert, M., M. (2005). Evolution of clams (cholinesterase-like adhesion molecules): structure and function during development. Front Biosci *10*, 2177.
Gilbert, M., Smith, J., Roskams, A.-J., and Auld, V.J. (2001). Neuroligin 3 is a vertebrate gliotactin expressed in the olfactory ensheathing glia, a growth-promoting class of macroglia. Glia *34*, 151–164.
Gohl, C., Banovic, D., Grevelhörster, A., and Bogdan, S. (2010). WAVE Forms Hetero- and Homo-oligomeric Complexes at Integrin Junctions in *Drosophila* Visualized by Bimolecular Fluorescence Complementation. J. Biol. Chem. *285*, 40171–40179.
Golub, O., Wee, B., Newman, R.A., Paterson, N.M., and Prehoda, K.E. (2017). Activation of Discs large by aPKC aligns the mitotic spindle to the polarity axis during asymmetric cell division. ELife *6*, e32137.
González-Mariscal, L., Betanzos, A., and Ávila-Flores, A. (2000). MAGUK proteins: structure and role in the tight junction. Seminars in Cell & Developmental Biology *11*, 315–324.
Gonzalez-Mariscal, L., Miranda, J., Ortega-Olvera, J.M., Gallego-Gutierrez, H., Raya-Sandino, A., and Vargas-Sierra, O. (2016). Involvement of Tight Junction Plaque Proteins in Cancer. Curr Pathobiol Rep *4*, 117–133.
Goossens, T., Kang, Y.Y., Wuytens, G., Zimmermann, P., Callaerts-Vegh, Z., Pollarolo, G., Islam, R., Hortsch, M., and Callaerts, P. (2011). The *Drosophila* L1CAM homolog Neuroglian signals through distinct pathways to control different aspects of mushroom body axon development. Development *138*, 1595–1605.
Grabbe, C. (2004). Focal adhesion kinase is not required for integrin function or viability in *Drosophila*. Development *131*, 5795–5805.
Gratz, S.J., Rubinstein, C.D., Harrison, M.M., Wildonger, J., and O'Connor-Giles, K.M. (2015). CRISPR-Cas9 Genome Editing in *Drosophila*. Current Protocols in Molecular Biology *111*.
Hall, S., and Ward, R.E. (2016). Septate Junction Proteins Play Essential Roles in Morphogenesis Throughout Embryonic Development in *Drosophila*. G3 *6*, 2375–2384.
Hall, S., Bone, C., Oshima, K., Zhang, L., McGraw, M., Lucas, B., Fehon, R.G., and Ward, R.E. (2014). Macroglobulin complement-related encodes a protein required for septate

junction organization and paracellular barrier function in Drosophila. Development *141*, 889–898.

Hamazaki, Y., Itoh, M., Sasaki, H., Furuse, M., and Tsukita, S. (2002). Multi-PDZ Domain Protein 1 (MUPP1) Is Concentrated at Tight Junctions through Its Possible Interaction with Claudin-1 and Junctional Adhesion Molecule. J. Biol. Chem. *277*, 455–461.

Harburger, D.S., and Calderwood, D.A. (2009). Integrin signalling at a glance. Journal of Cell Science *122*, 159–163.

Harris, T.J.C. (2012). Adherens Junction Assembly and Function in the Drosophila Embryo. In International Review of Cell and Molecular Biology, (Elsevier), pp. 45–83.

Harris, T.J.C., and Peifer, M. (2004). Adherens junction-dependent and -independent steps in the establishment of epithelial cell polarity in *Drosophila*. Journal of Cell Biology *167*, 135–147.

Hempstock, W., Sugioka, S., Ishizuka, N., Sugawara, T., Furuse, M., and Hayashi, H. (2020). Angulin-2/ILDR1, a tricellular tight junction protein, does not affect water transport in the mouse large intestine. Sci Rep *10*, 10374.

Higashi, T., and Miller, A.L. (2017). Tricellular junctions: how to build junctions at the TRICkiest points of epithelial cells. MBoC *28*, 2023–2034.

Higashi, T., Tokuda, S., Kitajiri, S. -i., Masuda, S., Nakamura, H., Oda, Y., and Furuse, M. (2013). Analysis of the “angulin” proteins LSR, ILDR1 and ILDR2 - tricellulin recruitment, epithelial barrier function and implication in deafness pathogenesis. Journal of Cell Science *126*, 966–977.

Higashi, T., Katsuno, T., Kitajiri, S., and Furuse, M. (2015). Deficiency of Angulin-2/ILDR1, a Tricellular Tight Junction-Associated Membrane Protein, Causes Deafness with Cochlear Hair Cell Degeneration in Mice. PLoS ONE *10*, e0120674.

Hildebrandt, A., Pflanz, R., Behr, M., Tarp, T., Riedel, D., and Schuh, R. (2015). Bark beetle controls epithelial morphogenesis by septate junction maturation in *Drosophila*. Developmental Biology *400*, 237–247.

Hough, C.D., Woods, D.F., Park, S., and Bryant, P.J. (1997). Organizing a functional junctional complex requires specific domains of the *Drosophila* MAGUK Discs large. Genes Dev. *11*, 3242–3253.

Huang, K.M., Wu, J., Duncan, M.K., Moy, C., Dutra, A., Favor, J., Da, T., and Stambolian, D. (2006). Xcat, a novel mouse model for Nance–Horan syndrome inhibits expression of the cytoplasmic-targeted Nhs1 isoform. Human Molecular Genetics *15*, 319–327.

Humbert, P.O., Grzeschik, N.A., Brumby, A.M., Galea, R., Elsum, I., and Richardson, H.E. (2008). Control of tumourigenesis by the Scribble/Dlg/Lgl polarity module. Oncogene *27*, 6888–6907.

Hynes, R.O. (2002). Integrins: Bidirectional, Allosteric Signaling Machines. Cell *110*, 673–687.

Ikenouchi, J., Furuse, M., Furuse, K., Sasaki, H., Tsukita, S., and Tsukita, S. (2005). Tricellulin constitutes a novel barrier at tricellular contacts of epithelial cells. Journal of Cell Biology *171*, 939–945.

Irie, M. (1997). Binding of Neuroligins to PSD-95. Science *277*, 1511–1515.

Itoh, M., Sasaki, H., Furuse, M., Ozaki, H., Kita, T., and Tsukita, S. (2001). Junctional adhesion molecule (JAM) binds to PAR-3. Journal of Cell Biology *154*, 491–498.

Janiszewska, M., Primi, M.C., and Izard, T. (2020). Cell adhesion in cancer: Beyond the migration of single cells. J. Biol. Chem. *295*, 2495–2505.

Juang, J.-L., and Hoffmann, F.M. (1999). *Drosophila* Abelson interacting protein (dAbi) is a positive regulator of Abelson tyrosine kinase activity. Oncogene *18*, 5138–5147.

Kale, G., Naren, A.P., Sheth, P., and Rao, R.K. (2003). Tyrosine phosphorylation of occludin attenuates its interactions with ZO-1, ZO-2, and ZO-3. Biochemical and Biophysical Research Communications *302*, 324–329.

Katoh, M., and Katoh, M. (2004). Identification and characterization of human GUKH2 gene in silico. Int. J. Oncol. *24*, 1033–1038.

Klapholz, B., and Brown, N.H. (2017). Talin - the master of integrin adhesions. J Cell Sci *130*, 2435–2446.

Kourtidis, A., Ngok, S.P., and Anastasiadis, P.Z. (2013). p120 Catenin: an essential regulator of cadherin stability, adhesion-induced signaling, and cancer progression. In Progress in Molecular Biology and Translational Science, (Elsevier), pp. 409–432.

Kurisu, S., and Takenawa, T. (2009). The WASP and WAVE family proteins. Genome Biol. *10*, 226.

Lahey, T., Gorczyca, M., Jia, X.X., and Budnik, V. (1994). The *Drosophila* tumor suppressor gene dlg is required for normal synaptic bouton structure. Neuron *13*, 823–835.
Lamb, R.S., Ward, R.E., Schweizer, L., and Fehon, R.G. (1998). *Drosophila coracle* , a Member of the Protein 4.1 Superfamily, Has Essential Structural Functions in the Septate Junctions and Developmental Functions in Embryonic and Adult Epithelial Cells. MBoC *9*, 3505–3519.
Lane, N.J., and Swales, L.S. (1982). Stages in the assembly of pleated and smooth septate junctions in developing insect embryos. J Cell Sci *56*, 245–262.
Laprise, P., Lau, K.M., Harris, K.P., Silva-Gagliardi, N.F., Paul, S.M., Beronja, S., Beitel, G.J., McGlade, C.J., and Tepass, U. (2009). Yurt, Coracle, Neurexin IV and the Na+,K+-ATPase form a novel group of epithelial polarity proteins. Nature *459*, 1141–1145.
Läubli, H., and Borsig, L. (2019). Altered Cell Adhesion and Glycosylation Promote Cancer Immune Suppression and Metastasis. Front. Immunol. *10*, 2120.
Laukoetter, M.G., Nava, P., Lee, W.Y., Severson, E.A., Capaldo, C.T., Babbin, B.A., Williams, I.R., Koval, M., Peatman, E., Campbell, J.A., et al. (2007). JAM-A regulates permeability and inflammation in the intestine in vivo. Journal of Experimental Medicine *204*, 3067–3076.
Lee, S., Zhou, L., Kim, J., Kalbfleisch, S., and Schöck, F. (2008). Lasp anchors the *Drosophila* male stem cell niche and mediates spermatid individualization. Mechanisms of Development *125*, 768–776.
Leoni, G., Neumann, P.-A., Sumagin, R., Denning, T.L., and Nusrat, A. (2015). Wound repair: role of immune–epithelial interactions. Mucosal Immunol *8*, 959–968.
Leptin, M., Bogaert, T., Lehmann, R., and Wilcox, M. (1989). The function of PS integrins during *Drosophila* embryogenesis. Cell *56*, 401–408.
Li, B., Zhuang, L., and Trueb, B. (2004). Zyxin Interacts with the SH3 Domains of the Cytoskeletal Proteins LIM-nebulette and Lasp-1. J. Biol. Chem. *279*, 20401–20410.
Li, H., Yang, L., Sun, Z., Yuan, Z., Wu, S., and Sui, R. (2018). A novel small deletion in the NHS gene associated with Nance-Horan syndrome. Sci Rep *8*, 2398.
Ling, C., Sui, R., Yao, F., Wu, Z., Zhang, X., and Zhang, S. (2019). Whole exome sequencing identified a novel truncation mutation in the NHS gene associated with Nance-Horan syndrome. BMC Med Genet *20*, 14.

Llimargas, M. (2004). Lachesin is a component of a septate junction-based mechanism that controls tube size and epithelial integrity in the *Drosophila* tracheal system. Development *131*, 181–190.

Maartens, A.P., Wellmann, J., Wictome, E., Klapholz, B., Green, H., and Brown, N.H. (2016). *Drosophila* vinculin is more harmful when hyperactive than absent, and can circumvent integrin to form adhesion complexes. J Cell Sci *129*, 4354–4365.

Mandell, K., and Parkos, C. (2005). The JAM family of proteins. Advanced Drug Delivery Reviews *57*, 857–867.

Masuda, S., Oda, Y., Sasaki, H., Ikenouchi, J., Higashi, T., Akashi, M., Nishi, E., and Furuse, M. (2011). LSR defines cell corners for tricellular tight junction formation in epithelial cells. Journal of Cell Science *124*, 548–555.

McNeil, E., Capaldo, C.T., and Macara, I.G. (2006). Zonula Occludens-1 Function in the Assembly of Tight Junctions in Madin-Darby Canine Kidney Epithelial Cells. MBoC *17*, 1922–1932.

Michel, M., Aliee, M., Rudolf, K., Bialas, L., Jülicher, F., and Dahmann, C. (2016). The Selector Gene apterous and Notch Are Required to Locally Increase Mechanical Cell Bond Tension at the *Drosophila* Dorsoventral Compartment Boundary. PLoS One *11*, e0161668.

Moh, M.C., and Shen, S. (2009). The roles of cell adhesion molecules in tumor suppression and cell migration: a new paradox. Cell Adh Migr *3*, 334–336.

Moyer, K.E., and Jacobs, J.R. (2008). Varicose: a MAGUK required for the maturation and function of *Drosophila* septate junctions. BMC Dev Biol *8*, 99.

Muller, B., Kistner, U., Veh, R., Cases-Langhoff, C., Becker, B., Gundelfinger, E., and Garner, C. (1995). Molecular characterization and spatial distribution of SAP97, a novel presynaptic protein homologous to SAP90 and the *Drosophila* discs-large tumor suppressor protein. J. Neurosci. *15*, 2354–2366.

Nagarkar-Jaiswal, S., Lee, P.-T., Campbell, M.E., Chen, K., Anguiano-Zarate, S., Cantu Gutierrez, M., Busby, T., Lin, W.-W., He, Y., Schulze, K.L., et al. (2015). A library of MiMICs allows tagging of genes and reversible, spatial and temporal knockdown of proteins in *Drosophila*. ELife *4*, e05338.

Narasimha, M., and Brown, N.H. (2004). Novel Functions for Integrins in Epithelial Morphogenesis. Current Biology *14*, 381–385.

Nayak, G., Lee, S.I., Yousaf, R., Edelmann, S.E., Trincot, C., Van Itallie, C.M., Sinha, G.P., Rafeeq, M., Jones, S.M., Belyantseva, I.A., et al. (2013). Tricellulin deficiency affects tight junction architecture and cochlear hair cells. J. Clin. Invest. *123*, 4036–4049.

Nelson, K.S., Furuse, M., and Beitel, G.J. (2010). The *Drosophila* Claudin Kune-kune Is Required for Septate Junction Organization and Tracheal Tube Size Control. Genetics *185*, 831–839.

Noirot-Timothée, C., and Noirot, C. (1980). Septate and Scalariform Junctions in Arthropods. In International Review of Cytology, (Elsevier), pp. 97–140.

Nonaka, M. (2004). Evolution of the complement system. Molecular Immunology *40*, 897–902.

Oda, H., Uemura, T., Harada, Y., Iwai, Y., and Takeichi, M. (1994). A *Drosophila* Homolog of Cadherin Associated with Armadillo and Essential for Embryonic Cell-Cell Adhesion. Developmental Biology *165*, 716–726.

Ohsawa, S., Sugimura, K., Takino, K., Xu, T., Miyawaki, A., and Igaki, T. (2011). Elimination of Oncogenic Neighbors by JNK-Mediated Engulfment in *Drosophila*. Developmental Cell *20*, 315–328.

Orth, M.F., Cazes, A., Butt, E., and Grunewald, T.G.P. (2015). An update on the LIM and SH3 domain protein 1 (LASP1): a versatile structural, signaling, and biomarker protein. Oncotarget *6*, 26–42.

Oshima, K., and Fehon, R.G. (2011). Analysis of protein dynamics within the septate junction reveals a highly stable core protein complex that does not include the basolateral polarity protein Discs large. Journal of Cell Science *124*, 2861–2871.

Pai, Y.-J., Abdullah, N.L., Mohd.-Zin, S.W., Mohammed, R.S., Rolo, A., Greene, N.D.E., Abdul-Aziz, N.M., and Copp, A.J. (2012). Epithelial fusion during neural tube morphogenesis. Birth Defects Research Part A: Clinical and Molecular Teratology *94*, 817–823.

Paul, S.M. (2003). The Na+/K+ ATPase is required for septate junction function and epithelial tube-size control in the *Drosophila* tracheal system. Development *130*, 4963–4974.

Perrimon, N. (1988). The maternal effect of lethal(1)discs-large-1: A recessive oncogene of *Drosophila melanogaster*. Developmental Biology *127*, 392–407.

Qurashi, A., Sahin, H.B., Carrera, P., Gautreau, A., Schenck, A., and Giangrande, A. (2007). HSPC300 and its role in neuronal connectivity. Neural Dev *2*, 18.

Raleigh, D.R., Marchiando, A.M., Zhang, Y., Shen, L., Sasaki, H., Wang, Y., Long, M., and Turner, J.R. (2010). Tight Junction–associated MARVEL Proteins MarvelD3, Tricellulin, and Occludin Have Distinct but Overlapping Functions. MBoC *21*, 1200–1213.

Ray, H.J., and Niswander, L. (2012). Mechanisms of tissue fusion during development. Development *139*, 1701–1711.

Requena, D., Álvarez, J.A., Gabilondo, H., Loker, R., Mann, R.S., and Estella, C. (2017). Origins and Specification of the *Drosophila* Wing. Current Biology *27*, 3826-3836.e5.

Resnik-Docampo, M., Koehler, C.L., Clark, R.I., Schinaman, J.M., Sauer, V., Wong, D.M., Lewis, S., D'Alterio, C., Walker, D.W., and Jones, D.L. (2017). Tricellular junctions regulate intestinal stem cell behaviour to maintain homeostasis. Nat Cell Biol *19*, 52–59.

Riazuddin, S., Ahmed, Z.M., Fanning, A.S., Lagziel, A., Kitajiri, S., Ramzan, K., Khan, S.N., Chattaraj, P., Friedman, P.L., Anderson, J.M., et al. (2006). Tricellulin Is a Tight-Junction Protein Necessary for Hearing. The American Journal of Human Genetics *79*, 1040–1051.

Ross, J.M. (1998). Cell-Extracellular Matrix Interactions. In Frontiers in Tissue Engineering, (Elsevier), pp. 15–27.

Rüffer, C., and Gerke, V. (2004). The C-terminal cytoplasmic tail of claudins 1 and 5 but not its PDZ-binding motif is required for apical localization at epithelial and endothelial tight junctions. European Journal of Cell Biology *83*, 135–144.

Rusu, A.D., and Georgiou, M. (2020). The multifarious regulation of the apical junctional complex. Open Biol. *10*, 190278.

Saitou, M., Ando-Akatsuka, Y., Itoh, M., Furuse, M., Inazawa, J., Fujimoto, K., and Tsukita, S. (1997). Mammalian occludin in epithelial cells: its expression and subcellular distribution. Eur J Cell Biol *73*, 222–231.

Saitou, M., Furuse, M., Sasaki, H., Schulzke, J.-D., Fromm, M., Takano, H., Noda, T., and Tsukita, S. (2000). Complex Phenotype of Mice Lacking Occludin, a Component of Tight Junction Strands. MBoC *11*, 4131–4142.

Sánchez-Pulido, L., Martín-Belmonte, F., Valencia, A., and Alonso, M.A. (2002). MARVEL: a conserved domain involved in membrane apposition events. Trends in Biochemical Sciences *27*, 599–601.

Sawyer, J.K., Harris, N.J., Slep, K.C., Gaul, U., and Peifer, M. (2009). The *Drosophila* afadin homologue Canoe regulates linkage of the actin cytoskeleton to adherens junctions during apical constriction. J Cell Biol *186*, 57–73.

Scheiffele, P., Fan, J., Choih, J., Fetter, R., and Serafini, T. (2000). Neuroligin Expressed in Nonneuronal Cells Triggers Presynaptic Development in Contacting Axons. Cell *101*, 657–669.

Schotman, H., Karhinen, L., and Rabouille, C. (2009). Integrins mediate their unconventional, mechanical-stress-induced secretion via RhoA and PINCH in *Drosophila*. Journal of Cell Science *122*, 2662–2672.

Schulte, J., Tepass, U., and Auld, V.J. (2003). Gliotactin, a novel marker of tricellular junctions, is necessary for septate junction development in *Drosophila*. J. Cell Biol. *161*, 991–1000.

Schulte, J., Charish, K., Que, J., Ravn, S., MacKinnon, C., and Auld, V.J. (2006). Gliotactin and Discs large form a protein complex at the tricellular junction of polarized epithelial cells in *Drosophila*. Journal of Cell Science *119*, 4391–4401.

Sharifkhodaei, Z., Gilbert, M.M., and Auld, V.J. (2019). Scribble and Discs Large mediate tricellular junction formation. Development *146*, dev174763.

Sharma, S., Ang, S.L., Shaw, M., Mackey, D.A., Gécz, J., McAvoy, J.W., and Craig, J.E. (2006). Nance–Horan syndrome protein, NHS, associates with epithelial cell junctions. Human Molecular Genetics *15*, 1972–1983.

Sharma, S., Burdon, K.P., Dave, A., Jamieson, R.V., Yaron, Y., Billson, F., Van Maldergem, L., Lorenz, B., Gécz, J., and Craig, J.E. (2008). Novel causative mutations in patients with Nance-Horan syndrome and altered localization of the mutant NHS-A protein isoform. Mol Vis *14*, 1856–1864.

Sharma, S., Koh, K.S., Collin, C., Dave, A., McMellon, A., Sugiyama, Y., McAvoy, J.W., Voss, A.K., Gécz, J., and Craig, J.E. (2009). NHS-A isoform of the NHS gene is a novel interactor of ZO-1. Experimental Cell Research *315*, 2358–2372.

Sharma, S., Datta, P., Sabharwal, J.R., and Datta, S. (2017). Nance-Horan Syndrome: A Rare Case Report. Contemp Clin Dent *8*, 469–472.

Shi, J., Barakat, M., Chen, D., and Chen, L. (2018). Bicellular Tight Junctions and Wound Healing. Int J Mol Sci *19*.

Soderholm, J.D. (2002). Augmented increase in tight junction permeability by luminal stimuli in the non-inflamed ileum of Crohn's disease. Gut *50*, 307–313.

Stevenson, B.R., Siliciano, J.D., Mooseker, M.S., and Goodenough, D.A. (1986). Identification of ZO-1: a high molecular weight polypeptide associated with the tight junction (zonula occludens) in a variety of epithelia. The Journal of Cell Biology *103*, 755–766.

Su, W.-H., Mruk, D.D., Wong, E.W.P., Lui, W.-Y., and Cheng, C.Y. (2012). Polarity protein complex Scribble/Lgl/Dlg and epithelial cell barriers. Adv Exp Med Biol *763*, 149–170.

Tanentzapf, G., and Tepass, U. (2003). Interactions between the crumbs, lethal giant larvae and bazooka pathways in epithelial polarization. Nat Cell Biol *5*, 46–52.

Tepass, U. (1996). Crumbs, a Component of the Apical Membrane, Is Required for Zonula Adherens Formation in Primary Epithelia of *Drosophila*. Developmental Biology *177*, 217–225.

Tepass, U. (2003). Claudin complexities at the apical junctional complex. Nat Cell Biol *5*, 595–597.

Tepass, U., and Hartenstein, V. (1994). The Development of Cellular Junctions in the *Drosophila* Embryo. Developmental Biology *161*, 563–596.

Thuveson, M., Gaengel, K., Collu, G.M., Chin, M., Singh, J., and Mlodzik, M. (2019). Integrins are required for synchronous ommatidial rotation in the *Drosophila* eye linking planar cell polarity signalling to the extracellular matrix. Open Biol. *9*, 190148.

Tian, Q., Li, Y., Kousar, R., Guo, H., Peng, F., Zheng, Y., Yang, X., Long, Z., Tian, R., Xia, K., et al. (2017). A novel NHS mutation causes Nance-Horan Syndrome in a Chinese family. BMC Med Genet *18*, 2.

Tokuda, S., Higashi, T., and Furuse, M. (2014). ZO-1 Knockout by TALEN-Mediated Gene Targeting in MDCK Cells: Involvement of ZO-1 in the Regulation of Cytoskeleton and Cell Shape. PLoS ONE *9*, e104994.

Tsukita, S., Furuse, M., and Itoh, M. (2001). Multifunctional strands in tight junctions. Nat Rev Mol Cell Biol *2*, 285–293.

Venken, K.J.T., Schulze, K.L., Haelterman, N.A., Pan, H., He, Y., Evans-Holm, M., Carlson, J.W., Levis, R.W., Spradling, A.C., Hoskins, R.A., et al. (2011). MiMIC: a highly versatile transposon insertion resource for engineering *Drosophila melanogaster* genes. Nat Methods *8*, 737–743.

Verghese, S., Waghmare, I., Kwon, H., Hanes, K., and Kango-Singh, M. (2012). Scribble Acts in the *Drosophila* Fat-Hippo Pathway to Regulate Warts Activity. PLoS ONE *7*, e47173.

Voelzmann, A., Liew, Y.-T., Qu, Y., Hahn, I., Melero, C., Sánchez-Soriano, N., and Prokop, A. (2017). *Drosophila* Short stop as a paradigm for the role and regulation of spectraplakins. Seminars in Cell & Developmental Biology *69*, 40–57.

Walsh, G.S., Grant, P.K., Morgan, J.A., and Moens, C.B. (2011). Planar polarity pathway and Nance-Horan syndrome-like 1b have essential cell-autonomous functions in neuronal migration. Development *138*, 3033–3042.

Wang, J. (2012). Pull and push: Talin activation for integrin signaling. Cell Res *22*, 1512–1514.

Ward, R.E., Lamb, R.S., and Fehon, R.G. (1998). A Conserved Functional Domain of *Drosophila* Coracle Is Required for Localization at the Septate Junction and Has Membrane-organizing Activity. Journal of Cell Biology *140*, 1463–1473.

Weihe, U., Milán, M., and Cohen, S.M. (2001). Regulation of Apterous activity in *Drosophila* wing development. Development *128*, 4615–4622.

Wiley, C.A., and Ellisman, M.H. (1980). Rows of dimeric-particles within the axolemma and juxtaposed particles within glia, incorporated into a new model for the paranodal glial-axonal junction at the node of Ranvier. Journal of Cell Biology *84*, 261–280.

Willott, E., Balda, M.S., Fanning, A.S., Jameson, B., Van Itallie, C., and Anderson, J.M. (1993a). The tight junction protein ZO-1 is homologous to the *Drosophila* discs-large tumor suppressor protein of septate junctions. Proc Natl Acad Sci U S A *90*, 7834–7838.

Willott, E., Balda, M.S., Fanning, A.S., Jameson, B., Van Itallie, C., and Anderson, J.M. (1993b). The tight junction protein ZO-1 is homologous to the *Drosophila* discs-large tumor

suppressor protein of septate junctions. Proceedings of the National Academy of Sciences *90*, 7834–7838.
Wittek, A., Hollmann, M., Schleutker, R., and Luschnig, S. (2020). The transmembrane proteins M6 and Anakonda cooperate to initiate tricellular junction assembly in epithelia of *Drosophila* (Cell Biology).
Wolpert, L. (2003). Cell boundaries: knowing who to mix with and what to shout or whisper. Development *130*, 4497–4500.
Woods, D.F., Hough, C., Peel, D., Callaini, G., and Bryant, P.J. (1996). Dlg protein is required for junction structure, cell polarity, and proliferation control in *Drosophila* epithelia. The Journal of Cell Biology *134*, 1469–1482.
Wu, V.M., Yu, M.H., Paik, R., Banerjee, S., Liang, Z., Paul, S.M., Bhat, M.A., and Beitel, G.J. (2007). *Drosophila* Varicose, a member of a new subgroup of basolateral MAGUKs, is required for septate junctions and tracheal morphogenesis. Development *134*, 999–1009.
Xu, W., Coll, J.L., and Adamson, E.D. (1998). Rescue of the mutant phenotype by reexpression of full-length vinculin in null F9 cells; effects on cell locomotion by domain deleted vinculin. J Cell Sci *111 (Pt 11)*, 1535–1544.
Zappia, M.P., Brocco, M.A., Billi, S.C., Frasch, A.C., and Ceriani, M.F. (2011). M6 Membrane Protein Plays an Essential Role in *Drosophila* Oogenesis. PLoS ONE *6*, e19715.
Zervas, C.G., Gregory, S.L., and Brown, N.H. (2001). *Drosophila* Integrin-Linked Kinase Is Required at Sites of Integrin Adhesion to Link the Cytoskeleton to the Plasma Membrane. Journal of Cell Biology *152*, 1007–1018.
Zihni, C., Mills, C., Matter, K., and Balda, M.S. (2016). Tight junctions: from simple barriers to multifunctional molecular gates. Nat Rev Mol Cell Biol *17*, 564–580.